

THE NERVOUS SYSTEM IS REGENERATED IN
SEA STAR LARVAE THROUGH RE-USE OF THE
EMBRYONIC NEURAL STEM CELL LINEAGE AND
RE-ACTIVATION OF STEM CELL SPECIFICATION

by

MINYAN ZHENG

Submitted in partial fulfillment of the requirements

For the degree of Doctor of Philosophy

Dissertation Advisor: Dr. Veronica F. Hinman

Department of Biological Sciences

CARNEGIE MELLON UNIVERSITY

July 2019

DEDICATION

Table of Contents

Abstract	5
Chapter 1: General Introduction	8
1.1 Regeneration and evolution	8
1.2 Animals naturally capable of regeneration use various strategies	10
1.2.1 Totipotent or pluri-potent stem cells.....	10
1.2.2 Trans-differentiation.....	11
1.2.3 De-differentiation	11
1.3 Common processes underlying regeneration and important questions in the field	12
1.4 Sea star larvae as models for regeneration studies	14
1.4.1 Regeneration in echinoderms	14
1.4.2 Sexual life cycle and larval stage	15
1.4.3 Sea star larvae as a model for regeneration.....	16
1.5 Sea star larval nervous system	17
1.5.1 Dorsal ganglia.....	18
1.5.2 Apical pole domain (APD) GRN governs serotonergic neurogenesis.	18
1.5.3 Ciliary bands	19
1.5.4 Ciliary band domain (CBD) associate GRN patterns neurons.	20
1.6 Overview of this study	22
Chapter 2: Materials and Methods	24
2.1 Culture and regeneration	24
2.1.1. Culture	24
2.1.2. Bisection	25
2.1.3 Morphology of regenerating larvae	25
2.1.4 Regeneration of larval nervous system.....	26
2.2 Gene expression detection	27
2.2.1 Whole mount <i>in situ</i> hybridization (WMISH).....	27
2.2.2 Double fluorescent <i>in situ</i> hybridization (FISH).....	28
2.2.2 EdU-FISH	29
2.3 Generation and examination of Sox_c-Kaede BAC	30
2.3.1 Test Kaede expression and conversion.....	30
2.3.2 Generation of Sox _c -Kaede BAC	33
2.4 Cell lineage tracing	34
2.4.1 Examination of specified Sox _c ⁺ cells in larvae.....	34
2.4.2 Examination of Sox _c ⁺ cell lineage in regenerating larvae.....	36
2.5 Double cell lineage tracing	40
2.5.1 Generation and examination of Sox _{b1} -Kaede BAC	40
2.5.2 Generation and examination of Sox _c -Cardinal BAC.....	41
2.5.3 Determine Sox _{b1} specification in regeneration.....	41
2.5.4 Determine Sox _{b1} ⁺ /Sox _c ⁺ cell fates in regeneration.....	43
Chapter 3: Embryonic genetic pathway controlling neurogenesis is recapitulated in regeneration	45
3.1 Introduction	45
3.1.1 Neuronal gene markers.....	45
3.1.2 Serotonergic neurogenesis in sea star larvae.....	48
3.1.3 General Introduction	49
3.2 Results	50

3.2.1 Sea star larvae regenerate the nervous system.....	50
3.2.2 Reconstruction of Anterior-Posterior body axis	57
3.2.3 Expression patterns of genes from the embryonic neuronal pathway in regenerating larvae.....	60
3.3 Conclusion and discussion: A model to be tested for neural regeneration	72
3.3.1 summary.....	72
3.3.2 Recapitulation of the genetic pathway controlling neurogenesis	73
3.3.3 Model.....	74
Chapter 4: Embryonic neural stem cell lineage is re-used to form the serotonergic neurons	75
4.1 Introduction	75
4.1.1 General introduction	75
4.1.2 Methods for cell lineage tracing	75
4.1.3 Recombinant bacterial artificial chromosomes (BAC) are used to track gene expression in echinoderms.....	77
4.2 Results	78
4.2.1 A Sox ^c -Kaede BAC is generated to trace the Sox ^c + cell lineage.....	78
4.2.2 Larval Sox ^c + cell lineage in the remaining posterior contributes to the regenerated serotonergic neurons	85
4.2.3 Larval Sox ^c + cells are derived from embryonic Sox ^c + neural stem cell lineage.....	90
4.2.4 Specifications of Sox ^c + cells resume in regeneration, resembling the embryo state.	98
4.3 Conclusion and discussion.....	101
Chapter 5: Sox^b1+ stem cells are specified into Sox^c+ cells to regenerate neurons	103
5.1 Introduction	103
5.2 Results	103
5.2.1 Sox ^b 1+ cell lineage gives rise to the nervous system in larvae.	103
5.2.2 Sox ^b 1+ cells in the regeneration leading edge are specified into Sox ^c + cells.....	109
5.2.3 Sox ^b 1+/Sox ^c + cells become neurons in regenerating larvae.....	119
5.2.4 There are multiple sources of Sox ^b 1+ cells in the regeneration leading edge.....	121
5.3 Conclusion and discussion.....	124
Chapter 6: General Discussion	126
6.1 Summary.....	126
6.1.1 The neuronal genetic pathway is recapitulated in regeneration.....	126
6.1.2 Novel application of BAC transgenesis in Echinoderm regeneration	127
6.1.3 The Sox ^c + neural stem cells at the regeneration leading edge come from three different sources and become neurons in regeneration	129
6.1.4 Larval Sox ^b 1+ cell lineage contributes to the larval nervous system in development and regeneration.....	132
6.1.5 Specification of Sox ^b 1+ cells is activated in regeneration, suggesting trans-fating from endo-mesodermal cells.....	133
6.2 A strategy for sea star larval nervous system regeneration	133
6.3 Sox^c+ stem cells are multipotent in regeneration.....	135
6.4 The regeneration leading edge is set back to an embryonic state.....	136
6.5 Regeneration capability and developmental plasticity in Metazoa	137

THE NERVOUS SYSTEM IS REGENERATED IN SEA STAR LARVAE THROUGH RE-USE OF THE EMBRYONIC NEURAL STEM CELL LINEAGE AND RE-ACTIVATION OF STEM CELL SPECIFICATION

Abstract

by

MINYAN ZHENG

Regeneration is a fascinating phenomenon widespread in the animal kingdom that by definition requires cells to reform lost tissues. Despite its wide distribution, the ability of regeneration varies dramatically among cell types and organisms. The central nervous system, for example, is particularly difficult to regenerate in mammals. In the field of neural regeneration, arguably long-lasting interests are the source of the regenerated neurons and the mechanism by which the neural reformation occurs. Transparent larvae of sea stars, *Patiria miniata*, have an extraordinary regenerative capacity and thereby offer the opportunity to interrogate the sources of neural regeneration and their mechanisms. This study combines BAC transgenesis, cell lineage tracing, molecular analyses and fluorescent microscopy to better identify the cellular sources of regeneration in the sea star larval nervous system.

Previously it was known that the serotonergic neurons and some other neurons in the nervous system of sea star embryos are derived from an embryonic multi-potent neural stem cell lineage expressing the gene *soxc*. To start characterizing the sources of regeneration *in vivo*, I generated a powerful molecular tool to trace cell lineage: a Sox_c-Kaede BAC construct that stably labels the Sox_c⁺ cell lineage and effectively differentiates regenerative Sox_c expression from developmental Sox_c expression through simple photo-conversions. This novel application of BAC transgenesis in larval regeneration sets the technical basis for interrogating the cellular sources of regeneration. It also holds great potential to be adapted and applied to many other model systems.

This study produced three important findings. First, there is a stem cell population expressing Sox_c located at the wound proximal area upon bisection. They consistently proliferate and eventually become serotonergic neurons and some other neurons in the nervous system of the decapitated larvae. Some of these Sox_c⁺ stem cells at the wound site are derived from larval Sox_c⁺ cell lineage in the remaining bottom half. And the larval Sox_c⁺ cells are indeed originated from the embryonic Sox_c⁺ stem cell lineage which generate the serotonergic neurons in embryos. Strikingly, these findings together for the first time demonstrate *in vivo* that an embryonic multi-potent neural stem cell lineage, which forms the embryonic nervous system, is maintained and populated in the organism during post-embryo development and is re-used upon bisection to regenerate the nervous system.

Second, some Sox^{c+} neural stem cells at the regeneration leading edge are derived from upstream stem cells that are programmed into neural fates, or specification, upon bisection. Specification of Sox^{c+} cells occur in embryonic stage but stops in larvae. Decapitation re-initiates the specification events to generate Sox^{c+} neural stem cells. These regeneration-specific Sox^{c+} cells arise from the highly potent Sox^{b1+} stem cells at the regeneration leading edge. Importantly, the Sox^{b1+}/Sox^{c+} cells are used in regeneration to form neurons at the anterior pole.

Last but not least, I observed that *de novo* Sox^{b1+} stem cells are specified upon decapitation to regenerate the multiple types of neurons. Sox^{b1+} cell lineage contributes to the nervous system in development and during regeneration. The genetic pathway of serotonergic neurogenesis is recapitulated in regeneration. Taken together, these findings shed light on the fundamental mechanisms and cellular basis of neural regeneration in metazoans.

Chapter 1: General Introduction

1.1 Regeneration and evolution

Regeneration is a fascinating phenomenon, which by definition requires cells to form lost tissues to restore the intrinsic body plan. The ability to regenerate is widely distributed throughout the animal kingdom; from basally branching animals like cnidarians to later branching animals such as vertebrates and insects (**Fig 1**).

Regenerative capacities of animals, however, differ profoundly among taxa (**Fig 1**).

Some animals are able to undergo extensive, whole-body regeneration (WBR) and are able to restore all types of cells. For example, the cnidarian, *Hydra vulgaris*, is able to regenerate whole polyps from single cells or segments. Likewise, *Schmidtea mediterranea*, a species of freshwater planarian in the phylum of *Platyhelminthes*, have nearly unlimited regenerative ability. They form a blastema that can differentiate to form the missing body parts. Some invertebrate deuterostomes also have extraordinary regenerative capability. The most representative taxon is Echinodermata: sea urchins, sea stars and their relatives (Czarkwiani et al. 2016; García-Arrarás et al. 2018; Carnevali and Burighel 2001; Vickery et al. 2001; Paul 2001). Adult sea stars are well known for their ability to regenerate arms or in some species, their whole bodies from severed arms. Sea cucumbers can regenerate almost all external and internal organs. Most, if not all larvae of echinoderms are also able to undergo whole-body regeneration. In contrast, the extent of regeneration is relatively limited in most chordates. Zebrafish and salamanders are the only vertebrates reported capable of extensively regenerating

multiple types of tissues including appendages, heart, transected spinal cord, brain and some other tissues. Mammals can only regenerate very few types of cells. The regenerative capacities for some mammals, including mouse and human are also age dependent.

Considering that the regenerative abilities are well represented in metazoans, yet the extent of regeneration varies dramatically, it remains fascinating why and how is such uneven distribution formed during evolution. To dissect this question, it will be informative to understand and compare the processes, molecular mechanisms and cellular basis of regeneration in different model systems across metazoans. These studies will have important implications in promoting and manipulating regeneration in vertebrates with limited potential as well as developing regenerative therapies for humans.

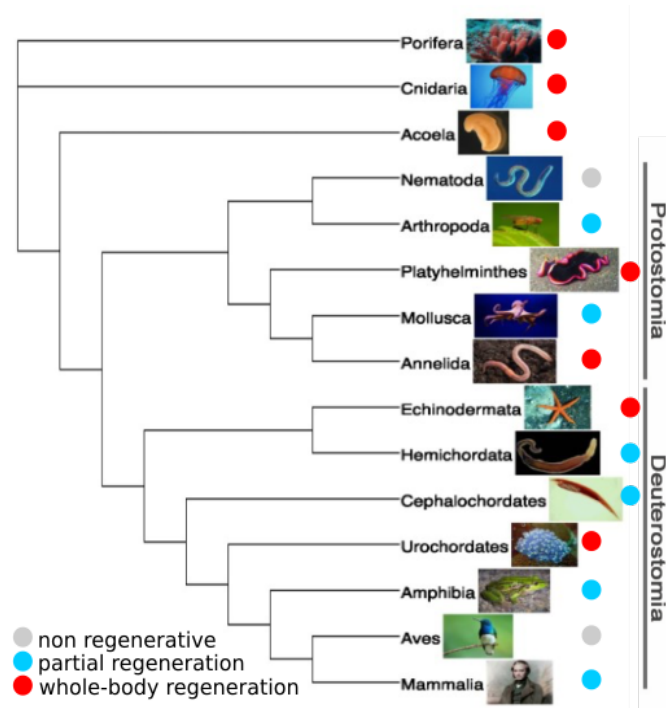


Fig1. phylogenetic distribution of regeneration

Regeneration is widely distributed in Metazoa. Animals display different regenerative capacity. This figure is adapted from published work ((Cary et al. 2019)).

1.2 Animals naturally capable of regeneration use various strategies

The fascinating phenomenon of regeneration drives scientists to understand its molecular and cellular basis in animals intrinsically capable of regeneration. Such animals are widely distributed in nature. Extensive studies show that the mechanisms of regeneration are not uniform. Three main strategies are adapted by different model systems.

1.2.1 Totipotent or pluri-potent stem cells

Schmidtea mediterranea, a species of freshwater planarians, have nearly unlimited regenerative ability. They possess a group of heterogeneous, pluripotent somatic stem cells, called neoblasts, that can proliferate and differentiate to replace body parts in regeneration and homeostasis (Sánchez Alvarado 2006) . Upon amputation, the neoblast in the near wound area will be activated to enter rapid cell cycles and form a blastema in place of the wound site (Reddien 2018). Body axes are reconstructed evidenced by expression of axial patterning genes. Multiple signalling pathways including WNT, BMP, ERK and JNK pathways are activated to regulate body axis reformation, cell proliferation and cell death (Reddien et al. 2007; Tasaki et al. 2011; Petersen and Reddien 2009; Almuedo-Castillo et al. 2014). While the blastema

differentiates to form the missing tissues, the remaining parts of the planarian undergo tissue remodelling to adjust the proportion and size. Therefore, a regenerated smaller planaria is the result of blastema differentiation and remaining tissue reproportion.

1.2.2 Trans-differentiation

The most studied cnidarian species *Hydra vulgaris* is able to regenerate whole polyps from single cells or segments. In contrast to planarians, regeneration is accomplished generally through trans-differentiation of cells (Galliot 2012; Frank et al. 2009; Gold and Jacobs 2013). There are also somatic stem cells, namely the interstitial cells, as precursors of several cell types (David 2012).

1.2.3 De-differentiation

Salamander limb regeneration is another well understood example of cell-reprogramming. Similar to planarians, amputated salamanders also form blastema to differentiate missing cell types. However, the sources of blastema in salamanders and axolotls are from cell dedifferentiation. The salamander skeletal muscle cells in the wound proximity de-differentiate to become pluripotent progenitor state. These de-differentiated progenitor cells form the blastema and differentiate to form the regenerated skeletal and muscle lineage (Wang et al. 2015; Wang and Simon 2016). Recent findings in axolotl using more advanced genetic labeling and single-cell analyses also support the de-differentiation mechanism in limb regeneration (Currie et al. 2016; Gerber et al. 2018).

1.3 Common processes underlying regeneration and important questions in the field

Despite the different strategies applied by different model systems, there are common processes underlying regeneration. A recent study characterizes the biological processes of regeneration transcriptomically in sea star larvae. When sea star larvae are bisected, active cell movements are engaged in sealing the wound, followed by thickening of the wound epithelia. Early responses activated within 3 hours post wounding are regarding signaling pathways activating wound responses, cilia functions, tumor suppressors, cell proliferation and cell deaths (Cary, Wolff, et al. 2019). A comparison of processes underlying regeneration of sea star larvae with transcriptomic studies in freshwater planarian (Kao et al. 2013) and cnidarian hydra (Petersen et al. 2015) reveals that there are common processes shared by these animals capable of WBRs. Following amputation, the organism detects the wound, activating immune signals and MAPK signaling either through the ERK or JNK pathway. Meanwhile, cell proliferation is activated to generate new cells, and cell deaths are upregulated in response of immune reactions. Cell deaths are also necessary for tissue remodeling to generate a properly proportioned animal. In addition, the organisms need to initiate the regeneration program instead of healing program. This can potentially be explained by the activity of tumor suppressor gene products. Following these immediate responses, patterning genes are expressed to reconstruct the body axis (Cary, Wolff, et al. 2019).

This significant finding of commonality of WBR exemplifies that regeneration presents a great opportunity to interrogate fundamental developmental biological processes in metazoans. It also raises a very interesting question: are these regenerative processes homologous or independently evolved? The shared gene expression trends suggest that they may be inherited from the same ancestor. But the different strategies of regeneration found in planaria *S. mediterranea* and hydra *H. magnipapillata* seem to counter this speculation. Therefore, understanding the regenerative strategy in sea star larvae will provide more important evidence in query of the evolutionary history of WBR.

To examine the mechanisms of regeneration used in sea star larvae, I investigated what are the cellular sources of regeneration and how are they directed to form new tissue? These questions have captured the interests of scientists for hundreds of years when they see a polyp or head growing back after injuries. Where do they come from? How do they reform? The earliest experimental inquiries of regeneration date back to the 1700s when Abraham Trembley cut the hydra polyp in half (Lenhoff et al. 1986; Galliot 2012). Since then, the sources of regeneration have arguably remained the most intriguing questions in the field (Reyer et al. 1973; Tanaka and Reddien 2011). 300 years after Abraham's study, we would like to take the challenge and find an answer to this long-lasting question in the context of sea star larvae.

1.4 Sea star larvae as models for regeneration studies

1.4.1 Regeneration in echinoderms

Nestled in a branch of bilateria, Deuterostomia is the clade of animals in which the first opening in the embryo, the blastopore, becomes the anus. The three phyla within this grouping have varying extents of regeneration. The phylum of Echinodermata contains a wide diversity of documented regenerative animals in both larva and adult forms (Carnevali and Burighel 2001; Paul 2001). For example, adult sea urchins are able to restore their tube feet and spines (Reinardy et al. 2015). Sea cucumbers can regrow the digestive systems after evisceration (Mashanov et al. 2005; Mashanov et al. 2010; Mashanov et al. 2012; García-Arrarás et al. 2018). One of the classes, the Asteroidea (sea stars) are especially well known for their ability to regenerate missing body parts. Adult sea stars can easily regenerate their arms. For most species, this process requires at least part of the central disc, the activity center of the sea star from which arms sprout. In some other species, the severed arms can even regenerate the whole-body. Thus this group provides a wide selection of species for research regarding tissue remodeling, tissue re-specification, re-differentiation, stem cells activities and competencies and has as a taxonomic grouping mature system for cellular and molecular understanding of regeneration.

Similar to adults, echinoderm larvae have an extraordinary regenerative capability. It is known that bipinnaria larvae of sea stars are able to undergo WBR, capable of regenerating all types of tissues including the nervous system. For example, upon

decapitation, the remaining posterior segments rapidly seal the wound. Following epithelialization, the posterior larvae undergo body re-proportioning and massive cell proliferations. Full restoration of the anterior occurs within 2 weeks post decapitation (Cary, Wolff, et al. 2019; Oulhen et al. 2016). This is consistent with previous findings in asteroids *Luidia foliolata* and *Pisaster ochraceus*: bisection of planktotrophic larvae leads to wound healing and complete regeneration of missing body parts in both halves over a period of 12-14 days (Vickery et al. 2002; Vickery and McClintock 1998).

1.4.2 Sexual life cycle and larval stage

Many species of echinoderms have a free swimming and feeding larval stage. The sexual life cycles of the sea star *P.miniata* begins from fertilized eggs, followed by hatching to become gastrula. After gastrulation, three germ layers are functionally distinguished from each other. The larval stage is marked by the formation of the mouth and the ciliary bands. This becomes the bipinnaria larvae of the sea star and the pluteus of sea urchin. Larvae may live in the plankton for weeks to months before metamorphosis. Feeding echinoderm larvae undergo dramatic metamorphosis, during which they re-arrange tissues and replace the bilateral symmetry with a pentaradially symmetrical body plan. Post-metamorphosis juveniles will keep feeding and growing to become sexually mature adults.

Echinoderm larvae have fully formed tissues and organs with multiple differentiated cell types. For example the sea star larval nervous system consists of the ciliary bands-associated neurons, oral neurons and the dorsal ganglia (Hinman and Burke 2018).

These neurons express the post-mitotic neuron marker gene *elav* (Yankura et al. 2013). The dorsal ganglia are mostly formed of serotonergic neurons. Detection of strong serotonin signals in the dorsal ganglia demonstrates the maturation and functionality of these differentiated neurons. Extensive literature of their development, and in particular the formation of their anterior-posterior (AP) axis, dorsal ventral axis and specification of tissues is known (Yankura et al. 2010; McCauley et al. 2010; Hinman et al. 2003). Thus these larvae represent an exceptional opportunity to adapt the tools and approaches that have empowered echinoderms as models for comparative developmental gene regulatory networks (GRNs) to regeneration.

1.4.3 Sea star larvae as a model for regeneration

Unlike the pluteus in sea urchins, bipinnaria of sea star *Patiria miniata* do not have interior skeletons. Larvae of *P.miniata* are much larger than those of the purple sea urchin. These features make them a perfect model for refined larval surgeries. Manual amputations can be consistently performed in well-controlled manners to induce regeneration. Methods to easily obtain and maintain thousands of genetically identical sea star embryos and larvae in a laboratory environment have been well described and characterized. After *in vitro* fertilization, *Patiria miniata* develops to become bipinnaria at 4 day-post-fertilization (dpf) at 15 °C.

In sea stars, sequencing and characterization of the genome of *Patiria miniata* (Cameron et al. 2015) allows for efficient gene level analyses and transcriptomic studies. A suite of well-established molecular tools are available to determine gene

expression patterns, gene functions and cell proliferation patterns which are an important basis for resolving the complicated gene regulatory networks in starfish. We also have accessible genetic tools that enable us to perform stable cell lineage tracing and visualization. Taken together, investigating the mechanisms of regeneration in sea star larvae is feasible and likely to generate fruitful results.

1.5 Sea star larval nervous system

In alignment with the pentaradial symmetry, adult sea stars have a radial nervous system. In contrast, the bilateral symmetric sea star bipinnaria present a more centralized nervous system. It consists of a centralized apical organ (Byrne et al. 2007), the dorsal ganglia, and peripheral neural organs including the neurons associated with ciliary bands, mouth and musculature of esophagus (Nakajima et al. 2004). The nervous systems associated with the apical organ and ciliary bands are characterized (Yankura et al. 2010; Cheatle Jarvela et al. 2016; Yankura et al. 2013) and are summarized here. Unlike the ciliary band neurons or the dorsal ganglia neurons, the nervous system associated with the foregut is derived from the endoderm instead of the ectoderm in sea urchins (Wei et al. 2011). Therefore, we speculate that the neurons located in the esophagus may originate from the endoderm in sea stars.

1.5.1 Dorsal ganglia

All echinoderm larvae possess apical organs. The apical organ is the central nervous organ that is located bilaterally at the anterior side. In sea star larvae, the apical organ is the bilateral anterior dorsal ganglia located opposite from the mouth. One distinctive characteristic shared by all forms of apical organs among echinoderm larvae is that there are clusters of serotonergic neurons as the main components (Byrne et al. 2007; Bisgrove and Burke 1986; Bishop et al. 2013). In sea urchin and sea star embryos, serotonergic neurons are derived from the anteriormost apical pole domain (APD). The APD is defined by a suite of anterior patterning genes including *foxq2*, *six3*, *zic*, *rx*, and etc. The expression of the APD genes is similar to those expressed in the vertebrate forebrain (Wei et al. 2009). In bipinnaria, serotonergic neurons are mainly found in the dorsal ganglia (**Fig 2.A**). There are also serotonergic neurons in the lower lip of the mouth and in the esophagus. However, it is easy to distinguish from others the serotonergic neurons in the dorsal ganglia due to their larger size. The number of these serotonergic neurons per larva varies from 30-50 and remains relatively fixed in bipinnaria (Hinman and Burke 2018).

1.5.2 Apical pole domain (APD) GRN governs serotonergic neurogenesis.

In sea stars, serotonergic neurons are first formed at the anteriormost apical pole domain (APD) in 3 day old embryos and move posteriorly as embryos grow (**Fig 2.B**). The embryonic ectoderm are pan-neurogenic marked by the expression of neural stem cell gene *soxb1*. On this broad neurogenic ectoderm, the neural stem cells expressing

soxc are partitioned through delta-notch signaling. *Soxc*⁺ cells are distributed in a “salt and pepper” pattern along the AP axis on the entire ectoderm (Yankura et al. 2010). However, serotonergic neurons are only formed at the APD. The APD GRN connects the axial information to the neural stem cell progression (**Fig 2.C**). This directs the precise location of serotonergic neurogenesis. The anterior patterning genes *foxq2* and *rx* are both expressed at the APD. With the presence of *foxq2* and *rx*, *soxc*⁺ neural stem cells undergo asymmetric divisions and progress to become *lhx2*⁺ restricted neural progenitors. Progression of *lhx2*⁺ progenitors also requires regulation of Foxq2 and Rx. After asymmetric divisions, *lhx2*⁺ progenitors give rise to post-mitotic neurons expressing *elav*. These post-mitotic neurons will produce serotonin when they mature. Knock-down of *lhx2* causes the loss of serotonergic neurons in dorsal ganglia. In comparison, knock-down of *soxc* leads to losses of both dorsal ganglia and the ciliary-band associated neurons. This shows that *Lhx2*⁺ cells are serotonergic restricted neural progenitors whereas *Soxc*⁺ cells are multipotent neural stem cells. On the other hand, axial patterning genes control the progression of stem cells. In both *foxq2* knock-down and *rx* knock-down, no *lhx2*⁺ cells are found. Similarly, when *foxq2* or *rx* is knocked down after *lhx2* expression, *lhx2*⁺ cells will not progress to express *elav* (Cheatle Jarvela et al. 2016).

1.5.3 Ciliary bands

All planktonic larvae of echinoderms have one or two ciliary bands surrounding their body. These bands of cilia are used to generate motility critical for swimming and feeding. Bipinnaria of *P.miniata* possess two loops of ciliary bands. The pre-oral ciliary

band outlines the oral ectoderm that extends dorsally and laterally towards the anterior (**Fig 2.A**). The post-oral ciliary band crosses the posterior ectoderm under the mouth, extending laterally and upwards to fuse at the anterior pole (Yankura et al. 2010). Together these two loops of ciliary bands traverse the entire body of the larva. In both sea urchins and sea star larvae, there are *elav* expressing post-mitotic neurons associated with the ciliary bands (Yankura et al. 2013). These neurons form axons projecting either along the ciliary bands or towards the mouth (Hinman and Burke 2018).

1.5.4 Ciliary band domain (CBD) associate GRN patterns neurons.

The ciliary band domain, where the ciliary bands will form, is marked by the expression of the genes *foxg* and *onecut*. *Foxg* is first expressed in the anterior oral ectoderm in gastrulae. The expression extends to the two ciliary bands domain where *onecut* expression is also found (Yankura et al. 2010). The CBD GRN allows neurons to form precisely at the correct location. Knocking down *foxg* leads to loss of neurons in the lateral side of the larvae. The CBD is restricted and regulated by anterior-posterior (AP) and dorsal-ventral (DV) axis patterning genes. Knocking down anterior patterning gene *six3* shifts CBD anteriorly. Likewise, manipulating DV axis patterning genes change the CBD as well. *Nodal* knock-down removes the ventral expression of *foxg* whereas *bmp2/4* knockdown leads to ventralization of the CBD (Yankura et al. 2013).

Interestingly, manipulations of axial patterning genes do not interfere with generation of post-mitotic neurons. Instead, they shift the location where ciliary bands and associated neurons are formed.

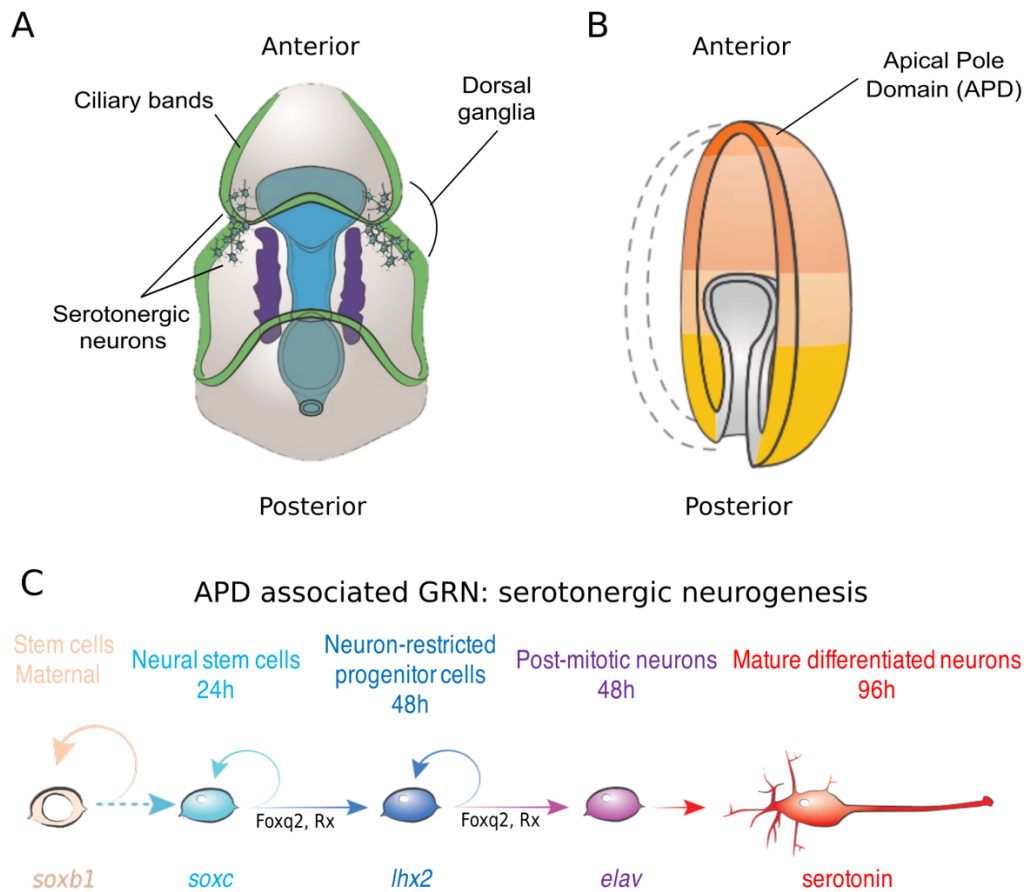


Fig 2. The bipinnaria apical organ and the apical pole domain (APD) associated gene regulatory network (GRN)

(A) A schematic of sea star larval nervous system. (B) The apical pole domain is the anteriormost domain of embryos. C, The APD-associated GRN regulate the neurogenesis of serotonergic neurons.

1.6 Overview of this study

In this study, I seek to understand the cellular sources of nervous system regeneration in bipinnaria of the indirectly developing sea star, *Patiria miniata*. I particularly focus on the cellular sources of the regenerated serotonergic neurons in the dorsal ganglia.

Through the innovative application of BAC transgenesis, I find three important cellular responses that are needed to reform neurons: (i) activation of embryonic Sox^{c+} neural stem cell lineage to enter an embryonic neuronal pathway; (ii) the resumption of Sox^{c+} neural stem cell specification from Sox^{b1+} stem cells; and (iii) the generation of new Sox^{b1+} stem cells at the regeneration leading edge.

Chapter 3 characterizes the regeneration of the larval nervous system and demonstrates that the gene expression trajectory is recapitulated in regeneration.

Chapter 4 shows for the first time that there is an embryonic neural stem cell lineage expressing Sox^c that is maintained in the larva. These embryonic neural stem cells are activated upon decapitation to regenerate serotonergic neurons. Chapter 5 reveals that the specification of Sox^{c+} cells occurs in embryos but stops in larvae. However, Sox^{c+} cell specification is recovered in regenerating larvae upon decapitation. We show Sox^{c+} cells that are activated to take the neuronal pathway at the regeneration leading edge are newly specified from the Sox^{b1+} lineage post decapitation. We also find that there are new lineages of Sox^{b1+} cell specification activated at the regeneration leading edge upon decapitation. Through these chapters, I have constructed a model of strategies used for neural regeneration in sea star larvae. In the general discussion, Chapter 6, I compare the status of cells at the regeneration leading edge to the embryonic cell states

and find multiple similarities. I also relate my findings of cell fate reprogramming in the process of neural regeneration to developmental plasticity. Finally, I extend from this study to discuss potential hypothesis of why the regenerative capacities are limited in some species.

Chapter 2: Materials and Methods

2.1 Culture and regeneration

2.1.1. Culture

Adult Sea star, *Patiria miniata*, were collected off the coast of California by Marinus Inc. They were housed in artificial sea water (Instant Ocean, Aquarium Systems) at 12-15°C. Embryos were cultured as described (Hinman et al. 2003). Briefly, gonads were obtained from the body cavities of adult females. The gonads were minced in cold seawater on ice with forceps to release the immature oocytes. The oocytes and ovary mixture was filtered through a 200 µm nylon mesh (to remove ovarian tissue) and a 100 µm nylon mesh (to remove small immaturable oocytes). The oocytes were then matured in artificial seawater containing 10 mM 1-methyladenine (Sigma) for 45 min to 1 h at 15°C. The mature oocytes were moved into fresh sea water. Maturation was examined as described (Cheatle Jarvela and Hinman 2014). Gonads were obtained dry into an Eppendorf tube from adult males. In approximately 1 ml of seawater, a bean-size piece of testes were minced to release sperm in cold sea water. About 3-5 drops of diluted sperm were used to fertilize the mature oocytes. Following fertilization, the fertilized eggs were filtered through a 100 µm nylon mesh to remove extra sperm. Embryos were cultured at 15°C. Testes can be stored for up to 1 week.

2.1.2. Bisection

P. miniata embryos were cultured in artificial seawater at 15 °C. Starting from 4 dpf, larvae were fed with *Rhodomonas lens* ad libitum every 2 days along with fresh artificial seawater. In this thesis, all regeneration studies were conducted on larval cultures bisected at 7 dpf. Manual bisection was performed stereotypically through the foregut, midway along the AP body axis (Fig.) with a #11 sterile scalpel as described earlier (Cary, Wolff, et al. 2019).

2.1.3 Morphology of regenerating larvae

Intact and bisected larvae were collected at the indicated time points. Before imaging, slides and coverslips were prepared: a poppyseed-size piece of clay was attached to each corner of the coverslip by scratching the corner of the coverslip against the plastilina clay. The coverslip was placed on the slide with the clay feet facing the slide. The coverslip was gently pressed down with a pipette tip to generate a 200-500 µm space between the coverslip and the slide. When imaging, larva was loaded in 100 µl of 15°C sea water. The coverslip was gently pressed down if necessary to remove air from covered area and mechanically immobilize the larvae. Samples were photographed using differential interference contrast (DIC) optics on a Leica DMI4000B microscope at 100× magnification using Leica Application Suite software (Leica; Wetzlar, Germany).

2.1.4 Regeneration of larval nervous system

2.1.4.1 Anti-serotonin Immuno-fluorescence (IF) staining

Immuno-fluorescence (IF) staining using anti-serotonin (Sigma) was performed as described previously (Cheatle Jarvela et al. 2016) with the following modifications. Intact and regenerating larvae incubated for the indicated times were fixed in 4% paraformaldehyde (PFA) in PBS with 0.1% Triton x-100 at room temperature for 60 minutes. They were post-fixed in 100% ice cold Methanol on ice for 10 min and then stepped into PBS/0.1% Triton x-100 for rehydration. Intact and regenerating larvae were treated with PBS/1% Triton x-100 for permeabilization at room temperature for 10 min. Intact and regenerating larvae were washed 4 times in PBS/0.1% Triton x-100, and blocked in 3% BSA/PBS/0.1% Triton x-100. They were next incubated with 1:250 rabbit anti-serotonin (Sigma), diluted in 3% BSA block, overnight at 4°C. Intact and regenerating larvae were then washed 6 times with PBS/0.1% Triton x-100, and incubated with 1:1000 anti-rabbit alexa-fluor 568, diluted in 3% BSA block. Samples were photographed with Zeiss 880 Laser Scanning Microscope at 200x magnification with 405 nm and 560 nm channels in Z-stack settings. Images were analyzed in FIJI and use green pseudo color for 560 nm channel.

2.1.4.2 Anti-synaptotagmin B 1e11 immunofluorescent (IF) staining

IF staining using 1e11, deposited to the DSHB by Burke, R.D. (DSHB Hybridoma Product 1E11) was performed as described (Nakajima et al. 2004) with the following modifications. Intact and regenerating larvae incubated for the indicated times were

fixed in 4% PFA in PBS with 0.1% Triton x-100 at room temperature for 15 minutes. Intact and regenerating larvae were post-fixed in 100% ice cold Methanol at -20 °C for 5 min, allowing for settling of larvae by gravity. Intact and regenerating larvae were then treated with 0.1M Glycine in PBS for 30 min at room temperature to quench autofluorescence. This was followed by 3 washes in PBS/0.1% Triton x-100. To detect synaptotagmin B, larvae were permeabilized in PBS/0.5% Triton x-100 for 30 min at room temperature and blocked in 3% BSA/PBS/0.1% Triton-x-100 for 30 min at room temperature. Intact and regenerating larvae were incubated in a dilution of 1:5 of 1e11 antibody in 3% BSA block overnight at 4 °C. They were next washed 6 times with PBS/0.1% Triton x-100 and incubated with 1:1000 anti-mouse alexa-fluor 568, diluted in 3% BSA block followed by nuclear staining in 1:10000 dilution of 10.9 mM DAPI. Samples were photographed with Zeiss 880 Laser Scanning Microscope at 200x magnification with 405 nm and 560 nm channels in Z-stack settings.

2.2 Gene expression detection

2.2.1 Whole mount *in situ* hybridization (WMISH)

Embryos, intact and regenerating larvae for WMISH were fixed in 4% PFA in a high salt MOPS-fix buffer (100 mM MOPS pH 7.5, 2 mM MgSO₄, 1 mM EGTA, and 0.8 M NaCl) for 90 minutes at room temperature or overnight at 4°C. Following fixation, embryos were washed in (v/v) 25%, 50%, 75% and 100% ice-cold 70% ethanol. Fixed embryos and larvae were stored at -20°C. WMISH was conducted to examine the spatial patterns

of gene expression using protocol described previously (Hinman et al. 2003; Yankura et al. 2010) with the following modification. Hybridization of *soxc* and *lhx2* riboprobes (final concentration of 0.2 ng/mL) was performed at 55°C for 5 days. Hybridization of *elav* riboprobes (final concentration of 0.2 ng/mL) was performed at 58°C for 5 days. Hybridization of *foxq2*, *wnt3*, *six3* and *foxj1* riboprobes (final concentration of 0.1 ng/mL) was performed at 58°C for 5 days. Anti-digoxigenin antibody was used at 1:2000 dilution to label the hybridized probes. Detection was performed through an alkaline phosphatase based color reaction as described. Larvae were imaged on a Leica DMI4000B inverted light microscope using DIC microscopy at 100x magnification and the Leica Application Suite software (Leica; Wetzlar, Germany).

2.2.2 Double fluorescent *in situ* hybridization (FISH)

Intact and regenerating larvae of *P. miniata* at the indicated time points were fixed in a solution of 4% paraformaldehyde in MOPS-fix buffer (0.1 M MOPS pH 7.5, 2 mM MgSO₄, 1 mM EGTA, and 0.8 M NaCl) for 90 min at room temperature and transferred into 70% ethanol for long term storage at -20 °C. Double FISH experiments were performed as previously described (McCauley et al. 2013) using digoxigenin-labeled antisense RNA probes (final concentration of 0.1-0.2 ng/mL) and dinitrophenol-labeled antisense RNA probes (final concentration of 0.1-0.2 ng/mL). Hybridized probes were detected using anti-DIG-POD antibody (1:1000, Roche), anti-DNP-HRP antibody (1:1000, Perkin Elmer) and tyramide signal amplification (Perkin Elmer). A 1:100 dilution of Cy3 or Fluorescein (FITC) labeled tyramide in amplification buffer was used to treat larvae for 7 min at room temperature in the dark. A Cy3- or FITC-labeled tyramide was

deposited near the hybridized probe in a horseradish peroxidase mediated reaction. This allowed for fluorescence detection of labeled probes. During PBST washes, larvae were incubated for a total of 20 min in solution with 1:10000 dilution of 10.9 mM DAPI, followed by PBST washes. Larvae were photographed with Zeiss 880 Laser Scanning Microscope at 200x magnification with 405 nm, 488 nm and 560 nm channels in Z-stack settings.

2.2.2 EdU-FISH

Labeling and detection of proliferating cells in *P. miniata* intact and regenerating larvae were performed using the Click-it Plus EdU 488 Imaging Kit (Life Technologies), with the following modifications. Larvae were incubated in a 10 μ M solution of EdU for 15 min or 6 h in seawater at 15 °C followed by immediate fixation in 4% PFA in PBS buffer with 0.1% Triton x-100. Fixation was performed at room temperature for 90 min. Larvae were then transferred to 70% ethanol for storage at – 20 °C. EdU-labeled intact and regenerating larvae were hybridized with digoxigenin-labeled antisense RNA probes (final concentration of 0.1-0.2 ng/mL). Hybridized probes were detected using anti-DIG-POD antibody (1:1000, Roche) and tyramide signal amplification (Perkin Elmer). Larvae were incubated in 1:100 dilution of Cy3-labeled tyramide for 7 min at room temperature in the dark. This allowed for fluorescence detection of labeled probes. Permeabilization and detection of EdU were performed following the manufacturer's protocol. During washes, intact and regenerating larvae were incubated for 20 min in solution with 1:10000 dilution of 10.9 mM DAPI, followed by PBST washes. Samples were

photographed with Zeiss 880 Laser Scanning Microscope at 200x or 400x magnification with 405 nm, 488 nm and 560 nm channels in Z-stack settings.

2.3 Generation and examination of Sox_c-Kaede BAC

2.3.1 Test Kaede expression and conversion

2.3.1.1 Generation and injection of kaede mRNA

Kaede-N1 was a gift from Michael Davidson (Addgene plasmid # 54726; <http://n2t.net/addgene:54726>; RRID:Addgene_54726). Kaede PCR product was cloned from the plasmid for generating capped mRNA (primers F: 5'- TAA TAC GAC TCA CTA TAG GGG TCG CCA CCA TGA GTC TGA T -3'; R: 5'-TTG CCG ATT TCG GCC TAT TGG -3'). Capped mRNA was generated with mMMESSAGE mMACHINE T7 transcription kit (ThermoFischer) using *kaede* PCR product as template. About 3µg *kaede* mRNA was used to make the 10µl injection buffer to reach a final concentration of 300 ng/µl. Microinjection was performed on de-jellied fertilized eggs following the protocol (Cheattle Jarvela and Hinman 2014). Injected fertilized eggs were sorted under 488 nm fluorescent light at 15 hour-post-fertilization (hpf). The sorted embryos were kept in a plate with artificial sea water (ASW) at 15°C until live imaging. These embryos were starved to avoid fluorescent background from their food.

2.3.1.2 Live imaging

Before imaging, slides and coverslips were prepared: a poppyseed-size piece of clay was attached to each corner of the coverslip by scratching the corner of the coverslip against the plastilina clay. The coverslip was placed on the slide with the clay feet facing the slide. The coverslip was gently pressed down with a pipette tip to generate a 200-500 μm space between the coverslip and the slide. When imaging, the sorted embryos were loaded in 70 μl 15°C sea water. The coverslip was gently pressed down if necessary to remove air from covered area and mechanically immobilize the embryos. The samples were imaged with the Andor Revolution XD spinning Disk confocal microscope using Andor IQ3 system. During imaging, the same laser power was used for 488 nm and 560 nm channels. At each time point, the laser powers applied to different embryos varied depending on the expression levels: 13% laser power at 17-68 hpf, 23.5% laser power after 4 dpf. Imaging was performed as quickly as possible to reduce the stress to embryos. Immediately after imaging, coverslip was carefully picked up with a pipette tip. Embryos were transferred back to the plate with ASW and kept at 15°C until needed.

2.3.1.3 Photo-conversion

Generating the conversion plot and the conversion rate plot

Photoconversion was completed manually with Andor Revolution XD spinning Disk confocal microscope using Andor IQ3 system. The sorted zygotes were loaded on a slide and manipulate them on 20x objective. A snapshot was taken using 488 nm and

560 nm fluorescent channels before conversion. The embryos were then converted following one of the three timelapse scenarios: 1. The embryo was exposed to 405 nm fluorescent source with 100% laser power for 250 seconds with snapshots taken every 5s; 2. The embryo was exposed to 405 nm fluorescent source with 100% laser power for 200 seconds with snapshots taken every 10s; 3. The embryo was exposed to 405 nm fluorescent source with 100% laser power for 150 seconds with snapshots taken every 50s. The time-lapse data were analyzed with FIJI. The embryo area and a background area with no Kaede signal were selected. The pixel values of 488 nm and 560 nm channels within the selected areas were measured and collected separately in each time point. The background pixel value was subtracted from the signal pixel value under each channel at each time point to generate the net pixel values. The net pixel values of both 488 nm and 560 nm were plotted over time to make the photo-conversion plot. The ratio of net 560 nm pixel value over net 488 nm pixel value was calculated and plotted over time to generate the conversion rate plot.

Generating the fluorescence intensity curve

Embryos were incubated individually in labeled 30 mm petri dish with ASW. Each embryo then was loaded on a slide following the steps described above. The 405 nm fluorescence channel with 100% laser power was used to convert embryos. At 24 hpf, 12 embryos were converted via exposure to 405 nm fluorescence for 80s. After conversion, embryos were immediately returned to ASW at 15°C until next imaging session 24 hours later. Using 488 nm and 560 nm channels, Z-stack images of each converted embryo were taken everyday up to 12 dpf. Out of the 12 converted embryos,

6 survived the repetitive imaging session. The net pixel values of 488 nm and 560 nm channels were collected and calculated following the steps described above. The net pixel values of both channels were plotted over time to generate the fluorescence intensity curve.

2.3.2 Generation of Sox-Kaede BAC

2.3.2.1 Sox-Kaede BAC recombination

The recombinant Sox-Kaede BAC was performed following the established protocol (Buckley and Etensohn 2019). The EL250 cells and the GFP recombination cassette were generous gifts from Dr. Buckley. The the GFP coding sequence was replaced with Kaede coding sequence in the recombination cassette. About 50ng of Sox-Kaede BAC was used to make 10 μ l of injection solution. Injection of the BAC was performed as described above. Injected embryos were kept in the injection dish at 15°C in sea water and sorted under 488 nm fluorescence at 24-48 hpf. The sorted embryo were incubated in 50 mm petri dish at 15°C in sea water until imaged at 2 dpf, 4 dpf and 7 dpf to determine Kaede expression pattern.

2.3.2.2 Live imaging to determine Kaede expression pattern

Slides and coverslips were prepared as described above. Individual larva from 2 dpf, 4 dpf and 7 dpf sorted larval culture were loaded on the slides in 70 μ l of 15°C sea water. Coverslip was gently pressed down if necessary to remove air from covered area and

mechanically immobilize the embryos. Z-stack images were taken with the Andor Revolution XD spinning Disk confocal microscope using Andor IQ3 system at 200x magnification with 488 nm and DIC channels. 13% laser power was used at 488 nm channel to image 2 dpf larvae. 4 dpf and 7 dpf larvae were imaged under 23.5% laser power at 488 nm channel. Immediately after imaging, coverslip was carefully picked up with a pipette tip. Embryos were transferred back to the plate with ASW and kept at 15°C until needed.

2.4 Cell lineage tracing

2.4.1 Examination of specified Sox^c+ cells in larvae

2.4.1.2 Injection and photo-conversion

About 50-100ng of Sox^c-Kaede BAC was used to make the 10 μ l injection buffer to reach a final concentration of 5-10 ng/ μ l. Microinjection was performed as described above. Injected zygotes were sorted under 488 nm fluorescent light at 24-48 hpf. The sorted embryos were kept in sea water at 15°C until photo-conversion. These embryos were starved to avoid fluorescent background from their food.

Before photoconversion, larvae were moved into 35 mm petri dish, one larva per dish. The dish were labeled with numbers or letters to track larvae over time. Slides and coverslips were prepared as described above. Sorted embryos were divided into 3 groups based on the developmental stage at which photoconversion was performed: 2 dpf embryonic conversion (N=13), 3 dpf embryonic conversion (N=2) and 4 dpf larval

conversion (N=12). Individual sorted embryo from 2 dpf, 3 dpf and 4 dpf larval culture were loaded on the slides in 70 μ l of 15°C sea water. The coverslip was gently pressed down if necessary to remove air from covered area and mechanically immobilize the embryos. Photoconversion was completed manually with Andor Revolution XD spinning Disk confocal microscope using Andor IQ3 system. The slide was loaded on the imaging stage and use 20x objective. The embryo were exposed to 405 nm fluorescent source with 100% laser power for 60-80 seconds with snapshots taken every 10s. After conversion, Z-stack images were taken for each converted larvae at 488 nm and 560 nm at 20% laser power and at DIC channel. Imaging was performed as quickly as possible to reduce the stress to larvae. Immediately after imaging, coverslip was carefully picked up with a pipette tip. Embryos were transferred back to the plate with ASW and kept at 15°C until imaging 3 day later.

2.4.1.3 Live imaging

The second imaging session for were 3 days post photoconversion. Therefore, the larvae converted at 2 dpf, 3 dpf and 4 dpf were imaged respectively at 5 dpf (N=10), 6 dpf (N=1) and 7 dpf (N=10). For each group, the sample size N decreased due to deaths of converted larvae from stress. Before imaging, slides and samples were prepared as described above. Z-stack images were taken with the Andor Revolution XD spinning Disk confocal microscope using Andor IQ3 system at 200x magnification under 488 nm, 560 nm and DIC channels. 20% laser power was used at 488 nm and 560 nm channels to image all larvae. Immediately after imaging, coverslip was carefully picked

up with a pipette tip. Embryos were transferred back to the plate with ASW and kept at 15°C until needed.

2.4.1.4 Quantification of Green Sox^{c+} cells and statistical analyses

The Z-stack images were analyzed with FIJI. Quantification of green Sox^{c+} cells was conducted manually in the 5 dpf (N=8), 6 dpf (N=1) and 7 dpf (N=9) larvae. Unhealthy, abnormal or dying larvae were not quantified. Quantification data of 5 dpf (2 dpf embryonic conversion) and 7 dpf (4 dpf larval conversion) were then processed for statistical analyses. Two group comparison was performed using Delta's Cliff comparison. The confidence interval width was 95%. Two side p-value was calculated with the Brunner-Munzel test. The Brunner-Munzel test was chosen because it does not require the assumption of equivariance of two groups. The probabilities of getting large values in both groups are equal. This test works on two independent samples, which may have different sizes.

2.4.2 Examination of Sox^{c+} cell lineage in regenerating larvae

2.4.2.1 Examination of cellular sources of Sox^{c+} cells at the regeneration leading edge

Injection, bisection and photo-conversion

Sox^c-Kaede BAC was injected at 5-10 ng/μl. Injection and sorting of embryos were performed as described above. Larvae were starved to avoid autofluorescence from algae *Rhodomonas lens*. Before bisection, multiple 35 mm labeled petri dish were

prepared for tracking larvae over time. Slides and coverslips were prepared as described above. Bisection was performed at the midline along the larval AP body axis on 7 dpf injected and sorted larval culture. Immediately after bisection, the posterior larvae were loaded individually on slides, one larvae per coverslip. Photoconversion was completed manually with Andor Revolution XD spinning Disk confocal microscope using Andor IQ3 system. The slide was loaded on the imaging stage and use 20x objective. The embryo was exposed to 405 nm fluorescent source with 100% laser power for 60-80 seconds with snapshots taken every 10s. After conversion, Z-stack images were taken with DIC, 488 nm channel (20% laser power) and 560 nm (20% laser power). After imaging, the coverslip was carefully picked up with a pipette tip. Larvae were transferred back to the same labeled individual plates with ASW and kept at 15°C until imaging 3 days later.

Live imaging at 3 day-post-bisection (dpb)

The second imaging session was 3 days post bisection. Z-stack images were taken with the Andor Revolution XD spinning Disk confocal microscope using Andor IQ3 system at 200x magnification under 488 nm, 560 nm and DIC channels. 20% laser power was used at 488 nm and 560 nm channels to image all larvae. Immediately after imaging, coverslip was carefully picked up with a pipette tip. Embryos were transferred back to the plate with ASW and kept at 15°C until needed at 7 dpb.

Quantification of neurons and determination of colors

The Z-stack images were analyzed with FIJI. Quantification of green, red and yellow Sox^c+ cells was conducted manually in 3 healthy 3 dpb larvae. To reduce false positive from phagocytic immune cells, only the cells located on the ectoderm or epithelia of the regeneration leading edge were quantified. To determine the color of the cell, the cellular area of each colored cell and a background area with no Kaede signal were selected. The pixel values of 488 nm and 560 nm channels within the selected areas were measured and collected respectively. The background pixel value was subtracted from the cellular pixel value at each channel to generate the net pixel value. The ratio of net 560 nm pixel value over net 488 nm pixel value of each cell was calculated to define the three colored groups as follows: red cells have pixel ratio of 560/488 >5; yellow cells have pixel ratio of 560/488 between 1/5 and 5; green cells have pixel ratio of 560/488 < 1/5. Because the expression level Kaede varies between cells, the net pixel values differ dramatically. Therefore, the logarithm with base 10 of each net pixel value was used to generate a color plot for all labeled cells at the regeneration leading edge in the 3 selected regenerating larvae. Cells were plotted in three different groups.

2.4.2.2 Quantification of *de novo* green Sox^c+ cells at the regeneration leading edge

The green Sox^c+ cells at the regeneration leading edge were quantified manually in 7 larvae at 3 dpb using FIJI. The data were compared to the 2 dpf embryonic conversion data. The effect size was Cliff's delta and the mean of data. The confidence interval width was 95%. Two side p-value was calculated with the Brunner-Munzel test. For Cliff's delta comparison and Mann Whitney test for mean comparison. The data were

compared to the 7 dpf larval conversion data. Delta's cliff did not apply to these two groups. Instead, the means of the two groups were compared. The confidence interval width was 95%. Two side p-value was calculated with the Mann Whitney test.

2.4.2.2 Determine whether Sox^{c+} cells become neurons in regenerating larvae

Live imaging

The third live imaging session was performed at 7 dpb. Sample was prepared as described above. Z-stack images were taken with the Andor Revolution XD spinning Disk confocal microscope using Andor IQ3 system at 200x magnification under 488 nm, 560 nm and DIC channels. 20% laser power was used at 488 nm and 560 nm channels to image all larvae. Images were analyzed using FIJI. Colored cells with neural morphology were the Sox^{c+} neurons.

Double IF staining with anti-GFP and anti-serotonin

A new batch of culture was started and injected with Sox^c-GFP BAC following the protocol described above. Sorted embryos were cultured in artificial seawater at 15 °C. Larvae were fed lightly with *Rhodomonas lens* ad libitum at 4 dpf followed with fresh artificial seawater exchange on the same day to reduce autofluorescence from the food. Bisection was conducted on the sorted larvae at 7 dpf. Decapitated larvae were kept at 50 mm petri dish at 15 °C in ASW. The regenerating larvae were fixed at 7 dpb in 4% PFA in PBS with 0.1% Triton x-100 for 1 h. The double IF staining and imaging was performed as described in serotonin IF staining with the following modifications. Larvae

and regenerating larvae were incubated with 1:100 mouse anti-GFP (DSHB Hybridoma Product DSHB-GFP-12A6) and 1:250 rabbit anti-serotonin (Sigma), diluted in 3% BSA block, overnight at 4°C. Intact and regenerating larvae were then washed 6 times with PBS/0.1% Triton x-100, and incubated with 1:1000 anti-mouse alexa-fluor 488 and 1:1000 anti-rabbit alexa-fluor 568, diluted in 3% BSA block. Nuclear staining, washes was performed as described in serotonin IF staining. Intact and regenerating larvae were photographed with Zeiss 880 Laser Scanning Microscope at 200x magnification with 405 nm and 560 nm channels in Z-stack settings.

2.5 Double cell lineage tracing

2.5.1 Generation and examination of Sox1-Kaede BAC

The Sox1-Kaede BAC was generated following the protocol used to generate the Sox2-Kaede BAC. Injection of Sox1-Kaede BAC was conducted using the same method of Sox2-Kaede BAC injection. Injected zygotes were sorted at 24-48 hpf. Live imaging was then performed to examine the expression pattern of Kaede. Individual larva from 2 dpf, 4 dpf and 7 dpf sorted larval culture were loaded on the slides as described above in 70 µl of 15°C sea water. Z-stack images were taken with the Andor Revolution XD spinning Disk confocal microscope using Andor IQ3 system at 200x magnification with 488 nm and DIC channels. 13% laser power was used at 488 nm channel to image 2 dpf larvae. 4 and 7 dpf larvae were imaged under 20% laser power at 488 nm channel. Immediately after imaging, coverslip was carefully picked up with a

pipette tip. Embryos were transferred back to the plate with ASW and kept at 15°C until needed. Images were analyzed with FIJI to determine the expression pattern of Kaede.

2.5.2 Generation and examination of Soxc-Cardinal BAC

The Soxc-Cardinal BAC was generated following the protocol used to generate the Soxc-Kaede BAC. Injection of Soxb1-Kaede BAC was conducted using the same method of Soxc-Kaede BAC injection. Injected zygotes were sorted at 24-48 hpf. Live imaging was then performed to examine the expression pattern of Kaede. Individual larva from 4 dpf and 7 dpf sorted larval culture were loaded on the slides in 70 µl of 15°C sea water as described above. Z-stack images were taken with the Zeiss 880 Laser Scanning Microscope at 200x magnification with 633 nm and DIC channels. 40% laser power was used at 633 nm channel to image the 4 and 7 dpf larvae. Images were analyzed with FIJI to determine the expression pattern of Kaede.

2.5.3 Determine Soxb1 specification in regeneration

2.5.3.1 Injection, bisection and photo-conversion

Equivalent concentration of Soxb1-Kaede BAC and Soxc-Cardinal BAC was mixed in 10µl of injection buffer. The final total DNA concentration was at 5-10 ng/µl. Injection and sorting of embryos were performed as described above. Larvae were starved to avoid autofluorescence from algae *Rhodomonas lens*. Before photoconversion and bisection, multiple 35 mm labeled petri dish were prepares. Photoconversion was

conducted with a lightbox. The sorted larvae were collected in 20 μ l of cold sea water and released in one drop on a 35 mm petri dish. The petri dish was placed on the lightbox. Samples were Photoconverted with 395 nm laser of 100% power for 40 seconds followed by addition of 2 ml cold ASW to increase survival rate. Immediately after photoconversion, bisection was performed at the midline along the larval AP body axis on 7 dpf sorted larvae. The posterior larvae were next loaded individually on labeled slides, one larvae per coverslip. Z-stack images were taken at DIC, 488 nm (green), 560 nm (red) and 640 nm (pseudo color blue) channels with Andor Revolution XD spinning Disk confocal microscope using Andor IQ3 system. To image all injected larvae with consistent setting for comparison, 20% laser power was applied to 488 nm and 560 nm and 40% laser power was applied to 640 nm. After imaging, the coverslip was carefully picked up with a pipette tip. The larvae were transferred back to the same labeled individual plates with ASW and kept at 15°C until imaging 3 days later.

2.5.3.2 Live imaging at 3 dpb

The second imaging session for this batch was at 3 days post bisection. Z-stack images were taken with the Andor Revolution XD spinning Disk confocal microscope using Andor IQ3 system at 200x magnification under 488 nm (20% laser power, green), 560 nm (20% laser power, red), 640 nm (40% laser power, pseudo color blue) and DIC channels. Immediately after imaging, coverslip was carefully picked up with a pipette tip. Embryos were transferred back to the plate with ASW and kept at 15°C until needed at 7 dpb.

A more refined live imaging session was conducted to generate better quality images using the Zeiss 880 Laser Scanning Microscope at 20x objective and 40x objective with a few selected larvae presenting interesting phenotypes. Labeled slides and coverslips were prepared as described above. Before imaging, the selected 3 dpb larvae were kept in individual labeled 35 mm petri dish. 500 mM high salt sea water was prepared in another dish. Each regenerating larva was transferred with minimum ASW into the high salt sea water and treated with salt shock for 1-2 min to remove the cilia of the larvae for immobilization. The larva was quickly transferred back to cold ASW and left in the ASW for 10 s. Individual larvae were loaded on the slides in 70 μ l of 15°C sea water, one larva under one coverslip. The coverslip was gently pressed down if necessary to remove air from covered area and mechanically immobilize the larvae. Z-stack images were taken using 488 nm, 561 nm, 633 nm and DIC. Because these images were not used for quantification analyses, the setting of each channel was variant dependent on the larva being imaged. The laser power used for 488 nm was varied between 2-7%. The laser power used for 561 nm was varied between 0.5-2.5%. And the laser power used for 633 nm was varied between 7-40%.

2.5.4 Determine Sox^{b1+}/Sox^{c+} cell fates in regeneration

The third live imaging session was performed at 7 dpb. Z-stack images were taken with the Andor Revolution XD spinning Disk confocal microscope using Andor IQ3 system at 200x magnification under 488 nm, 560 nm, 640 nm and DIC channels. 20% laser power was used at 488 nm, 560 nm channels and 40% laser power was used at 640 nm to

image all double injected larvae. Images were analyzed using FIJI. Colored cells with neural morphology are the neurons differentiated from the labeled lineages.

Chapter 3: Embryonic genetic pathway controlling neurogenesis is recapitulated in regeneration.

3.1 Introduction

3.1.1 Neuronal gene markers

Despite the dramatically different body plans and developmental strategies observed in the animal kingdom, most animals (with the exception of sponges) possess nerve cells or neurons (Rakic 2009), a very important and conserved cell type. Identification of nerve cells can be challenging when the morphology of neurons does not present axial projections or long processes. Molecular identification of neurons is difficult due to the complex gene expression profile in neuronal cell types and lack of specific gene expressed in all and only neuronal cell types. It is shown that up to 70% of the genome can be expressed in a single nerve cell (Bucher and Anderson 2015). However, among extensive studies of various animals across Metazoa, scientists have identified many conserved neural gene markers expressed in primitive stem cells, subtypes of neural progenitors and populations of neurons. Through these studies, it was noticed that the molecular mechanisms controlling the generation of nerve cells is shared in Cnidaria and Bilateria.

Neurogenesis starts when ectodermal cells acquire the capability to generate neurons. This is marked by the expression of transcription factors from the Sex-determining

region Y-related HMG box (Sox) B family. SoxB genes privilege the ectodermal cell populations with neurogenic potential (Hartenstein and Stollewerk 2015). In sea star embryos, the onset of neurogenesis is characterized by the embryonic expression of gene *soxb1* in the ectoderm. The SoxB1 transcription factor is a neural stem cell marker that is highly conserved across Metazoa. It maintains the neurogenic ectoderm in a proliferative state, inhibiting the differentiation of neural cells (Bylund et al. 2003; Elkouris et al. 2011). In echinoderms, Soxb1 is expressed along the broad neurogenic ectoderm and is upstream of neural specification through Notch signaling (McClay et al. 2018). In cnidarian *Nemastodella vectensis*, SoxB transcription factors are expressed in epithelial neural progenitor cells that are key in neurogenesis (Rentzsch et al. 2017). In acoels, Soxb1 is expressed in the neoblast which gives rise to committed neural progenitors that migrate to form neurons (Hartenstein and Stollewerk 2015). In later branching animals, SoxB1 family includes transcription factors Sox1, 2 and 3. They display strong functional redundancy and are often co-expressed in neural stem cells in developing central nervous systems (Miyagi et al. 2009). Both the SoxB1 and Notch pathway play important roles in the proper establishment and maintenance of the central nervous system (Holmberg et al. 2008; Cimadamore et al. 2013).

Specification of ectodermal cells with neurogenic potential is then followed by the separation of neural stem cells from the ectoderm. They migrate, proliferate and differentiate. A marker for multipotent neural stem cells in sea star is the Soxc transcription factor. Soxc⁺ neural stem cells give rise to multiple types of neurons in larvae (Cheatle Jarvela et al. 2016). In sea urchins, Soxc⁺ cells are neural progenitors

located in the endo-mesoderm, restricted area of ectoderm and in the APD. The Sox^c+ cells give rise to Brn1/2/4+ neural progenitors which become post-mitotic neurons (Garner et al. 2016). Sox^c family includes Sox4, Sox11 and Sox12 in vertebrates. Likewise, Sox4 and Sox11 control the establishment of neuronal properties (Bergsland et al. 2006).

The LIM/Homeobox protein Lhx is a conserved neural progenitor marker. Lhx2 is expressed in neural progenitors and is required for the generation of serotonergic neurons in sea stars. Similarly, Lhx1/5 is necessary for the maintenance and regeneration of serotonergic neurons in planarians (Currie and Pearson 2013). In mouse, Lhx2 is required for forebrain development (Porter et al. 1997). In sea stars, Lhx2 is downstream of SoxB1 and Sox^c. Likewise, Sox4/11 transfected cells express LIM2 in mammals and chicks (Bergsland et al. 2006).

Taken together, animals possessing nerve cells share a common genetic toolkit that controls the formation of neurons. This suggests that understanding how this genetic toolkit is re-wired or reprogrammed in the process of neural regeneration in the sea star may be very important to decoding regenerative mechanisms in other animals as well. It also holds great potential to be adapted in human regenerative therapies for neural degenerative diseases.

3.1.2 Serotonergic neurogenesis in sea star larvae

To determine how the nervous system, especially the serotonergic dorsal ganglia, is regenerated, it is key to understand the biology of neurogenesis. Fortunately, sea star larvae have been well established to answer important developmental questions (Hinman et al. 2003; McCauley et al. 2010; McCauley et al. 2013; Hinman and Cheatle Jarvela 2014; McCauley et al. 2015; Cheatle Jarvela and Hinman 2015; Cary et al. 2017; Cary et al. 2018; Cary, Cameron, et al. 2019), including generation of neurons (Yankura et al. 2010; Yankura et al. 2013; Cheatle Jarvela et al. 2016). Their nervous system and neurogenesis pathways have been carefully characterized. In sea star bipinnaria, the nervous system consists of the dorsal ganglia, which is mainly composed of serotonergic neurons, neurons associated with the two ciliary bands and neurons associated with the oral organs. The serotonergic neurons are first formed at the anteriormost apical pole domain (APD) in 3 day old embryos and move posteriorly as embryos grow. In bipinnaria, serotonergic neurons in the dorsal ganglia are located bilaterally on the dorsal side.

The APD GRN that regulates the formation of dorsal ganglia is described as follows. The embryonic, pan-neurogenic ectoderm expresses the neural stem cell marker *Soxb1*. From this broad neurogenic ectoderm, the neural stem cells expressing gene *soxc* are partitioned, distributed in a “salt and pepper” pattern along the anterior-posterior (AP) axis on the entire ectoderm (Yankura et al. 2010). The anterior patterning genes *foxq2* and *rx* are both expressed at the APD. These two transcription factors are required for the progression of *Soxc*⁺ neural stem cells. With the presence of FoxQ2

and Rx transcription factors, *soxc*⁺ neural stem cells located at the anterior undergo asymmetric divisions and progress to become *lhx2*⁺ restricted neural progenitors. Progression of *lhx2*⁺ progenitors also requires regulation of Foxq2 and Rx. After asymmetric divisions, *lhx2*⁺ progenitors give rise to post-mitotic neurons expressing *elav*. These post-mitotic neurons will produce serotonin when they mature. *Soxc*⁺ cells are multipotent neural stem cells giving rise to more than just serotonergic neurons (Cheatle Jarvela et al. 2016).

3.1.3 General Introduction

In this chapter, we begin to determine the mechanisms of neural regeneration. We characterize the biological stages of the regeneration of larval nervous system. And to understand whether the embryonic neurogenic pathway is involved in the regenerative processes, we examine the expression pattern of genes in the APD GRN. We also interrogate the proliferation patterns and gene expression trajectory of neurogenic cells in regenerating larvae.

3.2 Results

3.2.1 Sea star larvae regenerate the nervous system.

3.2.1.1 Posterior larvae regenerate the missing halves in two weeks.

Sea stars have extraordinary regenerative capacity. Bipinnaria undergo WBR and are able to regenerate all types of tissues including the nervous system. To test this, we performed larval surgeries that bisect the larvae across the midline along the AP body axis (**Fig 3. A, B**) and examined the regeneration of serotonergic neurons. The interest of this study is the regeneration of the anterior dorsal ganglia in the posterior larvae. Therefore, we first characterized the morphology of posterior regeneration (**Fig 3.C**).

Following amputation, the wound opening is sealed. At 3 day-post-bisection (dpb), the mouth has been regenerated, allowing for feeding. The regeneration leading edge, an extruding sphere, is formed at the regenerating anterior end. Meanwhile, the overall size and length of the posterior larva begin to differ from the 1 dpb larvae as a result of tissue re-proportion. By 7 dpb, at the anterior side of regenerating larvae have formed a primitive “head” with the regenerated pre-oral ciliary band. After regenerating for 10-14 day, the remaining posterior of the larva is re-proportioned while the anterior structure of the larva is regenerated (**Fig 3.C**).

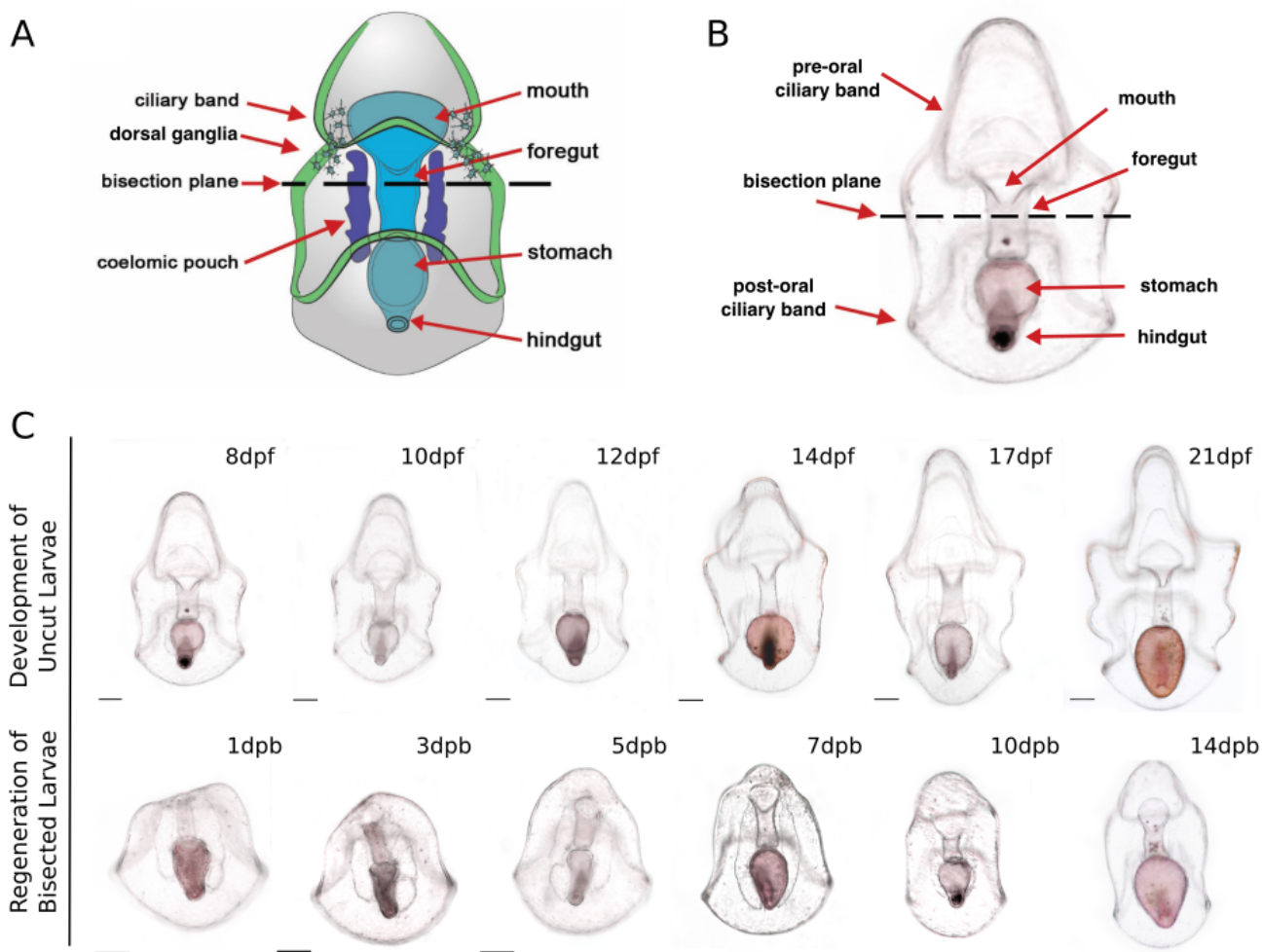


Fig 3. Sea star larvae undergo whole-body regeneration (WBR)

(A) A schematic of sea star larva. (B) A 7dpf sea star larva before bisection. Bisection is performed at the midline of the larvae along the anterior-posterior (AP) body axis through the foregut. (C) Morphology of posterior sea star regeneration. The panel on the top is the morphology of uncut control larvae at corresponding time points. The panel on the bottom is the morphology of regenerating posterior larvae. By 3 dpb, the wound is sealed and the mouth is reformed. In larvae from 3-5 dpb, a regeneration leading edge is formed at the anterior. By 7 dpb, a primitive anterior structure is formed in larvae. A segmented

posterior regenerates the anterior within 14 days. Scale bar: 100 μm . Dpf: day-post-fertilization; dpb: day-post-bisection

3.2.1.2 Sea star larvae regenerate the dorsal ganglia after complete removal.

The dorsal ganglia is featured by the distinctive clusters of serotonergic neurons. In 7 dpf larvae, serotonergic neurons are mainly detected in the dorsal ganglia and the lower lip of the mouth (**Fig 4. D'-E'**). The distribution of serotonergic neurons is also supported by the expression patterns of the postmitotic neuron marker *elav* (**Fig 6.K**). Serotonergic neurons in the dorsal ganglia present big cell bodies with long axonal processes. In comparison, serotonergic neurons on the lower lip of the mouth have much smaller cell bodies and shorter axonal processes. The genetic program controlling the formation of foregut associated serotonergic neurons remains unclear. However, they are likely to arise from the endoderm instead of the ectodermal APD (Wei et al. 2011). Therefore, our studies only focus the serotonergic neurons in the dorsal ganglia.

In 7 dpf larvae, the dorsal ganglia are completely removed (**Fig 4.F'-f**) through bisection. In all bisected posterior larvae, 0/45 show any remaining dorsal ganglia serotonergic neurons. 5/45 larvae show remaining small serotonergic neurons at the esophagus. This indicates that bisection across the foregut successfully removes all big serotonergic neurons in the dorsal ganglia. Interestingly, these serotonergic neurons are reformed at the regenerating leading edge within 5-7 days after the complete removal. In 5 dpb larvae, 8/14 display serotonin neurons at the regenerating leading edge (**Fig 4.G'-g**). In 7 dpb larvae, serotonergic neurons are found in 12/15 regenerating larvae at the anterior (**Fig 4.H'**). These serotonergic neurons all present clear neural morphology with axonal processes (**Fig 4.h**). Three weeks after decapitation, the regenerated

serotonergic neurons are bilaterally patterned at the dorsal side of the regenerating larvae, resembling the dorsal ganglia structure found in intact larvae (**Fig 4.I'-i**).

3.2.1.3 Sea star larvae regenerate the anterior ciliary bands

Besides the serotonergic neurons, bisection also removes the pre-oral ciliary band. In intact larvae, the pre-oral ciliary band outlines the anterior of the larva, extending laterally towards the anterior end (**Fig 4. A'-AA**). The neurons are associated with the ciliary bands and are distributed along the ciliary bands, shown by both synaptotagmin staining and the expression pattern of *e/av* (**Fig 6.K**). In 8 dpb posterior larva, a shorter, regenerated pre-oral ciliary band is detected outlining the primitive anterior structure (**Fig 4.B'-CC**). Together with the evidence of dorsal ganglia reformation, this demonstrates that the sea star larvae are capable of regenerating their larval nervous system, a structure and cell types that are extremely difficult to regrow in higher organisms.

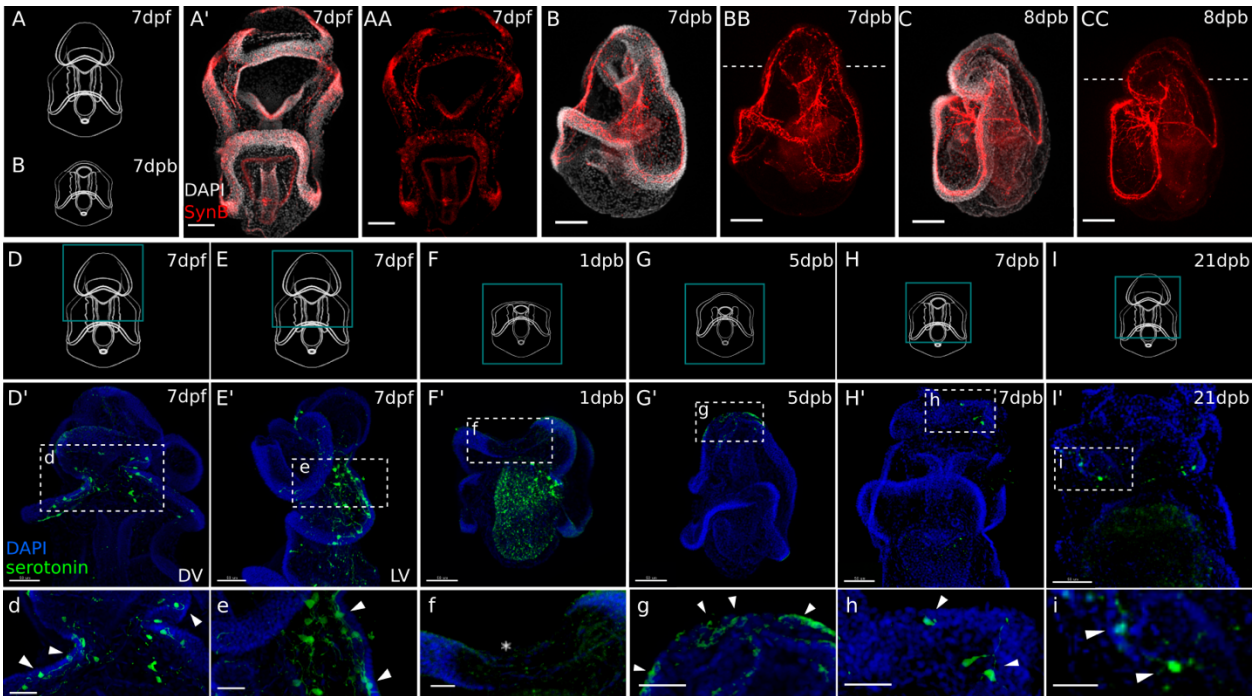


Fig 4. Regeneration of the larval nervous system

(A-B) Schematics of sea star larvae at the developmental stages corresponding to larvae in (A'-CC). (A'-CC) Immunofluorescence (IF) Staining with anti-synaptotagmin B (1e11). (A'-AA) Neurons are distributed at the pre-oral ciliary band, post-oral ciliary bands and along the mouth. (B-CC) Regenerated nervous system. (B-BB) Strings of nerve cell processes are projected from post-oral ciliary bands to the oral area. Bisection was performed at the dashed line. Above the dashed line is the regenerated anterior with neurons projecting to the oral area. (C-CC) A lateral view of regenerating larva. Above the dashed line is the regenerated tissue with reformed pre-oral ciliary band lining the primitive anterior. (D-I) Schematics of sea star larvae at the developmental stages corresponding to larvae in (D'-I') and (d-i). (D'-I') IF Staining with anti-serotonin shows the regeneration of the serotonergic dorsal ganglia. (d-i) The amplified view of highlighted

area with dashed-line box in (D'-I'). (D') The serotonergic neurons are located bilaterally in uncut larvae, on the dorsal side as shown in (E'). (d-e) Attached to the ectoderm, serotonergic neurons present axonal processes. (F'-f) Bisection completely removes the serotonergic neurons. (G') BY 5 dpb, serotonergic neurons are formed at the regeneration leading edge with clear neural morphology as shown in (g). (H') By 7 dpb, regenerated serotonergic neurons with mature neural morphology (h) are located at the lateral side of the regenerated anterior. (I'-i) Regenerated serotonergic neurons are bilaterally located to reform the dorsal ganglia by 21 dpb. Arrowheads highlight the serotonergic neurons. The asterisk shows missing neurons. Scale bar in (A-CC,D'-I'): 50 μm , in (d): 30 μm , in (e-i): 25 μm . Dpf: day-post fertilization; dpb: day-post bisection.

3.2.2 Reconstruction of Anterior-Posterior body axis

Previous studies have found that following early wound responses, the AP axial patterning genes are up-regulated in the regenerating larvae to recover the anterior-posterior positional information (Cary, Wolff, et al. 2019). Our results support this finding. In 3 dpb larvae, the conserved embryonic anterior patterning gene *foxq2* is expressed at the anteriormost leading edge, resetting the anterior identity (**Fig 5.A-B**). At 5 dpb, the expression of *foxq2* extends from the leading edge to the dorsal side of the primitive “head” of the regenerating larvae (**Fig 5.C-D**). Another embryonic anterior patterning gene *six3* is also expressed at anterior domain in the regenerating larvae (**Fig 5. E-H**). Similar to the AP patterning in embryos, *six3* expression domain is broader compared to the one of *foxq2*. On the other hand, Wnt family genes are engaged in posterior patterning in embryos, separating the ectoderm from the endo-mesoderm. In regeneration, *wnt3* is expressed in the *foxq2*-free posterior domain in 3 dpb larvae (**Fig 5,I-K**).

Taken together, the expression patterns of these conserved AP axial genes suggest the reconstruction of AP body axis. Axial reformation is a common mechanism shared by many organisms capable of WBR following wound detection. This homologous process observed in sea star larval regeneration demonstrates that the ontogeny of sea star WBR is not an evolutionary outlier. Therefore, the strategies identified in sea stars have great potential to be adapted to other model systems.

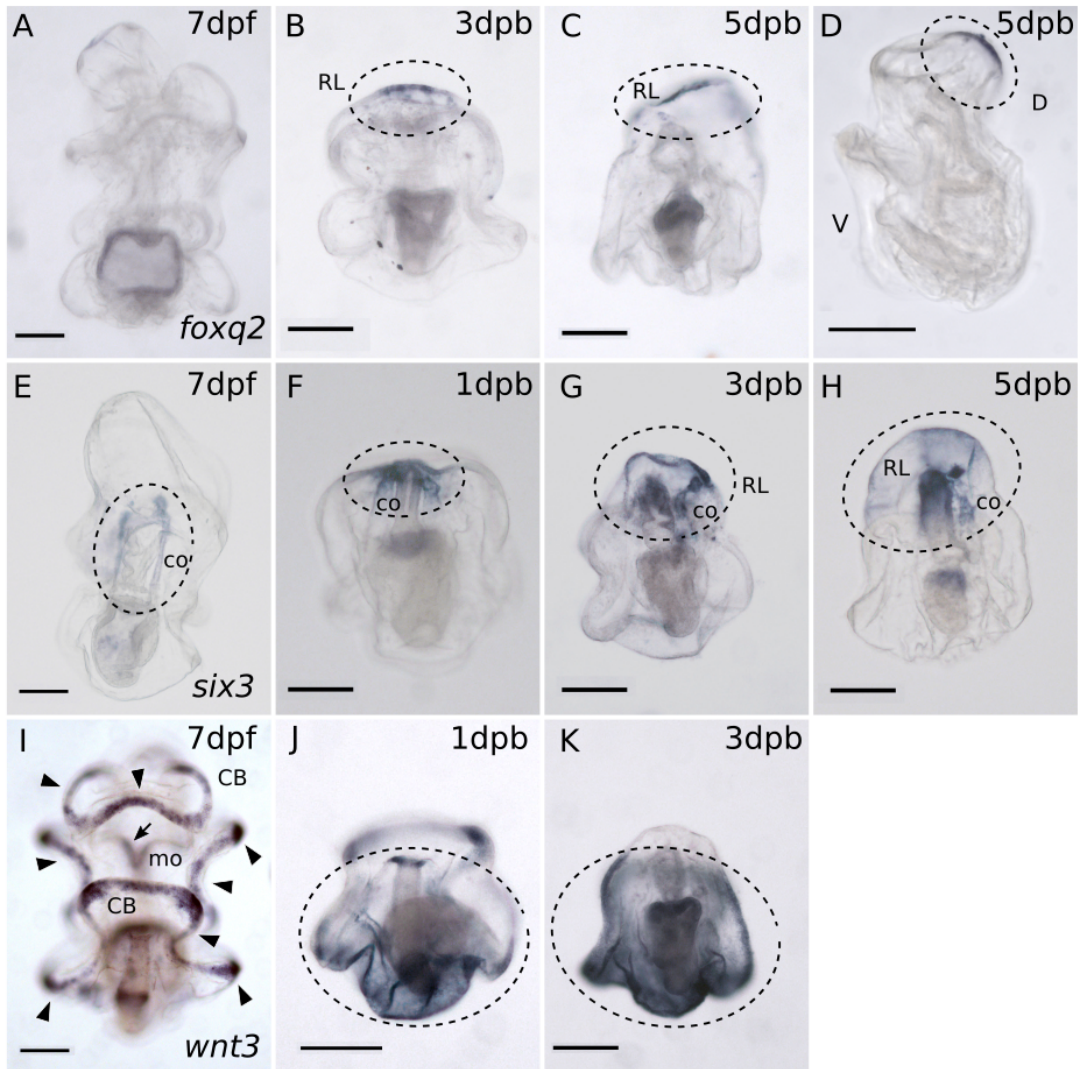


Fig 5. Whole-mount *in situ* hybridization (WMISH) results show the reconstruction of AP body axis.

(A-D) WMISH of anterior patterning gene *foxq2*. (A) *Foxq2* expression is barely detectable in intact larvae. Upon decapitation, (B) *foxq2* is first expressed in the anteriormost regeneration leading edge at 3 dpb. (C) *Foxq2* expression remains concentrated at the regeneration leading edge. (D) is a lateral view of a regenerating larva. The expression of *foxq2* is detected on the dorsal anterior. (E-H) WMISH of

anterior patterning gene *six3*. (E) *Six3* is expressed at the bilaterally located coeloms in uncut 7 dpf larvae. Upon decapitation, (F) *Six3* expression is immediately detected at the wound ectoderm and the regenerating coeloms in 1 dpb larva. (G-H) *Six3* expression extends to the entire regenerated anterior. (I-K) WMISH of posterior patterning gene *wnt3*. (I) In intact larvae, *wnt3* is expressed in the ciliary bands, marked by black arrowheads. It is also expressed in the mouth ectoderm indicated by the black arrow. Upon decapitation, (J) *wnt3* is expressed in the posterior domain. (K) The expression extends to the entire *foxq2*-free posterior domain. Gene expression is highlighted in circles with black dashed line. Scale bar: 100 μ m. RL, regeneration leading edge; co, coeloms; mo, mouth; CB, ciliary band; D, dorsal; V, ventral.

3.2.3 Expression patterns of genes from the embryonic neuronal pathway in regenerating larvae

The regeneration of serotonergic neurons following complete removal of cell types raises a very intriguing question: where do the reformed neurons come from? The regenerative strategies used in other models inspire us to hypothesize that there is a *Soxc*⁺ neural stem cell lineage present in the larvae that are used to regenerate serotonergic neurons. *Soxc*⁺ multipotent stem cells give rise to differentiated serotonergic neurons in embryos through the *lhx2* genetic pathway (**Fig 2.C**). We speculate that if present in the larvae, *Soxc*⁺ cells will contribute to the regenerated apical organ through a similar *lhx2* genetic pathway. Alternatively, the regenerated neurons may arise from totipotent or pluripotent stem cells through another genetic pathway that does not require the expression of *Soxc*. Another possibility is that the neurons are trans-differentiated from other cell types. However, both of these alternatives are difficult to examine in detail due to the limited molecular mechanisms known in sea star regeneration.

To interrogate whether *Soxc*⁺ neural stem cells are involved in regenerating the dorsal ganglia, we characterized the expression patterns of genes in the APD GRN with proliferation profiling. *Soxb1* is expressed maternally in the oocytes. Although it is not confirmed by gene perturbation studies, *Soxb1*, as a Yamanaka factor, is almost certainly upstream of *soxc* expression. Therefore, we started by examining the expression pattern of *soxb1* over the course of regeneration.

3.2.3.1 Immediate emergence of *Soxb1*+ proliferating cells at the wound site resembles the embryonic state.

Compared to the embryo stage, *soxb1* is expressed at a lower level on the ectoderm of larvae. The expression of *soxb1* is concentrated in the ciliary bands (**Fig 6.E-e, Fig 7.A**). A small proportion of *soxb1*+ cells in the ciliary bands are also proliferative, suggesting that *soxb1*+ cells may be involved in ciliary band expansion and larval growth (**Fig 6.E-e**). Strikingly, upon bisection, *soxb1* expression is dramatically up-regulated and concentrated at the wound site (**Fig 6. F-f, Fig 7. B**). A few *soxb1*+ cells at the wound site are in cell cycle. At 3 dpb, the concentrated expression of *soxb1* extends to the entire regeneration leading edge. Meanwhile, cell proliferation is drastically upregulated at the anterior side. Many of these dividing cells have *soxb1* expression (**Fig 6. G-g, Fig 7.C**). At 5 dpb, *soxb1* expression remains concentrated along the regeneration leading edge. Likewise, *soxb1*+ cells are actively dividing (**Fig 6. H-h, Fig 7.D**). Compared to 1 dpb larvae, the cell proliferation pattern has shifted from the posterior ciliary band to the regeneration leading edge. This is consistent with previous findings (Cary, Wolff, et al. 2019).

Taken together, the gene of Yamanaka factor and neural stem cell marker, *soxb1* is abruptly up-regulated at the wound site in response to decapitation. The expression remains concentrated at the regeneration leading edge as the cell proliferation pattern shifts to the anterior domain. During this process, *soxb1*+ cells are constantly undergoing cell division at the anterior domain. The proliferating *soxb1*+ cells are distributed within *soxb1* expression domain and *soxb1* expression is highly enriched at

the regeneration leading edge, this suggests that their daughter cells still express *soxb1*.

The regeneration leading edge is concentrated with the expression of *soxb1*. In sea star development, there is another time window when *soxb1* is highly enriched: the early embryo stage. In early embryos, yamanaka factors including *soxb1*, *klf13* and *myc* are all highly expressed, representing the totipotent or pluri-potent capacity. *Soxb1* expression at the regeneration leading presents similar enrichment of Yamanaka factor. This suggests that upon bisection, the wound site activates early embryo gene expression possibly through signaling enriched in early wound responses like the MAPK signaling pathway. This resets the regeneration leading edge to a pluripotent embryo state.

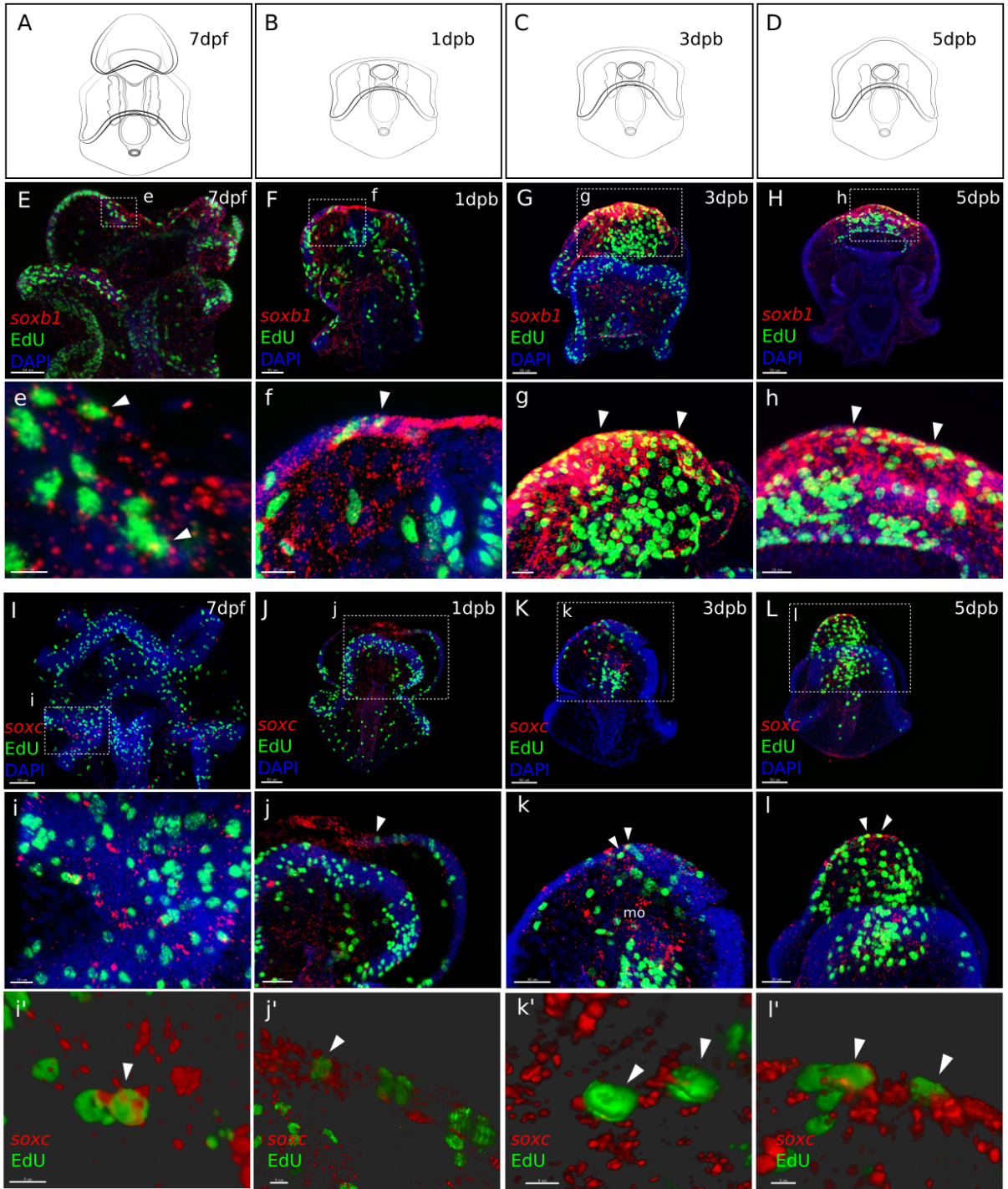


Fig 6. EdU labeled fluorescent *in situ* hybridization (EdU-FISH) results show that *soxb1*⁺ cells and *soxc*⁺ cells are proliferative at the regeneration leading edge.

(A-D) Schematics of sea star larvae at stages corresponding to each column. (E-H) EdU-FISH of gene *soxb1*. (e-h) Amplified view of the boxed area in (E-H). (E) *Soxb1*⁺ cells are detected in the ciliary band. Some of these cells are in cell cycle as shown in (e). (F) Upon bisection, *soxb1*⁺ cells are highly concentrated at the wound site and later in (G-H) at the regeneration leading edge. Throughout the course, *soxb1*⁺ cells consistently undergo cell cycles (f-h). (I-L) EdU-FISH of gene *soxc*. (i-l) Amplified view of the boxed area in (I-L). (l) *Soxc*⁺ cells are detected in the ciliary band. Some of these cells are in cell cycle as shown in (i). (J) Upon bisection, *soxc*⁺ cells are detected at the wound site and later in (K-L) at the regeneration leading edge including the mouth. Throughout the course, *soxc*⁺ cells consistently undergo cell cycles (j-l). (i'-l') 3D views of EdU⁺ *soxc*⁺ cells highlighted in (i-l), indicated by white arrowheads. This shows clear double detection of EdU and *soxc*: the EdU⁺ nucleus is surrounded by *soxc* signals. Scale bar in (E-H) and (I-L): 50 μm ; scale bar in (e): 10 μm ; (f-h): 20 μm ; (i): 10 μm ; (j-k): 20 μm ; (l): 30 μm ; (i'-l'): 5 μm . Dpf: day-post fertilization; dpb: day-post bisection; mo, mouth.

3.2.3.2 *Soxc*⁺ neural stem cells appear at the wound site consistently undergoing cell cycle

Soxc⁺ cells are multipotent neural stem cells in embryos. In larvae, *soxc* expression is found at the ciliary bands, in the dorsal ganglia and in the mouth (**Fig 6.I, Fig 7.E**). A small proportion of the *soxc*⁺ cells are in cell cycles, suggesting that *Soxc*⁺ stem cells may be required for maintenance of the nervous system (**Fig 6.i-l'**). Similar to *soxb1*, *soxc* expression is observed at the wound site following bisection. 3-4 *soxc*⁺ cells at the wound are in cell cycles (**Fig 6. J-j', Fig 7.F**). In 3 dpb larvae, *soxc* expression extends to the regeneration leading edge where more *soxc*⁺ cells undergo divisions. *Soxc* expression is also detected in the regenerating mouth where a few *soxc*⁺ cells proliferate (**Fig 6. K-k', Fig 7.G**). In 5 dpb larvae, *soxc* expression is concentrated to the regenerating anterior with some cells proliferating (**Fig 6. K-k', Fig 7.H**).

These data show that *soxc* expression domain is similar to *soxb1* domain in the regenerating anterior. There are also population of *soxc*⁺ cells undergoing cell cycles in the regeneration leading edge. However, this population is much smaller compared to the group of proliferating *soxb1*⁺ cells. Based on these results, it is possible that *soxc*⁺ cells are downstream of or specified from *soxb1*⁺ cells at the regeneration leading edge. Our result also shows that *soxc*⁺ cells have the potential to maintain neural stem cell state in regeneration and give rise to the regenerated serotonergic neurons.

3.2.3.3 *Soxc*⁺ cells progress to become *lhx2*⁺ neural progenitor cells which give rise to post-mitotic neurons.

To understand whether the regenerative *soxc*⁺ cells enter the serotonergic genetic pathway, we next examined the expression pattern of *lhx2* and *elav* in the course of regeneration. *Lhx2* is expressed in the restricted neural progenitors in embryos. In larvae, it is expressed in a few cells in the dorsal ganglia (**Fig 7.I**). Following bisection, the expression of *lhx2* is restored at 5-7 dpb in dispersed cells at the regenerating leading edge (**Fig 7.J**). At this time of regeneration, a few *lhx2*⁺ cells are proliferating in the regenerating anterior. Similarly, the expression of post-mitotic neural marker *elav* is also restored at the regenerating anterior at 5-7 dpb (**Fig 7.L**). Moreover, serotonergic neurons are also reformed at 5-7 dpb at the regenerating anterior. Thus it is likely that *lhx2* is involved in regenerating the serotonergic neurons.

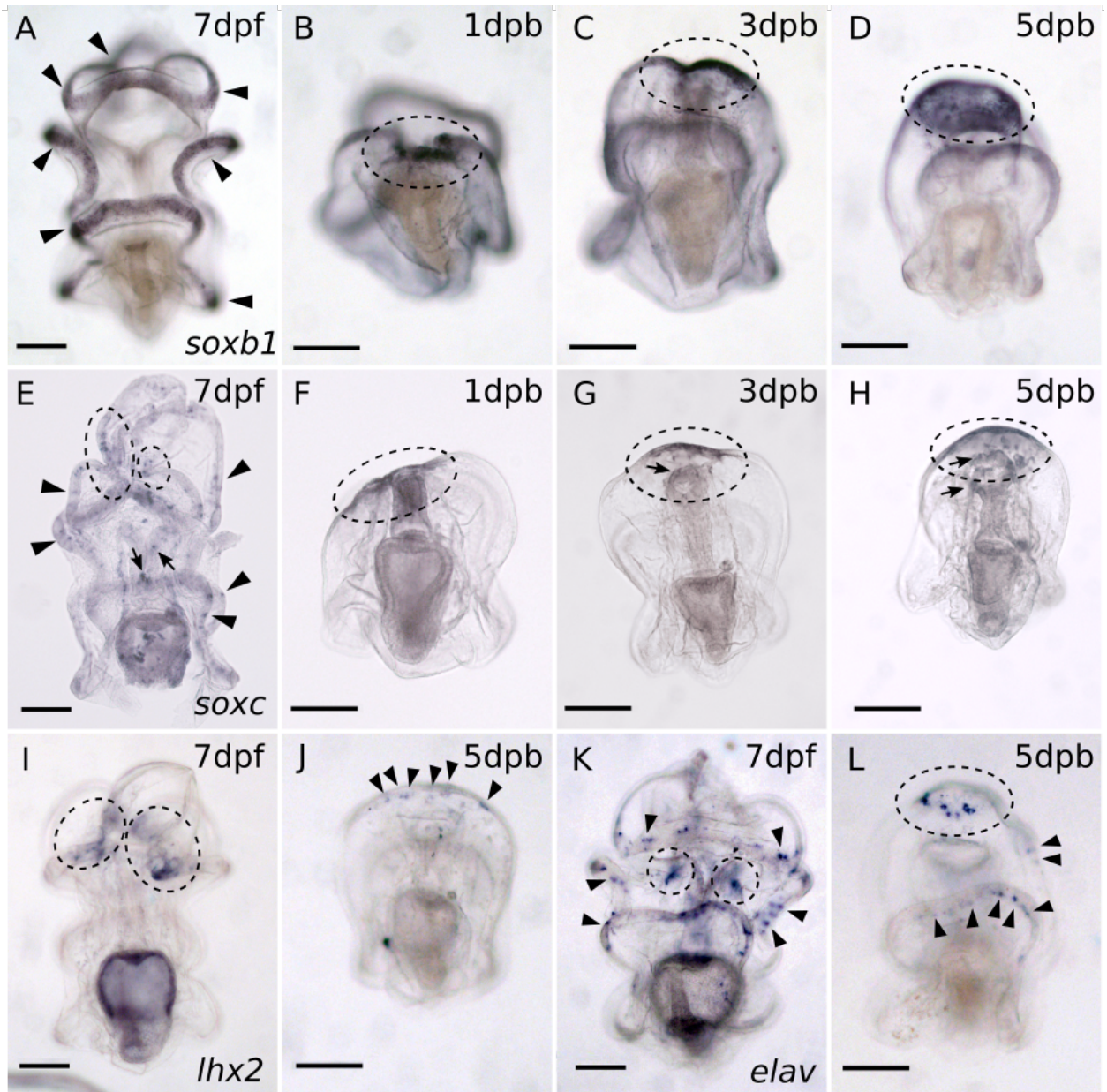


Fig 7. WMISH of genes in APD associated GRN

(A-D) WMISH of gene *soxb1*. (A) In intact larvae, *soxb1* expression is detected in the ciliary band, indicated by the black arrowheads. (B) Upon bisection, *soxb1* is expressed at the wound site and then at the regeneration leading edge as shown in (C-D). (E-H) WMISH of gene *soxc*. (E) In intact larvae, *soxc* expression is detected in the ciliary band,

indicated by the black arrowheads, and in the mouth and foregut, marked by the arrows. *Soxc* is also expressed in the dorsal ganglia, highlighted with black circles. (F) upon bisection, *soxc* expression is detected at the wound site and then in (G-H) at the regeneration leading edge, indicated by circles. In regenerating larvae, *soxc* is also expressed in the oral cells, arrows in (G-H). (I-J) WMISH of gene *lhx2*. (I) *Lhx2* is expressed at the dorsal ganglia in larvae. (J) In regenerating larvae, *lhx2* expression is first detected at 5 dpb at the regeneration leading edge. (K-L) WMISH of gene *elav*. (K) Post-mitotic neuron marker *elav* is expressed along the ciliary bands (black arrowheads) and the dorsal ganglia (circles). (L) In 5 dpb regenerated larvae, *elav* expression is detected at the regenerated (circle) and remains in the post-oral ciliary band (arrowheads). Scale bar: 100 μm . Dpf: day-post fertilization; dpb: day-post bisection.

To determine the trajectory of gene expression, we applied double FISH using probes of *soxc*, *lhx2* and *elav*. In 5 dpb larvae, *soxc/lhx2* co-expression is found in cells located at the lateral sides of the regeneration leading edge (**Fig 8. C**). At 5 dpb, cells coexpressing *lhx2* and *elav* are also observed at the regeneration leading edge (**Fig 8. D**).

Overall, these data show that *soxc*⁺ cells located at the lateral leading edge give rise to *lhx2*⁺ cells. And the *lhx2*⁺ cells at the leading edge become post-mitotic neurons expressing *elav*. Based on the time window during which these neurons are formed and their locations, it is highly likely that the *lhx2*⁺ progenitor cells at the leading edge give rise to the serotonergic neurons. The gene expression trajectory in regeneration resembles the genetic pathway used in serotonergic neurogenesis.

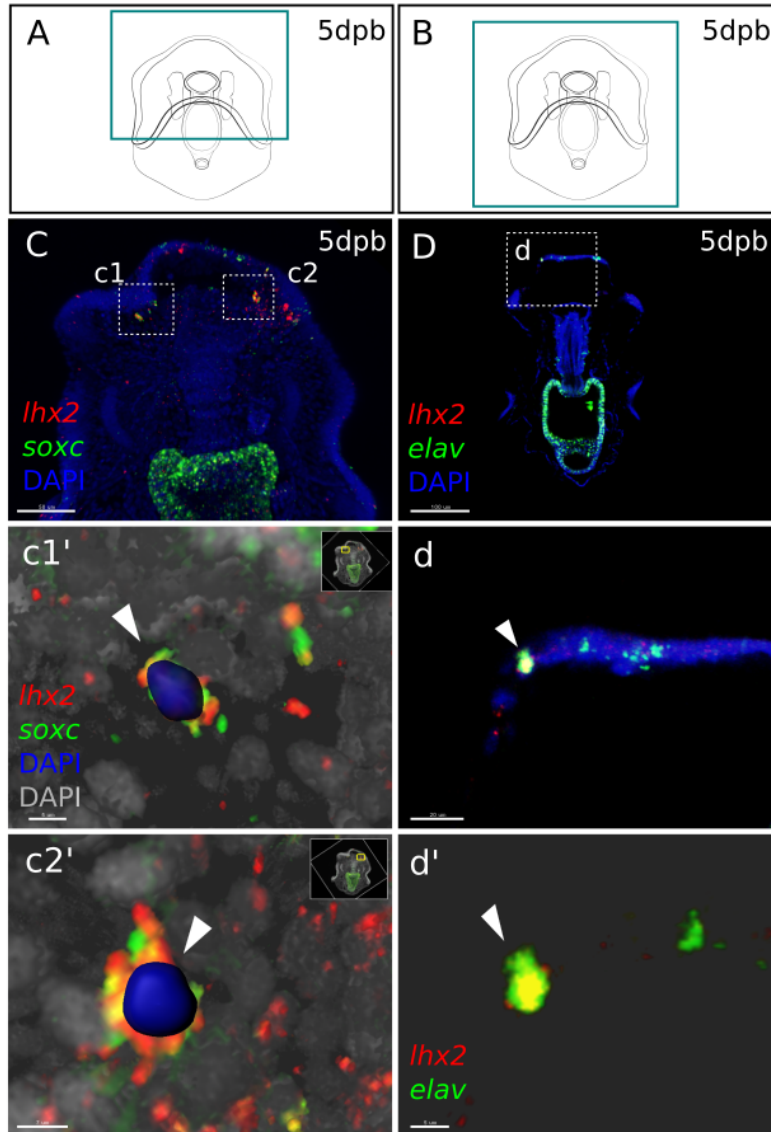


Fig 8. Double fluorescent *in situ* hybridization (FISH) shows the recapitulation of APD gene expression trajectory.

(A-B) Schematics of larvae at the regeneration stages corresponding to each column.
 (C) In 5 dpb larvae, *soxc* and *lhx2* are co-expressed in cells at the lateral regeneration leading edge. Scale bar: 50 μ m. (c1'-c2') show the 3D reconstructed view of boxed areas c1 and c2. In the highlighted cells (arrowheads), a nucleus labeled with DAPI is

surrounded by *lhx2* and *soxc* signals, indicating convincing co-expression in the same cell. Scale bar in (c1): 5 μm ; (c2): 7 μm . (D) In 5 dpb larvae, *lhx2* and *elav* are co-expressed in cells at the lateral regeneration leading edge, scale bar: 100 μm . This is amplified in (d), scale bar: 20 μm . (d') shows the 3D reconstructed view of the cell marked by arrowhead in (d), scale bar: 5 μm . Dpb: day-post-bisection.

3.3 Conclusion and discussion: A model to be tested for neural regeneration

3.3.1 summary

To conclude, we have characterized the regeneration of larval nervous system.

Following bisection which completely removes the dorsal ganglia, posterior larvae regenerate their anterior structures in 12 days. More quickly, they regenerate the serotonergic neurons at the lateral side of the anterior in 5-7 days post bisection. These serotonergic neurons can be correctly patterned to form regenerated dorsal ganglia by 3 weeks post amputation. The removed pre-oral ciliary band is also reformed at the regenerating anterior.

Following decapitation, the anterior-posterior body axis is reconstructed. We determined the expression patterns of highly conserved AP patterning genes. Similar to the embryo state, the anterior patterning gene *foxq2* is expressed at the anteriormost domain.

Another anterior gene *six3* is expressed in the regenerating anterior, broader than the *foxq2* domain, consistent with the embryonic expression pattern. Posterior gene *wnt3* is expressed broadly in the posterior end exclusively free from the *foxq2* domain. Previous work has shown the quantitative expression levels of AP patterning genes are upregulated in regeneration (Cary, Wolff, et al. 2019). This evidence confirms that the AP body axis is reformed in regenerating larvae.

We have examined the cell proliferation patterns and the expression patterns of genes governing serotonergic neurogenesis at different time points during regeneration. *Soxb1* and *soxc* are immediately expressed at the wound site and later broadened to the regeneration leading edge. The *Soxb1* expression domain is broader than *soxc* expression domain. Both *soxb1*⁺ cells and *soxc*⁺ cells are dividing at the regenerating anterior consistently over the course of regeneration. Later, *soxc*⁺ cells progress to become *lhx2*⁺ progenitor cells at the lateral side of the regeneration leading edge. And the *lhx2*⁺ cells give rise to post-mitotic neurons expressing *elav*.

3.3.2 Recapitulation of the genetic pathway controlling neurogenesis

In embryos, serotonergic neurons arise from the *soxc*⁺ stem cells through the *lhx2*⁺ regulatory pathway. And the embryonic *soxc*⁺ stem cells are partitioned from the *soxb1*⁺ neurogenic ectoderm. In regenerating larvae, *soxb1*⁺ wound ectoderm is highly proliferative and *soxb1* may be upstream of *soxc* expression. At the lateral sides of the dorsal ganglia, *soxc*⁺ cells give rise to *lhx2*⁺ progenitor cells which become post-mitotic neurons that are very likely to be the serotonergic neurons.

From this comparison, the *soxc-lhx2* and *lhx2-elav* progression in the embryonic neurogenesis is reapplied to neural regeneration. In addition, the high expression of yamanaka factor *soxb1* in early embryos is recapitulated in the regeneration leading edge. Extensive *soxb1*⁺ cell proliferation in regeneration also resembles the early embryo state. However, direct evidence showing that *soxc*⁺ cells make neurons in regeneration is still lacking. Also, it remains unknown where these *soxc*⁺ cells are

derived. Further study is needed to decide whether the *soxc*+ cells at the regeneration leading edge are partitioned from the *soxb1*+ cells.

3.3.3 Model

Based on the data from this chapter, we proposed a model that holds potential to delineate the sources of regenerated neurons (**Fig 9**). In the next two chapters, we tested and completed this model.

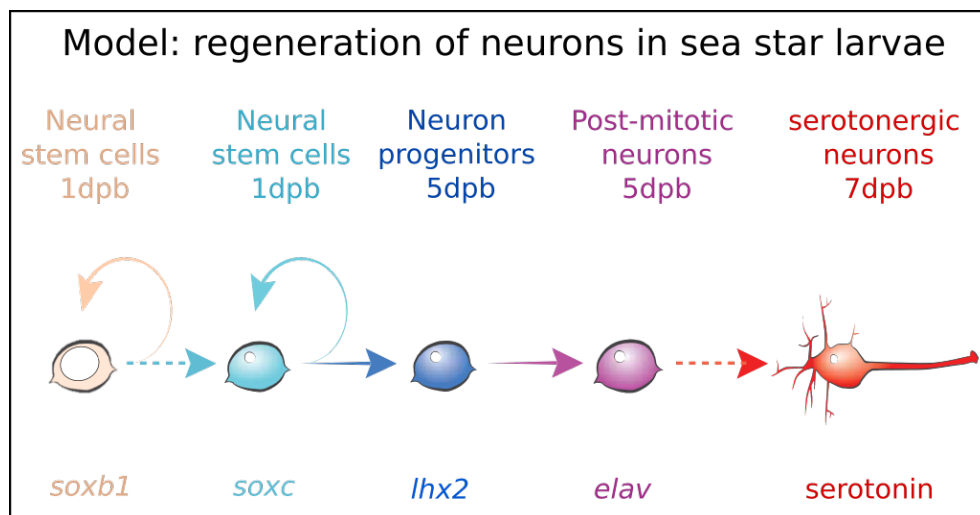


Fig 9. A proposed model for the regeneration of neurons in sea star larvae.

Chapter 4: Embryonic neural stem cell lineage is re-used to form the serotonergic neurons

4.1 Introduction

4.1.1 General introduction

In this chapter, we tested the model proposed in the previous chapter. Specifically, we focused on determining whether *Soxc*⁺ cells regenerate neurons and further understand the sources of the neurogenic cells in regeneration. In order to tackle this problem, a reliable system for cell lineage tracing was needed. Therefore, we generated an important, powerful tool that can systematically track the lineage of *Soxc*⁺ cells and differentiate between developmental lineage and regeneration lineage. The generation and testing of this molecular tool, the *Soxc*-Kaede BAC construct is described in this chapter. Then we took advantage of this method to transgenically label and track the *Soxc*⁺ lineage and successfully identify one source of the regenerated serotonergic neurons.

4.1.2 Methods for cell lineage tracing

One of the most challenging tasks in constructing a model for tissue formation is to know the history of the cells of interest. Echinoderms have become a model system to understand the gene regulatory networks (GRNs) controlling tissue formation in part

because the early cell lineages are stereotypic and well defined. The later larval stages present greater challenges because there are more cells and greater cell migrations. It is critical however that we know the initial state of the GRN in cells that contribute to new tissues so that we can establish how changes in GRNs are affected.

It is a significant challenge in developmental biology to be able to trace lineages over time in complex tissue environments. To trace cell lineage, cells of interest are labeled at a time point, the progeny of the labeled cells are revealed at a later time point. Common lineage tracing strategies are based on either visualization of cell lineage or computational analyses (Hsu 2015). Computational analyses are performed to construct cell lineage when the labeled cells are pooled for sequencing. With the development of elevated single cell sequencing technology, this tracing strategy becomes increasingly powerful (Gerber et al. 2018). Visualization strategies combine microscopic imaging with molecular labeling which requires the expression of a form of detectable biosensors, for example, fluorescent proteins (Tumbar et al. 2004), dyes (Kugelberg et al. 2005), nucleotide analogs like BrDU and EdU (Hsu et al. 2011), etc. These lineage tracing strategies are greatly empowered by advancement of transgenic labeling technologies including cre-lox based strategies (Wang et al. 2012; Beckervordersandforth et al. 2014), Cre and Flip based recombination (Jensen et al. 2008), CRISPR genome editing (Zafar et al. 2019; Spanjaard et al. 2018) and BAC transgenesis (Lai 2016; Suster et al. 2011).

Here we specifically focus on the visualization strategy. Most of the labeling methods used to track cells require transgenic expression of a construct containing inserted sequences and the coding sequence of a reporter gene (Kretzschmar and Watt 2012). To trace specific cell types, the inserted sequences must contain cis-regulatory sequences of the marker gene for the cell type. Inducible elements can also be incorporated to refine manipulations. The reporter genes normally encode fluorescent proteins or other tags that can be detected through visualization. This is particularly true for echinoderms which take advantage of transparent embryos and larvae allowing for *in vivo* imaging at single-cell resolution. For example, a β -catenin:GFP fusion construct was injected in starfish fertilized eggs to label cells that express β -catenin in embryos. This helped to interrogate the function of $\eta\beta$ -catenin in the specification and segregation of endo-mesoderm (McCauley et al. 2015).

4.1.3 Recombinant bacterial artificial chromosomes (BAC) are used to track gene expression in echinoderms.

Among all variants of constructs used in echinoderms, the recombinant bacterial artificial chromosome (BAC) construct is the most powerful tool to track gene expression in cells (Buckley et al. 2018). The nature of BACs makes it the perfect vector to bear genomic sequences of large sizes (50-300 kb). Scientists take advantage of such features and build BAC libraries in which each BAC harbors a truncated area of genomic DNA. The whole BAC library covers the entire genome of a species (Frengen et al. 1999; Cameron et al. 2000; Cameron et al. 2004; Cary et al. 2018). The resources

of genome-wide BAC libraries are already available for seven species of echinoderms. These BACs can easily be engineered through recombination, in a process that introduces the reporter gene at any wanted site such as the transcription start site, translation start site, within the first exon, etc (Buckley et al. 2018). Thus the resultant recombinant BAC not only bears all the necessary coding sequences, but also recovers the genomic environment in cells. Importantly, in echinoderms like sea urchins and sea stars, BACs injected into the zygotes are incorporated into the genome, most likely at the 4th or 5th cleavages, and replicated during mitosis (McMahon et al. 1984; Guay et al. 2017). This generates a chimeric transgenic embryo that stably marks the gene expression in cell lineages during development and potentially during regeneration. Recombinant BACs have been applied in sea urchins and sea stars to locate gene expression and track cells in order to understand processes such as the endomesoderm specification (de-Leon and Davidson 2010), control of neurogenic patterning (Barsi and Davidson 2016), inflammatory responses (Buckley et al. 2017), and endothelial development (Hinman et al. 2003).

4.2 Results

4.2.1 A Sox^c-Kaede BAC is generated to trace the Sox^c+ cell lineage.

To test the model, we needed to determine whether the Sox^c+ cells at the regeneration leading edge form neurons in regeneration. This requires tracing the Sox^c+ lineage in regenerating larvae. Previously, a construct of Sox^c-GFP BAC was available capable of transgenically labeling Sox^c+ cell lineage in development. However, this method was

not able to differentiate whether the Sox^c+ cells and neurons are formed before bisection or emerged during regeneration. Therefore, it was necessary to generate a method that labels Sox^c+ lineage of cells in live sea stars stably enough for embryos to develop into larvae, get decapitated and regenerate. Moreover, it was required that the technique was able to distinguish regeneration lineage from developmental lineage. Here we generated a Sox^c BAC with photo-convertible Kaede reporter and tested it in developing larvae. Based on the results, we propose that this can be a powerful approach to interrogate the questions in sea star larval regeneration. It also holds great potential to be adapted in other echinoderms and metazoans with less available genetic manipulations.

4.2.1.1 Expression and photo-conversion of Kaede proteins in sea stars

The photo-convertible green fluorescent protein Kaede was discovered by Ando and colleagues (Ando et al. 2002) and has been tested in various model systems including zebrafish (Hatta et al. 2006), mouse (Tomura et al. 2008), mammalian cell lines (Schmidt et al. 2009) and fruit flies (Chen et al. 2012). Scientists use Kaede to understand important questions regarding cell specification, cell fate decisions, stem cell maintenance, morphogenesis and regeneration. However, no studies regarding Kaede has ever been reported in echinoderms.

To examine whether kaede proteins can be expressed in sea star embryos and larvae, we generated and injected the mRNAs of *kaede* in starfish fertilized eggs. Green Kaede

fluorescent proteins are observed at 15 hpf in more than 80% of injected zygotes. All 26 embryos imaged show that *kaede* mRNAs are strongly expressed.

To characterize conversion of Kaede protein in sea stars, photo-conversion was next performed at 23 hpf. Based on the work of Ando and colleagues (Ando et al. 2002), we used a 405 nm fluorescent light to convert Kaede protein. Embryos mounted on a slide were exposed to a 405 nm laser for up to 200 seconds with snapshots taken every 10 seconds under channel 488 nm and 560 nm. In the process, the colors of the embryos gradually turned from green to yellow to red (**Fig 10.A, B, D**). The fluorescent intensity of each channel was extracted from the images to generate a photo-conversion plot.

As expected, the 560 nm fluorescence intensity gradually increases as the 488 nm intensity is progressively reducing with a converging point at ~40s (**Fig 10. A**). During 80-90s, the intensity value of 506 nm becomes 5 times of that of 488 nm (**Fig 10.B**), which renders a “red” embryo. The value of 488 nm intensity barely changes after 150s, suggesting the last phase of photo-conversion. Exposing embryos for 250s with snapshots taken every 5s and 150s exposure with 50s interval snapshots also support this trend of conversion.

4.2.1.2 How long can we detect Kaede in larvae?

Due to protein turnover in live cells, the Kaede proteins will be degraded and eventually become undetectable. Before moving to the next step of BAC generation, it was very important to characterize the Kaede protein decay process and clarify how long we can

effectively detect green and red Kaede proteins in embryos and larvae. To do this, we injected *kaede* mRNA in fertilized eggs and converted the green Kaede protein at 24 hpf with 80s exposure. Z-stack images of each converted embryo were taken every day up to 12 dpf. The fluorescent intensity values of the entire embryo were extracted to generate the fluorescent intensity plot (**Fig 10.C**).

Based on the fluorescent intensity plot, it is clear that Kaede proteins remain detectable for 6-7 days. The red fluorescence intensity increases slightly at 2 dpf. One explanation is that the intensity of the red proteins is too high to be diluted in the early days of development. Thus the growth in size leads to the increasing red fluorescence. On the other hand, the green fluorescent intensity rises dramatically at 2 dpf, likely due to the growing of the embryo and the continuous translation of *kaede* mRNA. For both red and green Kaede, the intensity drops at 3 dpf, suggesting that the protein degradation becomes distinguishable. However, some amount of red and green proteins in the embryos still remain detectable in the larvae until 7 dpf when another decrease of intensity is observed. After 7 days, the red signals are too weak to be consistently identified. And the quality of green signals becomes rather poor. Therefore, we conclude that the Kaede proteins can be effectively detected for 7 days (**Fig 10.C, E**).

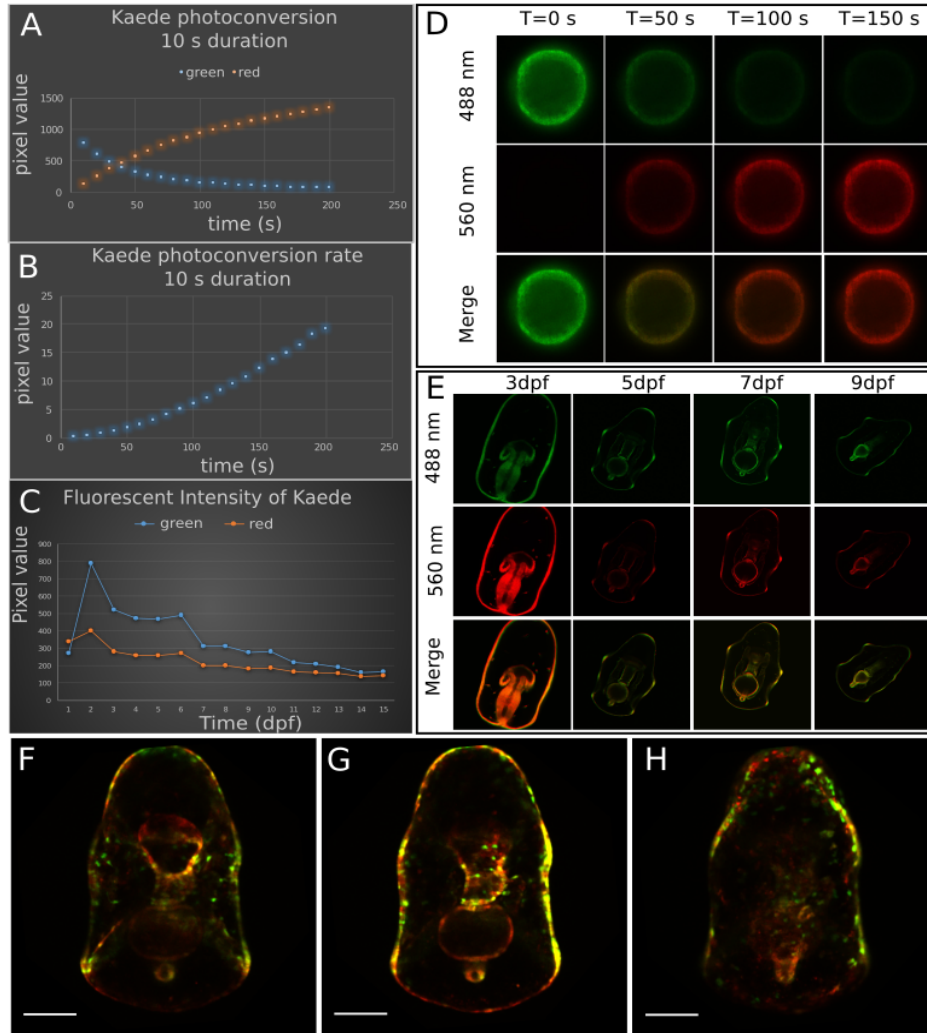


Fig 10. Examination of Kaede protein expression in sea star larvae.

(A) Photo-conversion plot of Kaede protein in sea star embryos injected with *kaede* mRNA. (B) Photo-conversion rate of Kaede protein in sea star embryos. (C) Fluorescent intensity of Kaede protein over time in sea star larvae injected with *kaede* mRNA. This shows that Kaede can be detected for 6-7 days. (D) Photo-conversion of Kaede in sea star embryos. Green Kaede protein is gradually converted to red protein. (E) Detection of Kaede in larvae injected with with *kaede* mRNA. This shows that Kaede can be stably detected for 7 days. (F-H) Examination of Sox-Caede BAC in sea star

larvae. Kaede photo-conversion is performed in larvae. Expression pattern of Sox2-Kaede BAC in sea star larvae recapitulates sox2 expression. Scale bar: 100 μ m. Dpf: day-post-fertilization.

4.2.1.3 Soxc Kaede BAC expression recapitulates soxc expression in development

To examine Kaede function in BACs, we generated a Soxc-Kaede BAC that carries the regulatory sequences of the *soxc* gene and the coding sequence of the *kaede* gene (**Fig 11.A**). After genome incorporation, the cells expressing Soxc will also express Kaede in the injected zygotes. After BAC injection, the embryos start to express Kaede at 24-28 hpf in patches of cells on the ectoderm. At 48 hpf, green Kaede is observed in patches of cells on the ectoderm and the archenteron. During 4-7 dpf, the expression of Kaede extends to the ectoderm including ciliary band domains, the mouth, esophagus and the stomach (**Fig 10.F-G**). This expression pattern of Kaede recapitulates the larval *soxc* expression pattern and the *soxc in situ* hybridization results reported previously (Yankura et al. 2013; Cheattle Jarvela et al. 2016). This proves that the injected Soxc-Kaede BAC stably label the Soxc+ cell lineage.

Taken together, echinoderm zygotes have the ability to incorporate exogenous DNA like BACs into their genome. Injecting Soxc-Kaede BACs in starfish fertilized eggs results in chimeric transgenic embryos. Cells expressing Soxc are marked by Kaede expression. Their daughter cells are marked by inheriting Kaede proteins. Thus, the Soxc+ stem cell lineage is stably labeled. Unpublished data and previous work from our lab have shown that *soxc* expression is continuous from hatched embryos to bipinnaria larvae. In addition, Kaede proteins can be successfully detected for up to 7 days in sea star larvae. Collectively, these produce a time window long enough to interrogate important questions in regeneration. The feature of Kaede enables the differentiation of the regenerative Soxc expression from the larval Soxc expression simply by photo-

conversion upon amputation. This allows us to trace the sources of regenerative Sox^{c+} cells and understand the contribution of each population of Sox^{c+} cells in regeneration.

A particular great feature of echinoderm zygotes is that the genomic integration of exogenous BACs are concatenate. When co-injected with multiple BACs, the embryos will add all different BACs into the genome. And the incorporation of several BACs occurs in the same blastomere. This affords an opportunity to label different cell lineages in larvae through co-injection of different BACs. It potentially offers a chance to interrogate the relationship between genes and the connections between diverse cell lineages in regeneration. Cell lineage tracing with Kaede BACs also provides the basis for high throughput sequencing analyses on specific cells in regenerating larvae.

4.2.2 Larval Sox^{c+} cell lineage in the remaining posterior contributes to the regenerated serotonergic neurons

With the Sox^c-Kaede BAC available, we next sought to understand the sources of regenerated neurons. We specifically focused on determining whether the cells expressing *soxc* after bisection contribute to the regenerated neurons. Importantly, we find that there is a larval Sox^{c+} cell lineage in regeneration. These are Sox^{c+} cells present before amputation and continuing expressing Sox^c after bisection. This larval Sox^c lineage is used to re-make serotonergic neurons.

To investigate this question, we have performed the Sox_c-Kaede BAC transgenesis (**Fig 11. A, C**). After injection, the larvae are grown to 7 dpf when bisected and photo-converted. At this point, the Sox_c⁺ cell lineage in the decapitated larvae is marked by converted red Kaede. In the posterior segments, labeled cells are found in a few or all of these locations: post-oral ciliary band, lateral ciliary band, esophagus and gut. As shown in **Fig 11.B**, in regeneration, when new Sox_c is generated, new Kaede is also expressed. Thus the cells with regeneration-induced new Sox_c expression will be marked with green Kaede. As a result, the red cells in the regenerating larvae are the historic labeled cells that only express Sox_c before bisection. The green represents the Sox_c⁺ cells specified upon decapitation with regeneration-specific *de novo* expression of Sox_c. The yellow cells are consistent larval Sox_c⁺ cell lineage. These cells express Sox_c in the intact larvae and continue to express Sox_c in their progeny after wounding.

After 3 days of regeneration, Sox_c⁺ cells are enriched at the regeneration anterior. These cells exhibit all three colors (**Fig 14. A-C**). This is supported by quantification of the fluorescent intensity at each channel for each Sox_c⁺ cell at the regeneration leading edge. The results show three groups representing red, yellow and green cells (**Fig 14.D**). This indicates that the Sox_c⁺ cells at the leading edge are derived from multiple sources including both larval Sox_c⁺ cell lineage and regeneration-induced specification. Another interesting finding to note is that the yellow, larval Sox_c cells are only observed in the lateral sides of the regeneration leading edge (**Fig 14.E-F**). This implies that the yellow cells may contribute the regenerated serotonergic neurons which are reformed at the lateral side of the anterior.

In 7 dpb larvae, the yellow cells derived from the larval Sox^{c+} cell lineage form the regenerated neurons that display axonal processes (**Fig 11.e-e2**). These neurons are located dorsally at the lateral side of the anterior, projecting both within the dorsal ganglia and towards the mouth (**Fig 11.E**). This suggests the yellow regenerated neurons are serotonergic neurons. To confirm that the regenerated serotonergic neurons are contributed by Sox^{c+} cells, we label the Sox^{c+} lineage with GFP via microinjection of Sox^c-GFP BAC. This is followed by detection of GFP and serotonin through double IF staining. The results indicate that the GFP⁺/Sox^{c+} cells do form serotonergic neurons in regeneration (**Fig 11.D-d**).

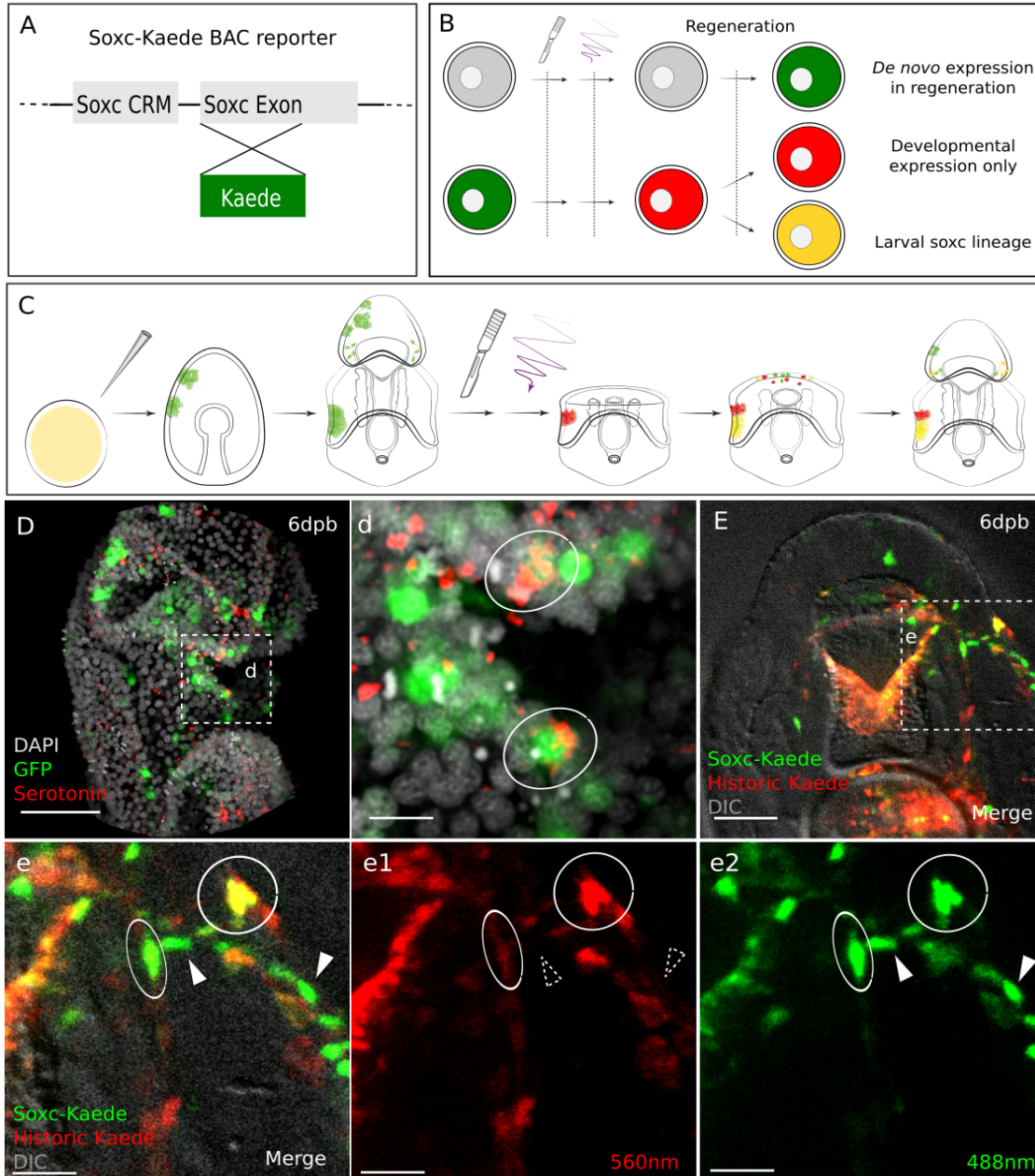


Fig 11. Larval Sox+ lineage and *de novo* Sox+ lineage make serotonergic neurons in regeneration.

(A) The design of Sox+Kae+ BAC construct. (B) Photo-conversion scenario of labeled Sox+ cells upon bisection. (C) A schematic of experimental plan: sea star zygotes are

injected with the Soxc-Kaede BAC. Injected embryos are incubated till larvae for bisection. Photo-conversion is immediately performed on bisected posterior segments. After regenerating for different periods of time, larvae are observed to examine the Soxc+ lineages in regeneration. (D) Bisected larvae injected with Soxc-GFP BAC were examined through double IF staining with anti-GFP and anti-serotonin. Soxc+ cells labeled with GFP become serotonergic neurons in regenerated larvae. Scale bar: 100 μm . (d) Amplification of the boxed area in (D) shows that serotonin and GFP are detected in the same cells, highlighted by circles. Scale bar: 15 μm . (E) Regenerated larvae injected with Soxc-Kaede BAC display neurons with multiple colors. Scale bar: 50 μm . (e) Amplification of boxed area in (E) shows that the yellow, larval Soxc+ cell lineage forms serotonergic neurons at the regenerating dorsal ganglia, highlighted in circles. The neurons contain (e1) historic red Kaede, shown in circles, and (e2) newly formed green Kaede in circles. *De novo* Soxc+ cells specified upon bisection also form serotonergic neurons at the regenerating dorsal ganglia, indicated by the white arrows. These neurons contain (e2) only newly formed green Kaede (arrowheads). (e1) No historic red Kaede is found at the corresponding locations (arrowheads with dashed lines). Scale bar in (e-e2): 20 μm . Dpb: day-post-bisection.

Taken together, we have used *Soxc*-Kaede BAC transgenesis to stably label the *Soxc*⁺ lineage during development and regeneration. Through photoconversion upon bisection, we find that there are both newly specified *Soxc*⁺ cells and the larval *Soxc*⁺ cell lineage at the regeneration leading edge. Remarkably, through cell lineage tracing, we are able to demonstrate that the larval *Soxc*⁺ cell lineage makes serotonergic neurons in regenerating larvae.

4.2.3 Larval *Soxc*⁺ cells are derived from embryonic *Soxc*⁺ neural stem cell lineage

In embryos, *Soxc*⁺ cells generate the APD associated serotonergic neurons. Similarly, in regeneration, the larval *Soxc*⁺ lineage gives rise to the neurons in the dorsal ganglia. This interesting coincidence raised the question: is the larval *Soxc*⁺ cell lineage originated from the embryonic *Soxc*⁺ cells? Is the embryonic *Soxc*⁺ cell lineage maintained in the larval stage and activated upon decapitation to make serotonergic neurons? To understand this, we started by characterizing *soxc* expression and *soxc*⁺ cell proliferation in uncut larvae.

4.2.3.1 *Soxc*⁺ cells are populated in larvae

Soxc FISH results confirm that *soxc* is expressed in intact larvae at 7dpf. *Soxc*⁺ cells are located in the dorsal ganglia, distributed in pre- and post-oral ciliary bands. There are also a few *soxc*⁺ cells observed in the esophagus (**Fig 12.A**). 15 min of EdU incubation reveals that *soxc*⁺ cells are actively proliferating in the dorsal ganglia (**Fig 12.a1-a2'**). We quantify the ratio of *soxc*⁺ proliferating cells over all *soxc*⁺ cells using

Imaris. 18.9% of *soxc*⁺ cells are EdU positive in larvae compared to 20.8% in embryos (**Fig 12.C**). Thus *soxc*⁺ cells are maintained and dividing in the larval stage. Similar to *soxc*, *Lhx2*⁺ cells are also expressed in the dorsal ganglia despite at a low expression level. 15 min EdU incubation shows that a few *lhx2*⁺ cells in the dorsal ganglia are actively dividing. This suggests that the *soxc*⁺ neural stem cell population in the dorsal ganglia may progress into *lhx2*⁺ pathway in a *foxq2* free environment to generate more serotonergic neurons in the dorsal ganglia.

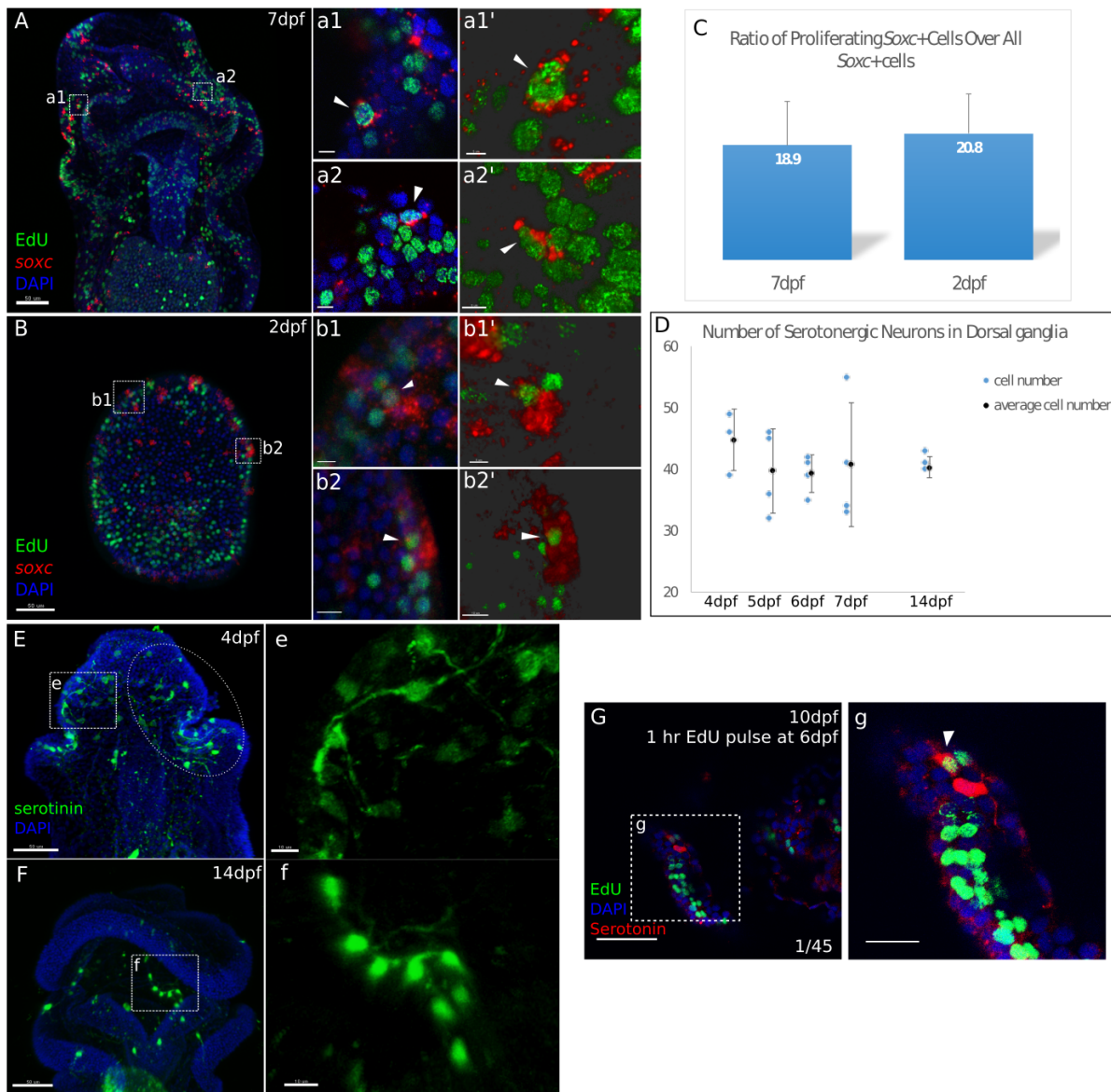


Fig 12. Sox+ cells remain proliferative in larvae.

(A) EdU-FISH with 15 min EdU incubation and soxc probe detection show that soxc+ cells actively proliferate in larvae. Boxed areas are amplified in (a1) (a2) showing the soxc+ cells at the dorsal ganglia are dividing (arrowheads), scale bar: 5 μ m. (a1') (a2') show the 3D reconstructed view of overlapping EdU and soxc. Scale bar: 5 μ m.

Similarly, (B-b2) a proportion of *soxc*⁺ cells actively divide in 2 dpf embryos. A 3D reconstructed view of overlapping EdU and *soxc* is shown in (b1'). Scale bar in (b1-b'1): 5 μm , and (b2'). Scale bar in (b2-b2'): 10 μm . (C) Quantification of proliferating *soxc*⁺ cells show that the ratio of dividing *soxc*⁺ cells over all *soxc*⁺ cells are comparable in embryos and larvae. (D) Quantification of serotonergic neurons in larvae shows a stable number of neurons over time. (E-f) IF staining with anti-serotonin in larvae at different developmental stages. (E) In 4 dpf larvae, serotonergic neurons in dorsal ganglia is highlighted in circles. (F) In 14 dpf larvae, number of serotonergic neurons is comparable to that of 4 dpf larvae. (e-f) Amplified view shows clear morphology of axonal processes, scale bar: 10 μm . (G) IF staining with anti-serotonin in larvae with 1 h EdU pulse and 4 d development. 1/45 larva shows newly formed serotonergic neurons from cell division. (g) Amplified view of boxed area in (G) shows the newly formed serotonergic neurons with pulsed EdU in the nucleus. Scale bar in (A,B,E-G): 50 μm . Dpf: day-post-fertilization.

To determine whether proliferating *soxc*⁺ cells in the dorsal ganglia actively generate more serotonergic neurons, we performed EdU pulse for 1, 7, 24 hours respectively in 3 stages: 4 dpf, 6 dpf and 9 dpf larvae. After 2-5 days of development, we used serotonin IF staining to detect the new serotonergic neurons formed from cell division. Out of the 45 imaged larvae, only 1 larva pulsed with EdU for 1 h at 6 dpf showed 1 newly formed EdU incorporating serotonergic neurons in the dorsal anterior at 10 dpf (**Fig 12.G-g**). The rest 44 larvae did not present serotonergic neurons incorporated with EdU. Instead of 3 days of development after the EdU pulse, we also tested different time windows from 2 to 5 days of developing in case neurogenesis in larvae takes shorter or longer than 3 days. However, IF staining of these larvae did not present convincing positive results. This suggests that there are very few serotonergic neurons formed from progenitor cell division after 4 dpf. This is supported by the quantification of serotonergic neurons in the dorsal ganglia over different time points in larval stages (**Fig 12.D**). Despite small fluctuations due to individual variances, the number and morphology of serotonergic neurons from 4 dpf to 14 dpf presents no significant differences (**Fig 12.E-f**). Therefore, the proliferating *soxc*⁺ cells are not used to produce more serotonergic neurons. Instead, they may be a pool of stem cells for generating other neuronal cell types. They can also be involved in homeostatic maintenance of the nervous system in larvae.

4.2.3.2 Specification of *Soxc* cells stops in larvae: the *Soxc*⁺ cells in larvae are resultant from cell divisions instead of specifications.

There are two possible sources of the larval *Soxc*⁺ lineage. First, the larval *Soxc*⁺ lineage may inherit part of the embryonic *Soxc*⁺ cell progeny. But the majority of *Soxc*⁺

cells in larvae are specified from non-Soxc+ cells post embryonically. Second, all of the Soxc+ cells in 7 dpf larvae are continuation of the embryonic Soxc+ lineage. In this case, all specification of Soxc+ cells will be completed in embryo stage.

In order to determine the correct scenario, we performed Soxc-Kaede BAC transgenesis to label the Soxc+ cell lineage. We applied photo-conversion in 2 dpf embryos and 4 dpf larvae respectively and quantified the events of cell specification 3 days after (**Fig 13.A**). Similar to the previous cell lineage tracing experiment, continuing lineage contain both red and green Kaede and thereby show yellow signal. The newly specified Soxc+ cells display green color only. Comparing the number of green cells in larvae 3 days post photo-conversion, we find that ~0 green cells are found in larvae converted at 4 dpf (**Fig 12.D-E**). However, a number of newly specified cells are present in larvae converted in 2 dpf (**Fig 13.B-C**). Comparing the two dataset shows significant differences in numbers of new specification events (**Fig 13.F**). This evidence strongly supports the second hypothesis. It indicates that the Soxc+ cells are actively being specified in embryos. And in larvae, the specification of Soxc+ cells has stopped. Therefore, we can conclude that the larval Soxc+ cells are derived from the embryonic Soxc+ cell lineage, generated from cell divisions, not specifications.

In summary, our data show that the larval Soxc+ cell lineage regenerate serotonergic neurons, and the larval Soxc+ lineage is a continuation of the embryonic Soxc+ cell lineage. Significantly, we have demonstrated that there is an embryonic neural stem cell lineage that is maintained and populated in larvae. Upon bisection, this embryonic

neural stem cell lineage located in the posterior larvae is activated to continue expressing Sox_c at the regeneration leading edge (cell migration may be involved). Moreover, this embryonic Sox_c⁺ cell lineage is induced to enter the embryonic serotonergic neuronal pathway to reform the serotonergic neurons in regeneration.

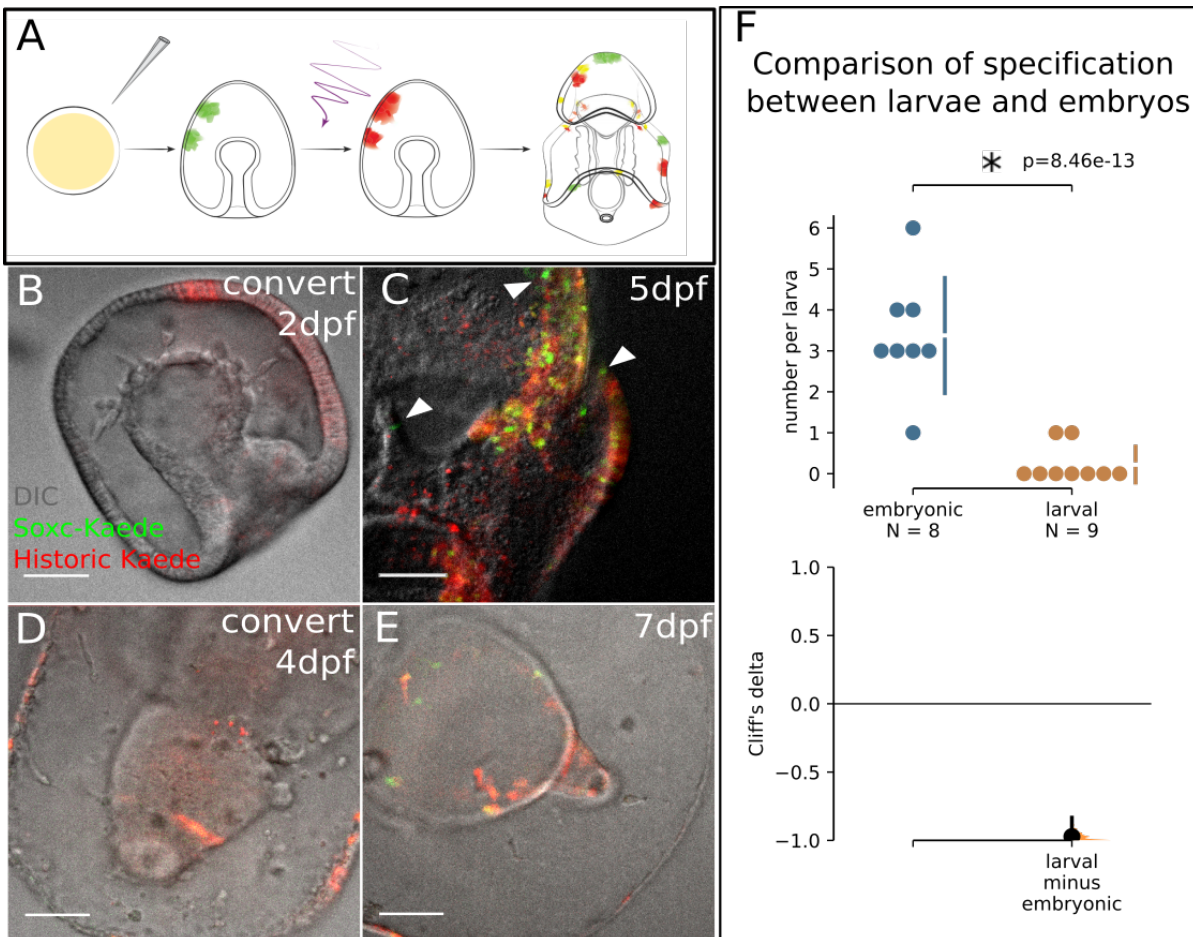


Fig 13. Larval Sox_c⁺ cell lineage is embryonically derived.

(A) A schematic for the experimental plan to determine the source of larval Sox_c⁺ cell lineage. (B-E) shows the specification of Sox_c⁺ cells occur in embryos but stops in larvae. (B) Embryo injected with Sox_c-Kaede BAC is converted at 2 dpf. Red Kaede marks all labeled Sox_c⁺ cells. (C) After 3 days, besides the red and yellow cells, there

are several newly specified, green Sox^{c+} cells indicated by arrowheads in the 5 dpf larva. However, (D) when converted at 4 dpf (larval stage), only yellow cells and red cells are observed 3 days later as shown in (E), suggesting no specification of Sox^{c+} cell occurs in the larva. (F) Quantification of Sox^c specification in embryos and larvae. Sox^{c+} cell specification event is close to 0, significantly decreased compared to the embryonic state. Scale bar in (B-E): 50 μ m. Dpf: day-post-fertilization.

4.2.4 Specifications of Sox^{c+} cells resume in regeneration, resembling the embryo state.

Interestingly, we have shown that the Sox^{c+} cell specification has stopped by larval stage. However, there are green, newly specified Sox^{c+} cells located in the regeneration leading in 3 dpb larvae (**Fig 14.A-C, a1-a3**). Thus decapitation initiates the making of new Sox^{c+} cells and resumes the specification in regeneration.

Quantification results show that the number of specified green Sox^{c+} cells at the regeneration leading edge at 3 dpb has significantly increased compared to the ~0 specification in larval conversion (**Fig 14.G**). Considering that Kaede proteins can be stably detectable for 7 days, this indicates that cells never taken Sox^c mediated neuronal fates since 3 dpf are reprogrammed to become neuronal tissues upon decapitation. This fate reprogramming induced by wounding is a homologous process also present in planarians and cnidarian hydra (Sánchez Alvarado and Yamanaka 2014).

Inspiringly, the number of specified Sox^{c+} cells in the regeneration leading edge is comparable to that of the embryo conversion (**Fig 14.H**). Therefore, not only is specification of Sox^{c+} cells resumed in regeneration, but the extent of specification in the regenerating leading edge also recapitulates the embryonic level. This finding strongly supports the hypothesis that the competent regeneration leading edge is reset to the embryonic state in gene expression, cell capacity and fate specification.

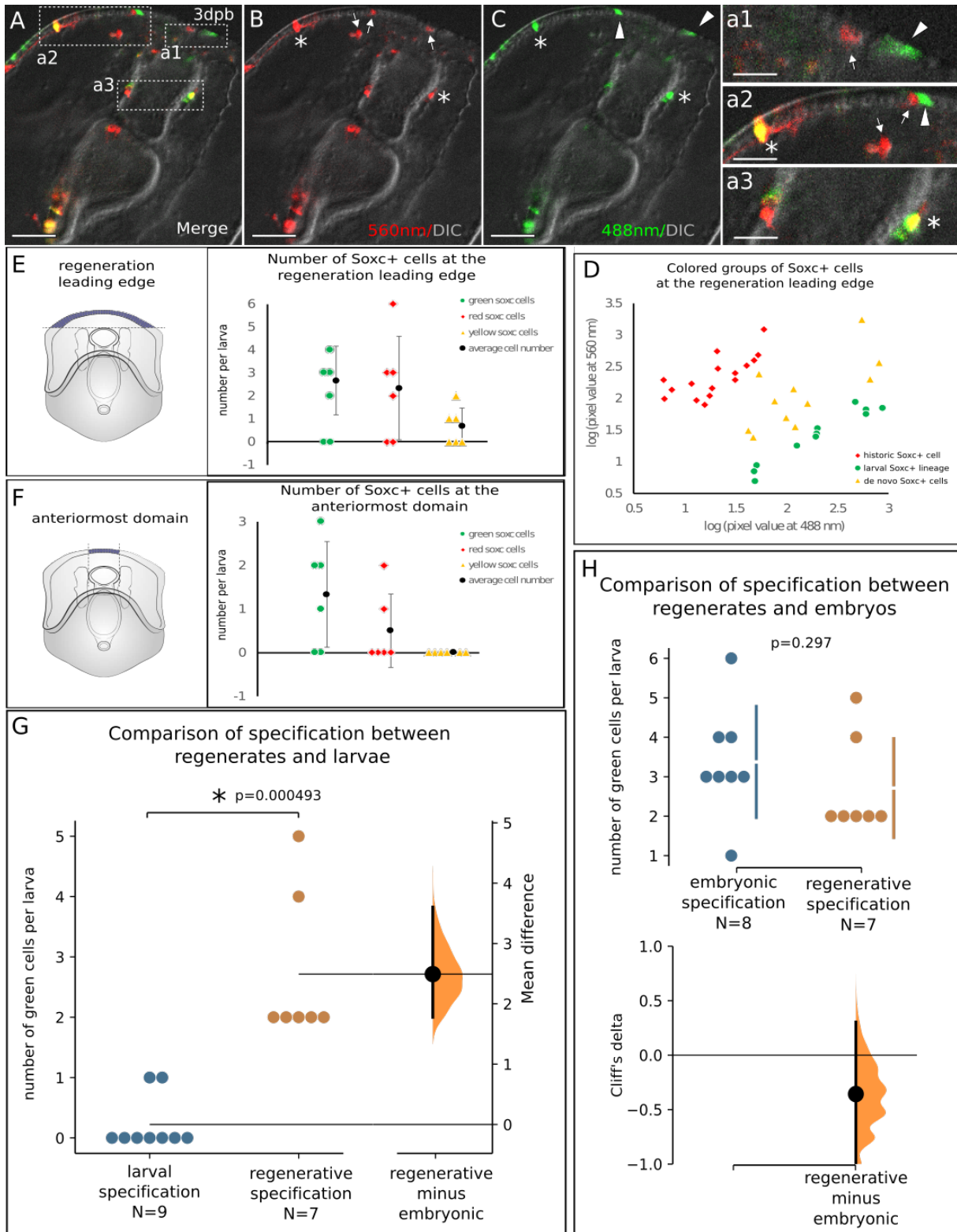


Fig 14. Specification of Sox+ cells resumes in regeneration.

(A-C) In *Soxc*-Kaede transgenic regenerating larvae, there are multiple sources of *Soxc*⁺ cells at the regeneration leading edge. Some *Soxc*⁺ cells are derived from the yellow, larval *Soxc* lineage (marked by asterisks). Some *Soxc*⁺ cells are differentiated cells no longer express Kaede (arrows). There are also green *Soxc*⁺ cells that are newly specified upon decapitation (arrowheads). The boxed areas in the regeneration leading edge is amplified in (a1) and (a2). *Soxc*⁺ cell lineage in the mouth and foregut are amplified in (a3). (D) Quantification of fluorescent intensity of cells in the regeneration leading edge generates 3 colored groups. (E-F) All yellow, larval *Soxc*⁺ cell lineage is located at the lateral side of the regeneration leading edge. (E) Cells of all three colors are detected in the regeneration leading edge. (F) Only green cells and red cells are at the anteriormost. (G) Quantification of *Soxc* specification in regenerating and intact larvae. *Soxc*⁺ cell specification event significantly increases in regenerating compared to the larval stage. (H) Quantification of *Soxc* specification in regenerating larvae and embryos. *Soxc*⁺ cell specification event is comparable in regenerative and embryonic stage, indicating that specification of *Soxc* is resumed in regeneration. Scale bar in (A-C): 50 μm . Scale bar in (a1): 10 μm , in (a2): 20 μm , in (a3) 15 μm . Dpb: day-post-bisection.

4.3 Conclusion and discussion

To conclude, Sox^{c+} cells are partitioned from the *soxb1*⁺ ectoderm in embryos. Specification to generate more Sox^{c+} neuronal fated cells actively progresses in embryonic stages but is completed by 4 dpf larval stage. The Sox^{c+} cells are distributed along the pre- and post oral ciliary bands, in the dorsal ganglia and the oral regions. This embryonic Sox^{c+} neural stem cell lineage is maintained and continues to proliferate to generate more Sox^{c+} cells in larvae. Particularly, the *soxc*⁺ cells in the dorsal ganglia are actively dividing, suggesting that they may be involved in making other neuronal cell types or take part in the homeostatic maintenance of neurons.

Upon bisection, the Sox^{c+} stem cell populations in the anterior are removed. The posteriorly located embryonic Sox^{c+} cell lineage is activated by wounding to enter the embryonic serotonergic neuronal pathway. The yellow, embryonic Sox^{c+} cells are distributed at the lateral sides of the leading edge, possibly resulting from cell migration towards the wounded anterior. These Sox^{c+} cells at the regeneration leading edge progress to become *lhx2*⁺ progenitor cells which give rise to post-mitotic neurons expressing *elav* at the lateral sides of the regeneration anterior. IF staining has shown that these post-mitotic neurons are serotonergic neurons.

Remarkably, we have demonstrated for the first time *in vivo* that there is an embryonic neural stem cell lineage marked by Sox^c expression, which generates the serotonergic neurons in embryos, and is maintained and populated in larvae. And upon decapitation, this embryonic Sox^{c+} neural stem cell lineage is activated to re-take the embryonic

serotonergic neuronal pathway, reforming the serotonergic neurons in regenerating larvae. Taken together, we have identified one source of regenerated neurons.

This chapter raised another interesting question: where do the newly specified Sox^{c+} cells come from? The specification of new Sox^{c+} cells has stopped by larval stage. However, decapitation initiates the specification events, supported by the green Sox^{c+} cells at the regeneration leading edge. The number of new Sox^{c+} cells are specified in regeneration is similar to the embryonic state. What are the sources of these newly specified Sox^{c+} cells? Do they also form neurons in regeneration? Based on the embryonic biology in sea stars and previous studies in other metazoans, we hypothesized that the green Sox^{c+} cells are specified from the Sox^{b1+} cell in the regeneration leading edge. We next tested this hypothesis and completed our model in Chapter 5.

Chapter 5: Soxb1+ stem cells are specified into Sox^c+ cells to regenerate neurons

5.1 Introduction

In this chapter, we further tested the model for neural regeneration. We specifically focused on identifying the sources of the newly specified, green Sox^c+ cells in the regeneration leading edge. We also determined whether these regeneration-specific Sox^c+ cells become neurons.

5.2 Results

5.2.1 Soxb1+ cell lineage gives rise to the nervous system in larvae.

To test the model for neural regeneration, we needed to determine whether the Soxb1+ cells at the regeneration leading edge become Sox^c+ cells and form neurons in regeneration. This required the tracing of both Soxb1+ cell lineage and Sox^c+ cell lineage in regenerating larvae. Here we generated a Soxb1-Kaede BAC for tracing and distinguishing the regenerative Soxb1 cell lineage. We also generated a Sox^c-Cardinal BAC to label Sox^c expression. This enabled the co-injection and double labeling of Soxb1+ cell lineage and Sox^c+ cell lineage.

5.2.1.1 Soxb1-Kaede BAC expression recapitulates *soxb1* expression in development.

We generated a Soxb1-Kaede BAC that carries the regulatory sequences of *soxb1* gene and the coding sequence of *kaede* gene. Therefore, the cells express Soxb1 protein will also express of Kaede in the injected zygotes. After BAC injection, the zygotes started to express Kaede at 24-28 hpf in broad patches of cells on the ectoderm. At 2 dpf, green Kaede was expressed broadly in patches of cells on the ectoderm. This expression pattern of Kaede recapitulates the embryonic *soxb1* expression pattern reported previously (Yankura et al. 2013; Yankura et al. 2010). Although detailed characterization of Kaede expression was not performed at larval stages, Kaede expression in 7 dpf was detected on the ectoderm including the ciliary bands, dorsal ganglia and the ectodermally derived neurons (**Fig 15.A-f**). This recapitulates the *soxb1 in situ* results in larvae (**Fig 7.A**). These data together prove that the injected Soxb1-Kaede BAC stably label the Soxb1+ cell lineage. Our data and previous work have shown that *soxb1* expression is continuous from hatched embryos to bipinnaria larvae. This produces a time window long enough to interrogate the fates of the lineage in regeneration.

5.2.1.2 Soxk-Cardinal BAC expression recapitulates *soxk* expression in development.

Echinoderm embryos are great models for cell lineage and cell fate studies. When co-injected with multiple BACs, they will incorporate all different BACs into the genome. It is noticeable that incorporation only occurs in the same blastomere. This, therefore, affords an opportunity to label different cell lineages in larvae through co-injection of different BACs. To understand the relationship between Soxb1+ cell lineage and the

Soxc⁺ cell lineage in regeneration, double labeling of both Soxb1⁺ cells and Soxc⁺ cells was required throughout the course of regeneration. Therefore it was necessary to generate another Soxc BAC with a different reporter gene.

Here we generated a Soxc-Cardinal BAC that carries the cis-regulatory sequences of gene *soxc* and the coding sequence of the gene *cardinal*. Cardinal is a far-red fluorescent protein. Thus the detection of this protein does not interfere with the photo-conversion and the detection of Kaede. This sets the basis for co-injection. We next tested the expression patterning of Soxc-Cardinal in development. Similar to the Soxc-Kaede BAC injection results, the embryos started to express Cardinal at 24-28 hpf in on the ectoderm. Cardinal was continuously expressed in development. By 4-7 dpf, Cardinal expression was observed on the ectoderm, including the ciliary bands and the ectodermally derived dorsal ganglia, as well as in the mouth and esophagus. This recapitulates the *soxc* expression patterns and proves that the Soxc-Cardinal BAC stably labels the Soxc⁺ cell lineage.

5.2.1.3 Soxb1⁺ stem cell lineage becomes neurons

In larvae injected with Soxb1-Kaede BAC, all of the 18 imaged larvae presented Soxb1⁺ cells in the ciliary bands and on the ectoderm. 2/18 larvae showed inconclusive Kaede signals in the endodermal foregut. From all 18 larvae, we observed cells with evident neuron morphology, projecting axonal processes. These Soxb1⁺ neurons were distributed along the ciliary bands (**Fig 15.C**), at the dorsal ganglia (**Fig 15.F-f**), on the oral ectoderm projecting to the foregut (**Fig 15.E-e**), at the hindgut-anus domain (**Fig**

15.C) and elsewhere on the ectoderm (**Fig 15.D**). There were also Soxb1+ cells without neuron morphology in the ciliary bands (**Fig 15.A**) and elsewhere on the ectoderm (**Fig 15.B**). The ciliary-band associated neurons form projections lining the ciliary band. The neurons on the ectoderm were either projecting to the mouth or to the Soxb1+ ciliary band associated nerve cells. These data show that the Soxb1+ cell lineage forms multiple nerve cells at different locations in the larvae and thereby generate the larval nervous system. This is strong evidence supporting that Soxb1 is a master regulator that primes the neural stem cell fates, consistent with findings from multiple studies describing work in different model systems (Ross et al. 2018; Corsinotti et al. 2017; Oosterveen et al. 2013).

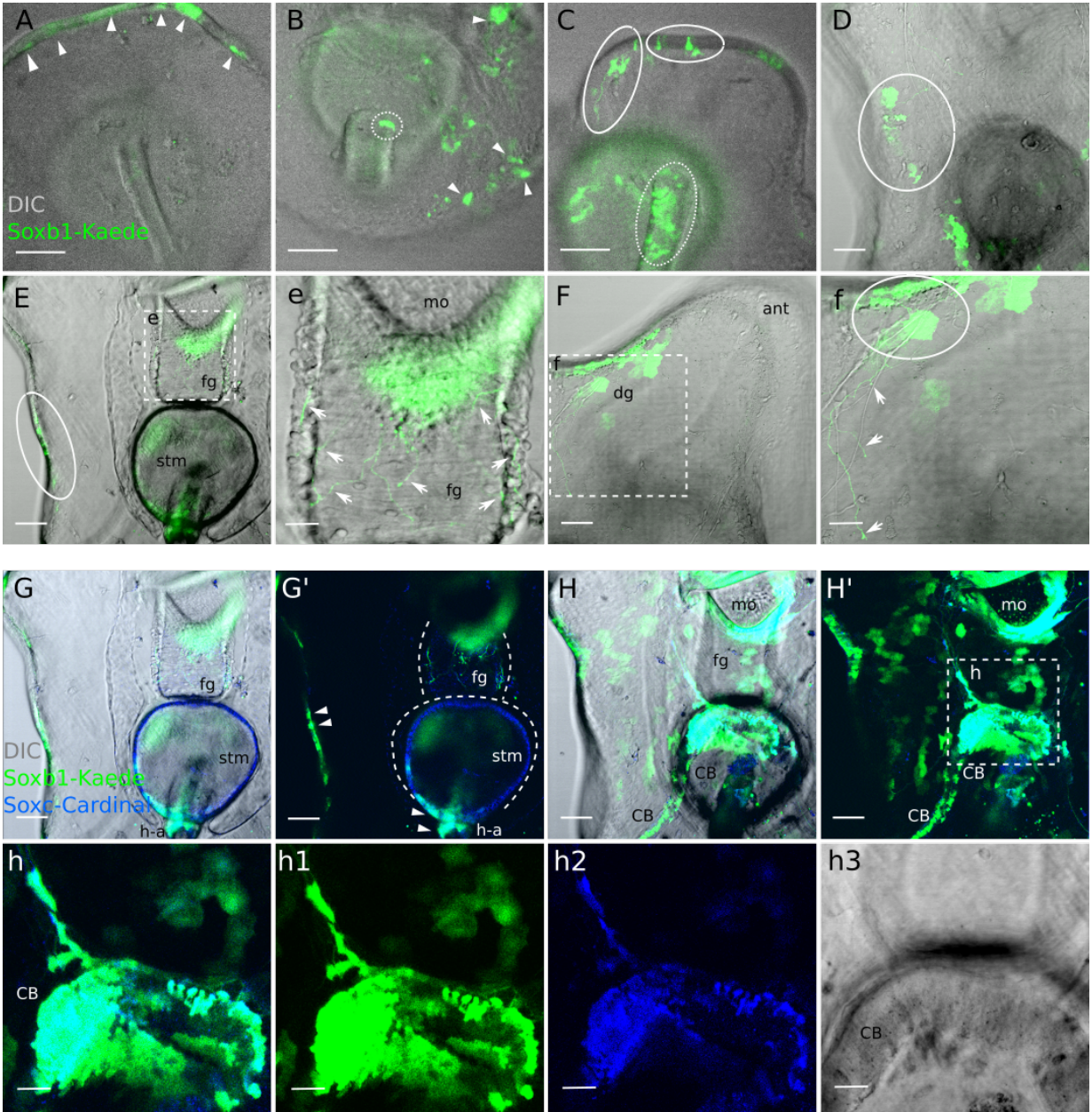


Fig 15. Ectodermal Sox1+ cells are derived from neurogenic Sox1+ cell lineage.

(A-f) Sox1+ cell lineage is neurogenic. In 7 dpf larvae, (A) Sox1 lineage forms cells in the ciliary band. These cells do not have clear neuron morphology (arrowheads). (B) Sox1 lineage forms cells clear neuron morphology (arrowheads) and cells at the

hindgut-anus area (circle with dotted line). (C) *Soxb1* lineage forms neurons along the ciliary band (circle with solid line), in the hindgut (circle with dotted line), (D) on the ectoderm (circle with solid line) with clear axonal projections (arrows). (E) *Soxb1*⁺ neurons are located in the lateral ciliary band (solid circle) and on the oral ectoderm (boxed area). (e) The amplification of the boxed area in (E) shows clear projections from the mouth neurons to the foregut. (F-f) *Soxb1*⁺ neurons are located in the dorsal ganglia (solid circle) with axonal processes (arrows). (G-H') Co-injection of *Soxb1*-Kaede BAC and *Soxc*-Cardinal BAC shows ectodermal *Soxc*⁺ lineage is derived from *Soxb1*⁺ cell lineage. (G-G') Green *Soxb1*-Kaede and blue *Soxc*-Cardinal are overlapping on the ectodermal cells along the ciliary band (arrowheads). *Soxb1*⁺ *Soxc*⁺ cells are also found at the junction of endoderm and ectoderm in the hindgut-anus domain (arrowheads). But endodermal tissues including the foregut and the stomach (highlighted with dashed lines) contain blue only, *Soxc*⁺ cells. Similarly, (H-h3) show that the ectodermal blue *Soxc*⁺ cells contain are also labeled with green *Soxb1*-Kaede, (h-h3) particularly the post-oral ciliary band and the ciliary band projecting neurons. Scale bar in (A-H'): 50 μm , in (e): 20 μm , in (f): 15 μm , in (h-h3): 20 μm . CB, ciliary band; fg, foregut; dg, dorsal ganglia; ant, anterior; mo, mouth; stm, stomach; h-a, hindgut-anus domain.

5.2.2 Soxb1+ cells in the regeneration leading edge are specified into Sox^c+ cells.

Neural stem cell marker Soxb1 is expressed on the entire ectoderm in embryos, upstream of all neurogenesis events in development. In regeneration, *soxb1* expression is immediately concentrated in the broad anterior regeneration leading edge where sit the Sox^c+ cells derived from resumed specification activated by injuries. To complete our model for neural regeneration, it was necessary to understand where these newly specified Sox^c+ cells come from as well as their fates. We speculated that these regeneration-specific Sox^c+ cells are specified from Soxb1+ cells. To test this hypothesis, we needed to label both Soxb1+ cell lineage and Sox^c+ cell populations to determine their relationship. Thus, we co-injected Soxb1-Kaede BAC and the Sox^c-Cardinal BAC into the fertilized eggs, followed by photo-conversion of Kaede at 7 dpf immediate before bisection. However, the expression of 2 fluorescent proteins with 3 different colors labeling 2 cell lineages in regeneration and development generated much complexity in drawing conclusions from all possible results. We carefully described all possible scenarios for cellular color combinations in the regenerating larvae.

5.2.2.1 Coinjection of Soxb1-Kaede BAC and Sox^c-Cardinal BAC shows overlapping expression patterns in larvae.

Larvae co-injected with both *Soxb1*-Kaede and *Soxc*-Cardinal BACs present both Kaede expression and Cardinal expression over the course of development. Compared to the single injections, the Kaede expression domain is smaller and the Cardinal+ cells are more dispersed. This phenomenon is likely due to the lower concentrations of each BACs applied in the co-injection. However, in the co-injected larvae, the *Soxb1*+ cell lineage marked by Kaede is distributed on the ectoderm and the nervous system. This is supported by the *Soxb1*-Kaede BAC single injection results and the WMISH patterns. Likewise, the labeled *Soxc*+ cells in double injected larvae are observed in the dorsal ganglia, ciliary bands, and mouth. The pattern is incorporated in the expression domains of *Soxc* in single injections and WMISH. These data suggest that each BAC successfully labels the lineage of interest and the labeling is the same in both single injections and double injections.

Interestingly, we find that the majority of both *Soxb1* and *Soxc* lineages overlap in developing larvae. In the few intact unconverted larvae, *Soxb1*+ cells are marked by green Kaede proteins whereas *Soxc*+ cells are labeled by far-red (pseudocolor blue) Cardinal. All *Soxc*+ cells on the ectoderm overlap with *soxb1* driven green Kaede (**Fig 15.G-H**). Some *Soxb1*+ cells located at the hindgut-anus domain also express *Soxc*-Cardinal. There are endodermal *Soxc* only cells in the foregut and gut (**Fig 15.G'**). Similarly, in 13 out of the 15 immediately converted posterior larvae, all of the blue cells are also red, suggesting all of the *Soxc*+ cells are derived from *Soxb1*+ cells. These cells are neurons on the ciliary bands, cells on the mouth and in the esophagus. Out of the 15 larvae, 2 larvae show *Soxc*+ only (blue positive, red negative) signals in the

foregut or gut. However due to the low expression level of Cardinal, whether these blue positive, red negative signals are cells remains indecisive.

Strikingly, these results demonstrate that the ectodermal Sox^c+ cells in sea star larvae are originated from the Sox^b1+ cell lineage. In the previous chapter, I have shown that the larval Sox^c+ cell population is a continuation of the embryonic Sox^c+ cell lineage. The specification of new Sox^c expression has stopped by the end of the embryonic stages. Here we have shown that all the embryonic specification events to generate cells with new Sox^c+ expression happen in the embryonic Sox^b1+ cells. Therefore, we can conclude that the embryonic Sox^b1+ cells are the sources for the ectodermally derived Sox^c+ cell lineage in sea star larvae.

5.2.2.2 All possible scenarios of cellular color combinations

After 3 days of regeneration, bisected and photo-converted larvae display multi-color cells. Because Sox^c+ marker Cardinal is not photo-convertible, each cell with blue color (pseudocolor for far-red Cardinal) in regeneration may have three explanations for its sources. One is that the blue cells contain historically generated Cardinal from larval Sox^c+ expression but no longer express Sox^c in regeneration. These are likely the differentiated cells from the Sox^c+ lineage. Another is that the blue cells contain historically generated Cardinal from larval Sox^c+ expression and are still expressing Sox^c in regeneration. In this situation, the Sox^c+ cells are from the embryonic Sox^c+ cell lineage, which corresponds to the yellow cells in Sox^c-Kaede BAC injections. The last explanation is that the blue cells have never expressed Sox^c in development and

thereby have no historic Cardinal. These blue cells are the newly specified Sox^c+ cells, mapping to the green cells at the regeneration leading edge in the single injections. Therefore, we summarize all explanations for each possible color combination in the regenerating larvae based on whether or not the cells contain Cardinal expressed before bisection (**Table 1**).

When a cell has historic Cardinal from the larval expression of Sox^c

If a cell expresses Sox^b1 and Sox^c before bisection, displaying both green Kaede and blue Cardinal in larvae. After bisection and the photo-conversion, the cell will display red Kaede and blue Cardinal in the posterior. At 3 dpb, if the cell presents red and blue colors, it is no longer expressing Sox^b1. If it stops expressing Sox^c in regeneration, this suggests the cell is differentiated or a trans-fating cell that quits the neural fates. If it continues to express Sox^c, this cell is derived from the embryonic Sox^c+ cell lineage that is specified from embryonic Sox^b1+ cells.

When a cell expresses Sox^c but no Sox^b1 before bisection will show only blue color before and after photoconversion. In 3 dpb larva, if the cell displays both blue and green colors, the cell starts to express Sox^b1 in the regenerating larva. Sox^b1 expression is activated upon injuries. If it stops to express Sox^c, this is likely a differentiated mesodermally derived neuronal cell that is dedifferentiated to express Sox^b1 stem cell marker. If the cell continues to express Sox^c in regeneration, this cell is mesodermally derived Sox^c+ cell lineage that is contributing to become an ectodermal Sox^b1+ stem cell.

When a cell has no larval Sox_c expression or historic Cardinal

When a cell does not have historic Cardinals, if the cell presents only green color after conversion and regeneration, this cell only expresses Sox_b1 in regeneration. Thus the cell is likely derived from the endo-mesoderm, non-neuronal fated progenitors and becomes ectodermal and neuronal in regeneration. If it presents only a yellow color, this cell is from the larval Sox_b1 neural stem cell lineage. If it presents only a red color, it is a differentiated cell from the Sox_b1 lineage.

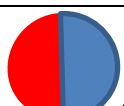
If the cell presents both blue and red colors, this cell is used to express Sox_b1 in development but longer express Sox_b1 in regeneration. Instead, it starts to express Sox_c in regeneration. This is likely originated from an ectodermal, differentiated, non-Sox_c fated cell. In regeneration, this cell de-differentiate or trans-differentiate to become a Sox_c fated neural stem cell.

If the cell presents both blue and yellow colors, this cell is from the larval Sox_b1 stem cell lineage and is specified to express Sox_c in regeneration.

If the cell displays both blue and green colors, this cell only expresses Sox_b1 and Sox_c in regeneration. It may be derived from an endo-mesodermal, non-neural fated cell and is trans-fated to become an ectodermal neural stem cell expressing Sox_b1. And the Sox_b1 cell is specified to express Sox_c.

However, whether the cells have historic Cardinal is difficult to determine in many conditions. This leads to inconclusive results. Therefore, detailed and careful comparisons of cells at different stages are required for this experiment.

Post-bisection	Post photo-conversion	regeneration
 Soxb1 Soxc	 Soxb1 Soxc	 Soxb1 Soxc
		 Soxb1 Soxc
 none Soxc	 none Soxc	 Soxb1 Soxc
 none none	 none none	 Soxb1 Soxc
 none none	 none none	 Soxb1 none
		 Soxb1 none

		 Soxb1 Soxc
		 Soxb1 none
		 Soxb1 Soxc
 Soxb1 none	 Soxb1 none	
Table 1 photo-conversion scenario for double injected regenerating larvae		

5.2.2.3 Green Kaede and Cardinal coexpression in the regenerating larvae shows that Soxb1+ cells are specified into Soxc+ cells

Through double injection and cell lineage tracing, we have identified that the newly specified Soxc+ cells are derived from Soxb1+ cells at the regeneration leading edge. All 15 injected larvae present cells with multiple colors. Specifically, 4/15 larvae display cells with both green Kaede and blue Cardinal at the regeneration leading edge. For example, in the larva shown in **Fig 16.A**, there are 4 cells located at the left side of the regeneration leading edge that present green Kaede and blue Cardinal (**Fig 16.a-a3**). And these cells do not have historic red Kaede proteins. It is important to note that the larva does not have any blue only cells at 0 dpb. Thus by the time bisection is performed, all labeled Soxc+ cells are originated from the Soxb1 lineage in the larva.

This is consistent in 13/15 larvae. Therefore, the Cardinal in the green/blue cells at the regeneration leading edge marks the regenerative Sox_c expression after bisection. Based on the scenarios we characterized above, these 4 green/blue cells only express Sox_b1 and Sox_c in regeneration. Remarkably this demonstrates that cells derived from a non-Sox_b1 lineage is trans-fated to express stem cell marker Sox_b1 in regenerating larvae. Because *soxb1* expression is mainly observed on the ectoderm in uncut larvae, the green cells showing regeneration-specific Sox_b1 expression are likely derived from the mesoderm or the endoderm. Our results also confirm that the newly formed Sox_b1⁺ stem cells are specified to become Sox_c⁺ neural stem cells at the anterior regeneration leading edge.

Secondly, there are also other sources of newly specified Sox_c cells. In 3/15 larvae, there are a few blue only cells observed at 3 dpb (**Fig 16.c-c3**). These cells are dispersed in the post-oral and lateral ciliary bands. Due to the lack of blue cells in the larvae at bisection, the cells labeled solely by Cardinal in 3 dpb larvae express Sox_c only in regeneration. These newly specified Sox_c⁺ cells are originated from sources other than the embryonic Sox_c⁺ stem cell lineage, the larval Sox_b1⁺ cell lineage or the regenerative Sox_b1⁺ cells. This demonstrates that there are other sources for neural stem cells, and they may arise from non-ectodermal tissues.

Finally, yellow cells are also observed in 3 dpb larvae (**Fig 16.b-b3**). They are dispersed at the regeneration leading edge, in the esophagus, and along the ciliary bands. No

Cardinal expression is observed in the yellow Sox_b1⁺ cells. Therefore, these cells are larval Sox_b1⁺ cell lineage that does not express Sox_c in regeneration.

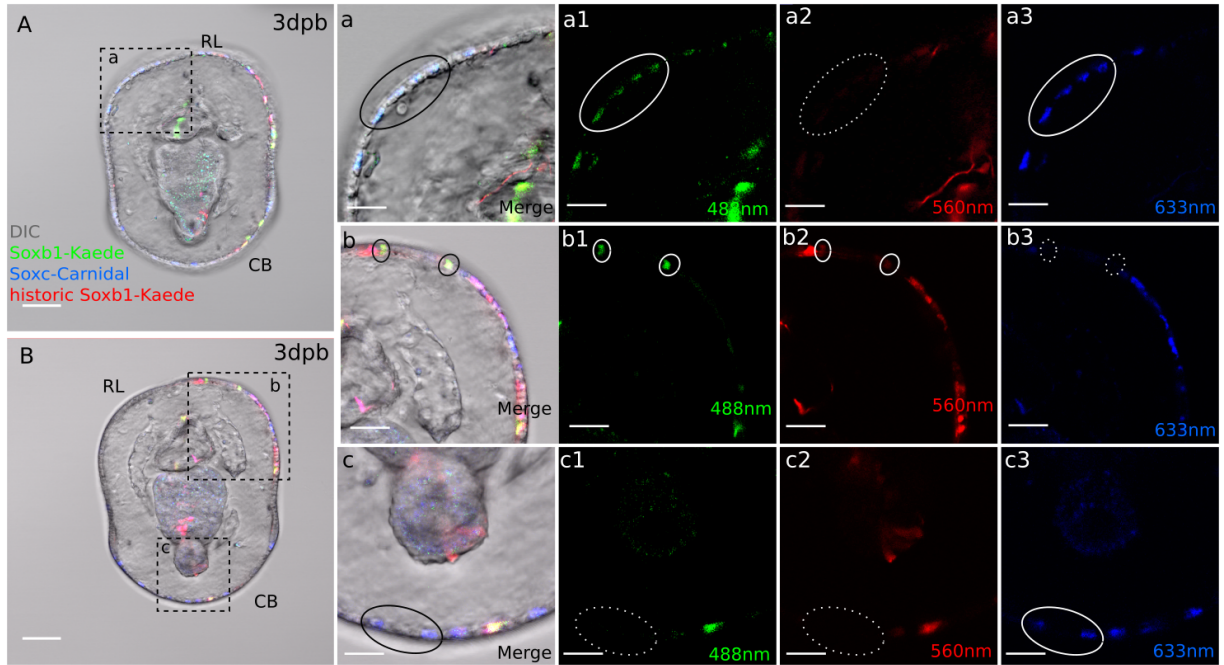


Fig 16. Sox_c⁺ cells are specified from Sox_b1⁺ cells at the regeneration leading edge.

(A) Some Sox_c⁺ cells at the regeneration leading edge are specified from *de novo* Sox_b1⁺ cells. The boxed area is amplified in (a). In 3 dpb transgenic larvae, cells with *de novo* Sox_b1 and Sox_c expression are located at the lateral side of the regeneration leading edge (black solid circle). These cells have (a1) newly formed, regenerative Sox_b1 and (a3) Sox_c expression (both highlighted with the white solid circles) (a2) but have no historic Sox_b1 (white dotted circle). (B-b) Sox_b1 cells at the regeneration leading edge have multiple sources. (b) is the amplified view of the boxed area. Apart from the *de novo* Sox_b1 cells, there are also yellow, larval Sox_b1 lineage at the

regeneration leading edge (black solid circle). These cells are not specified in Sox-mediated pathways. They are labeled with (b1) green and (b2) red Kaede (white solid circle), (b3) but not Cardinal (white dotted circle). (B-c) There are other sources of Sox cells in regeneration. (c) There are blue only, Sox⁺ cells in the posterior ciliary band (black solid circle). These Sox⁺ cells (c3) express only Cardinal (white solid circle). So they are not specified from historic or *de novo* Sox1 cell lineage because (c1) they do not contain green or (c2) red Kaede (white dotted line). Scale bar: 50 μ m. RL, regeneration leading edge; CB, ciliary band.

5.2.3 Soxb1+/Soxc+ cells become neurons in regenerating larvae.

We next sought to understand the role of regenerative Soxb1+/Soxc+ lineage in regeneration. In embryos and larvae, the neurogenic Soxc+ cells in the larvae are derived from the Soxb1+ cell lineage. Similarly, wounding activates the *de novo* expression of Soxb1 in cells with non-Soxb1 mediated fates. This is followed by the specification to express neural stem cell marker Soxc. Therefore, we speculated that the Soxb1+/Soxc+ is also neurogenic in regeneration. Here we tested this hypothesis and focused on determining whether injury-activated Soxb1+/Soxc+ cells form regenerated neurons.

We identified that the newly specified Soxb1+/Soxc+ lineage gives rise to regenerated neurons by tracing the cell lineage in double injected larvae. In 7-8 dpb larvae injected with Soxb1-Kaed BAC and Soxc-Cardinal BAC, anterior neurons are regenerated at the lateral side of the regeneration leading edge. Out of all 15 imaged regenerating larvae, 4 display green/blue cells that are specified to express Soxb1 and Soxc at 3 dpb. Interestingly, all 4 larvae present green/blue regenerated neurons at the regeneration leading edge at 7 dpb. As shown in **Fig 17.A**, there are two green/blue cells located at the left side of the anterior with early neuron morphology (**Fig 17.a-a3**). They are descendants of the Soxb1+/Soxc+ cells observed at 3 dpb (**Fig 16.a**). In addition, the neurons located at the lateral leading edge suggests that they may be the regenerated serotonergic neurons. Together, this demonstrates that similar to the embryonic state, the regeneration specific Soxb1+/Soxc+ cell lineage is used to make neurons in regeneration.

Secondly, we show that the larval Soxb1+ cell lineage is reused to generate neurons through Sox_c mediated neuronal pathway in regeneration. Next to the two neurons, there is another neuron at the left side of the regeneration leading edge labeled with green, red and blue (**Fig 17.A-a3**). The triple colored cell is derived from the larval Soxb1+ cell lineage. The Soxb1+ cell is specified into a Sox_c+ neural stem cell before or after bisection. And this Sox_c+ stem cell generates a differentiated neuron with processes located at the lateral anterior. These data suggest that the larval Soxb1+ cell lineage contributing to the larval nervous system is reused to regenerate neurons via the Sox_c mediated pathway after decapitation.

Last, we confirm that the Soxb1+ cell lineage contributes to the larval nervous system in development and regeneration. In **Fig 17.C**, the posterior larva show numerous nerve cells with convincing axonal morphology labeled with either red or yellow. A few red neurons are distributed at the regenerating mouth and the esophagus (**Fig 17.B-C, b-c**), projecting within the oral domain. Besides the mouth associated nerve cells, other red neurons are located in the post-oral ciliary band and form processes towards the mouth (**Fig 17.c-c3**). These red cells carry the Kaede marker when larvae are photo-converted upon bisection. Therefore, they are differentiated neurons formed in development before the injury of the larvae, indicating that the neuronal descendants of Soxb1+ cell lineage are important components of the larval nervous system. Upon bisection, Soxb1 expression is still observed in some Soxb1+ cells. This yellow larval Soxb1+ cell lineage contributes to the neurons in the regeneration leading edge (**Fig 17.a**), the oral nerve

cells (**Fig 17.b-c**) and the ciliary band associated neurons (**Fig 17.c**) in the regenerating larvae through the *Soxc* mediated pathway or not (**Fig 17.c**). Together, these data demonstrate that the larval *Soxb1*⁺ cell lineage not only gives rise to the nervous system in development but also contributes to the nervous system during regeneration.

5.2.4 There are multiple sources of *Soxb1*⁺ cells in the regeneration leading edge.

In the converted 3 dpb larvae injected with both BACs, regardless of Cardinal expression, there are cells labeled with green or yellow at the regeneration leading edge (**Fig 17.A-a3**). This demonstrates that the *Soxb1*⁺ cells located at the regenerating anterior have multiple cellular sources. The yellow cells are derived from the larval *Soxb1*⁺ cell lineage that has the historic Kaede from larval *Soxb1* expression and the new Kaede made during regeneration. More interestingly, the green cells possess regeneration-specific *Soxb1* expression. This indicates that injuries not only resumes the specification into *Soxc*⁺ cells, but also activates the *de novo* expression of the upstream regulator *Soxb1*. Through specification events, the non-ectodermally derived cells are reprogrammed to take the *Soxb1* mediated ectodermal neuronal fates.

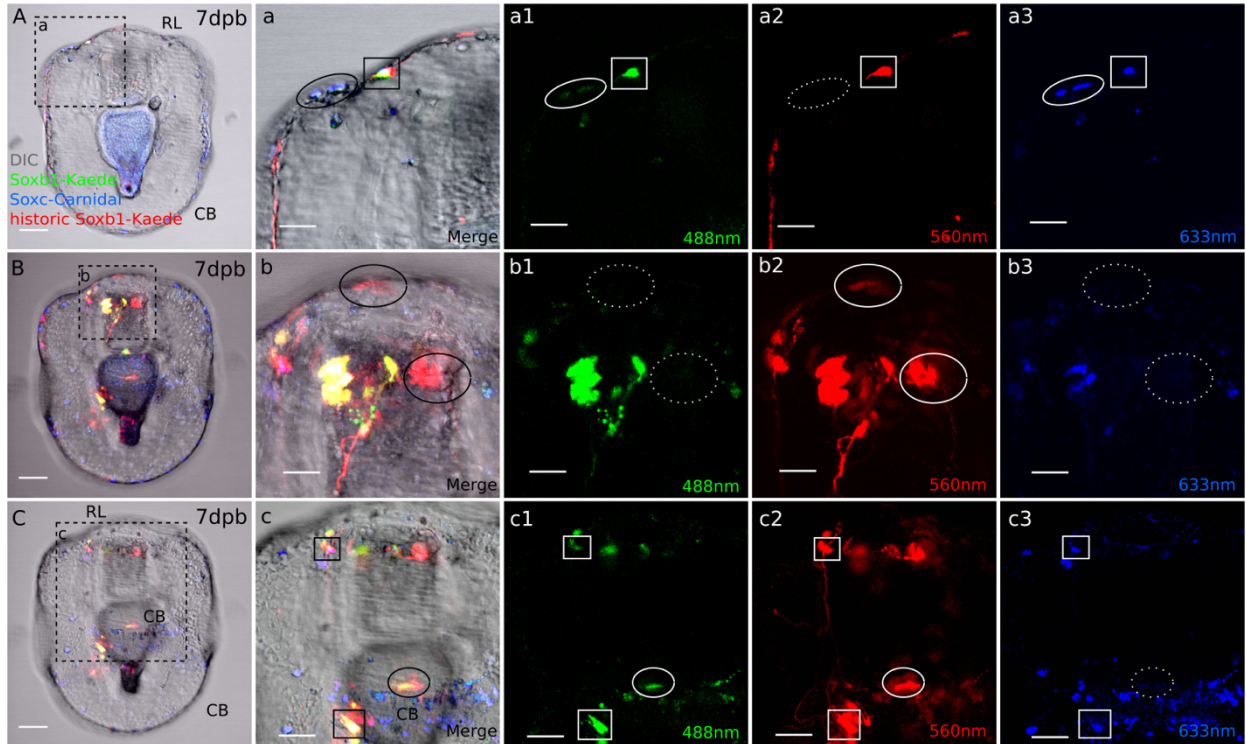


Fig 17. Soxb1+ cell lineage forms the regenerated nervous system.

(A) *De novo* Soxb1 cells form neurons through the Sox_c-mediated pathway in the regenerating anterior. (a) Amplification of boxed area in (A). There are two neurons at the lateral side of the regenerating anterior (black solid circle) derived from the newly specified Soxb1+/Sox_c+ cells. They contain (a1) regenerative green Soxb1-Kaede and (a3) blue Sox_c-Cardinal (white solid circle), (a2) but do not have historic Soxb1 expression (dotted white circle). Apart from the *de novo* Soxb1 cells, the larval Soxb1+ cell lineage also contributes to the regenerated neurons at the anterior marked by the black solid square in (a). (a1-a3) This neuron contains all three colors (white solid box), suggesting it is derived from the larval Soxb1+ cell lineage through the Sox_c-mediated pathway. (B) Historic Soxb1 cells present neural morphology. (b) There are red only, historic Soxb1+

neural cells at the regeneration leading edge and the oral domain (black solid circles). These cells are likely to be differentiated cells or cell taken other fated in regeneration, no longer express Soxb1. (b2) They contain the historic Kaede marker, (b1) but do not express new green Kaede or (b3) Cardinal (white dotted circle). (C-c) Besides the anterior, larval Soxb1+ cell lineage also contributes to neurons at the oral ectoderm and the post-oral ciliary band (black solid box). (c1-c3) They have all three colors (white solid box), suggesting the Sox-c-mediated pathway is involved. (c) In the ciliary band, there is also a neural descendant of larval Soxb1+ cell lineage through non-Sox-c-mediated pathway (black solid circle). The neuron (c1-c2) have both green and red Kaede (white circle) but (c3) does not express Sox-c-Cardinal (white dotted circle). Scale bar in (A,B,C): 50 μm , in (a-a3): 20 μm , in (b-b3): 15 μm , in (c-c3) :30 μm . RL, regeneration leading edge; CB, ciliary band.

5.3 Conclusion and discussion

Through double injection of the *Soxb1*-Kaede BAC and the *Soxc*-Cardinal BAC, we show that bisection activates *de novo* expression of *Soxb1* in cells derived from non-*Soxb1* governing lineages, possibly from non-ectodermal lineages. With a few exceptions, other *de novo* *Soxb1*⁺ stem cells at regenerating anterior are further specified to express *Soxc*. The newly formed *Soxb1*⁺/*Soxc*⁺ cells then enter multiple neuronal fates and form neurons in regenerating anterior. In bisected larvae, there are multiple sources of *Soxb1*⁺ cells. Apart from the green regeneration-specific *Soxb1*⁺ cells, there are also yellow cells derived from the larval *Soxb1*⁺ cell lineage. The neuron morphology of the yellow cells indicates that the larval *Soxb1*⁺ cell lineage is reused to form neurons in regeneration. This is likely through the *Soxc* mediated pathway supported by the blue Cardinal observed in the yellow neurons. Apart from the neurons located at the regeneration leading edge, larval *Soxb1*⁺ cell lineage also forms yellow nerve cells associated to the regenerating mouth and the post-oral ciliary bands. Likewise, historic red neurons differentiated from *Soxb1*⁺ stem cells are detected in the mouth and ciliary bands. Evidently, the larval *Soxb1*⁺ cell lineage contributes to the nervous system in both development and regeneration.

In this chapter, we have identified two other sources of the regenerated neurons: the yellow larval *Soxb1*⁺ cell lineage and the green *de novo* *Soxb1*⁺ neural stem cells at the regeneration leading edge. Moreover, the *de novo* *Soxb1*⁺ stem cells regenerate neurons through the *Soxc* neuronal pathway. In the working model, we validate that the *soxb1-soxc-elav* pathway is recapitulated.

This chapter raised another interesting question: where do the newly specified Soxb1+ cells come from? Based on the common regenerative strategies used in other model systems, we speculated that there are two possible origins of the Soxb1 *de novo* expression. There may be totipotent or pluripotent germline cells or stem cells in sea star larvae that function similar to the neoblast in freshwater planarians. Upon decapitation, these “neoblast” cells are specified into Soxb1 neural fates. In agreement with this hypothesis, there are consistently massive cell proliferation detected in the larvae, especially in the ciliary bands. Alternatively, tissues from non-germline, non-Soxb1 lineages are reprogrammed to trans-fate into Soxb1 stem cells. Soxb1 is expressed in a low level on the larval ectoderm. Therefore, non-Soxb1 lineages are likely to be endo-mesodermal tissues. As a result, they de/trans-differentiate and express neural stem cell marker Soxb1. Further studies are necessary to distinguish between the hypotheses.

Chapter 6: General Discussion

6.1 Summary

The larvae of the sea star *Patiria miniata* have been used as a model system to study fundamental questions in developmental biology. This study extends the larval model *P. miniata* that are naturally capable of whole-body regeneration as a model for research in the field of regeneration and stem cell reprogramming. Using starfish larvae, this work seeks to understand the strategies and mechanisms underlying nervous system regeneration, with a particular focus on identifying the cellular sources of the regenerated neurons. Previous work has shown that *P. miniata* undergo homologous regenerative processes shared by planarians and cnidarians (Cary, Wolff, et al. 2019). Therefore, we believe that the regenerative mechanism characterized in this thesis is an important reference to unravel the molecular and cellular basis of regeneration in Metazoa, providing key evidence for determining the evolutionary history of regeneration phenomena.

6.1.1 The neuronal genetic pathway is recapitulated in regeneration.

In embryos, the APD GRN governs the *soxc+* neural stem cells to form the anterior serotonergic neurons that become the dorsal ganglia through *lhx2+* neural progenitors. In Chapter 3, we show that this genetic pathway controlling embryonic serotonergic neurogenesis is recapitulated to regenerate the serotonergic neurons. We characterize the expression pattern of the APD GRN associated genes in the context of serotonergic neural regeneration. Following bisection, the anterior patterning gene *foxq2* and *six3* is

expressed at the regenerating anterior whereas the *wnt3* is expressed in the *foxq2*-free posterior domain, suggesting that the AP body axis is reconstructed. Both *soxb1* and *soxc* are expressed immediately after bisection at the wound site and the regenerating leading edge. Proportions of both *soxb1*⁺ cells and *soxc*⁺ cells are consistently proliferating in the regenerating anterior. However, the *soxb1* expression domain is spatially broader than *soxc*. In all examined time points there are more proliferating *soxb1* cells than dividing *soxc*⁺ cells, suggesting that the *soxb1* may be upstream of *soxc* in regulating the formation of neurons. At the lateral side of the regeneration leading edge, *Soxc*⁺ cells then give rise to the *lhx2*⁺ neural progenitors which become *elav*⁺ post-mitotic neurons. The progression of *soxc*⁺ neural stem cells and the *lhx2*⁺ neural progenitors is detected at 7 dpb, the time when regenerated serotonergic neurons are first observed at the lateral side of the regenerating anterior. GFP and serotonin double IF staining also provides evidence to support that the embryonic *soxc-lhx2-elav* genetic pathway is recapitulated to reform serotonergic neurons during regeneration. However, whether and how the AP patterning genes communicate with neuronal genes to direct neural regeneration remains unknown. In the future, it will be of interest to us to perform the expression perturbation analyses of AP patterning genes in the context of regeneration to understand this question.

6.1.2 Novel application of BAC transgenesis in Echinoderm regeneration

To identify the cellular sources of regenerated neurons, tracing the lineage of neural stem cells in regenerating larvae is an important and necessary approach. Therefore, a molecular tool needs to meet the following standards:

- (1) The method can stably label the neural stem cell lineage over the course of development and regeneration preferably via transgenesis;
- (2) The approach is able to differentiate stem cell lineage formed in regeneration from the developmentally generated neural stem cells;
- (3) The labeled stem cell lineage can be detected through visualization and microscopy.

The previously available method Soxc-GFP BAC labeling did not satisfy standard (2). Therefore, we generated the Soxc-Kaede BAC that is ideal for labeling cell lineage and detecting cell origins and fates in the context of regeneration. When delivered into zygotes through microinjection, the BAC is incorporated in the embryonic genome. The expression of photo-convertible protein Kaede is controlled by the cis-regulatory module of gene *soxc*. Thus the Soxc⁺ neural stem cell lineage is labeled with Kaede protein. When photo-converted upon decapitation, the Kaede historically generated before bisection is irreversibly converted to red. In contrast, the regenerative Soxc expression drives the formation of new, green Kaede proteins. Therefore the developmental cell lineage and the regeneration cell lineage are easily distinguished through photo-conversion. In Chapter 4, we characterize and validate the function of the Soxc-Kaede BAC in the embryo and larvae of *P.miniata*. We then take advantage of this powerful tool to interrogate the cellular basis of regenerated neurons.

Apart from the Soxc-Kaede BAC, we also generated the Soxb1-Kaede BAC and the Soxc-Cardinal BAC for multiplex cell lineage tracing studies. This facilitates the query

for relationships between lineages in development, regeneration and fate decision of cells.

This is the first time that the BAC transgenesis system incorporated with a photo-convertible reporter protein is applied in the context of regeneration in echinoderms. We believe that the Kaede BAC labeling is a very powerful and promising method that can be easily adapted in other echinoderm models for lineage tracing studies. It also holds great potential to be applied in other metazoan model systems with less available genetic tools.

6.1.3 The Sox^c+ neural stem cells at the regeneration leading edge come from three different sources and become neurons in regeneration

Knowing that the *soxc-lhx2-elav* neuronal genetic pathway is recapitulated at the regeneration leading edge, Chapters 4 and 5 seek to understand the cellular origins of the Sox^c+ cells located at the regeneration leading edge and whether they form differentiated neurons in regeneration. Through Kaede BAC transgenesis and neural stem cell lineage tracing, we find that there are three different sources of Sox^c+ neural stem cells located at the regeneration leading edge.

6.1.3.1 Embryonic Sox^c+ cell lineage is activated to enter the embryonic neuronal pathway.

Sox^c-Kaede expressions in regenerating larvae indicate that there is a combination of sources for regenerative Sox^c+ cells. The first origin is the embryonic Sox^c+ cell lineage. Using Sox^c-Kaede cell lineage tracing, we find that all of the larval Sox^c+ neural stem cells are descendants of the embryonic Sox^c+ cell lineage through cell divisions. Quantification of the *de novo*, green Sox^c+ cells show that specification to generate new Sox^c+ cells is completed in embryo stages. This embryonic Sox^c+ lineage is maintained in the larvae and continues to express Sox^c, marked by yellow from existing red Kaede and new green Kaede.

Upon bisection, the posteriorly located embryonic Sox^c+ cell lineage relocates to the lateral sides of the regeneration leading edge. The relocation of the lineage may occur through cell migration or the changes in the local tissue environment from healing and re-proportioning. When the AP body axis is reconstructed, these yellow Sox^c+ cells are positioned at the anterior molecular environment. They are activated to enter the embryonic neuronal pathway and form the regenerated serotonergic neurons at the regenerating dorsal ganglia.

6.1.3.2 Sox^c+ cells specified from the regenerative Sox^b1+ stem cell lineage give rise to anterior serotonergic neurons

The second population of regenerative Sox^c+ cells at the leading edge is derived through Sox^b1+ cell specification. In 3 dpb regenerating larvae, apart from the yellow

embryonic Sox^{c+} cell lineage, there are newly specified, green Sox^{c+} cells at the regeneration leading edge. These cells are originated from a non-Sox^c lineage. By comparing the numbers of green Sox^{c+} cells in embryonic photo-conversion, larval photo-conversion, and bisection photo-conversion, we show that specification events to form *de novo* Sox^{c+} cells are resumed in regeneration to the extent similar to embryo states.

Using double lineage labeling with Sox^b1-Kaede BAC and Sox^c-Cardinal BAC, we show that upon bisection, the *de novo* green Sox^b1 cells located at the regeneration leading edge are specified to become Sox^{c+} cells. These regeneration-specific Sox^b1⁺/Sox^{c+} cell lineage also forms neurons at the regeneration leading edge.

Together, we identify the *de novo* Sox^b1⁺ cells emerged upon decapitation as another origin to both the regenerative Sox^{c+} neural stem cells and the newly formed neurons in the regenerating anterior.

Interestingly, we note that almost all Sox^{c+} cells are Sox^b1 positive in immediately converted larvae. There are more converted Sox^b1⁺ cells (red) than Sox^b1⁺/Sox^{c+} cells (red/blue). But there is almost no convincing evidence of Sox^{c+} only cells (blue) in the larvae. This demonstrates that the larval Sox^{c+} cells are a continuation of the embryonic Sox^{c+} cells which may be specified from the embryonic Sox^b1⁺ stem cell lineage.

6.1.3.3 Other sources

It is worth noting that not all Sox_c cells specified upon bisection, or the regeneration-specific Sox_c⁺ cells, are derived from the *de novo* Sox_b1⁺ cells at the leading edge.

These are the blue cells located at the anterior labeled only with Sox_c marker Cardinal and free from Sox_b1 reporter Kaede. They emerge through specification upon injury.

This indicates that there are other sources of the regenerative Sox_c⁺ cells besides the embryonic Sox_c⁺ cell lineage or the *de novo* Sox_b1⁺ stem cells.

6.1.4 Larval Sox_b1⁺ cell lineage contributes to the larval nervous system in development and regeneration.

In chapter 5, we have found that the Sox_b1⁺ cell lineage plays a major role in neurogenesis in development and regeneration. In double-labeled regenerating larvae, red and yellow Sox_b1⁺ neurons are distributed at the regenerating mouth, the esophagus and the post-oral ciliary band which are important organs of the larval nervous system. Red neurons represent the historic nerve cells generated by the developmental Sox_b1⁺ cell lineage. In contrast, the yellow neurons are regenerated neurons derived from the larval Sox_b1⁺ stem cells. Together, these data demonstrate that the larval Sox_b1⁺ cell lineage plays a vital role in neurogenesis, giving rise to the nervous system in both development and regeneration.

6.1.5 Specification of Soxb1+ cells is activated in regeneration, suggesting trans-fating from endo-mesodermal cells.

In chapter 5, we have shown that there are newly specified, green Soxb1+ cells located at the regeneration leading edge. Some of the *de novo* Soxb1+ cells are specified to become Soxc+ neural stem cells and generate neurons through the embryonic neuronal pathway. Others do not take the Soxc-mediated cell fates. Specification of Soxb1+ cells is activated upon bisection. They may originate from the germline derived stem cells similar to the neoblast in freshwater planarians. Alternatively, they can be trans-differentiated from the endo-mesoderm tissues. Further studies need to be performed to distinguish between the hypotheses.

6.2 A strategy for sea star larval nervous system regeneration

In this study, we proposed a strategy used by sea star larvae to regenerate the nervous system. As shown in **Fig 18**. Upon bisections, the following cellular behaviors are activated:

- 1, Pre-existing posterior embryonic Soxc+ stem cell lineage is relocated to the regeneration leading edge and activated to enter the embryonic *soxc-lhx2-elav* neuronal pathway, regenerating the anterior serotonergic neurons;

2, The specification of *de novo* Soxb1+ stem cells is resumed upon decapitation to become regeneration-specific Soxc+ neural stem cells. These cells are used to form neurons at the regeneration leading edge;

3, The specification of non-neural lineage is activated to trans-fate into *de novo* Soxb1+ stem cells. These cells may serve as a pool of stem cells required for neural regeneration;

4, The pre-existing larval Soxb1+ stem cell lineage is activated to form neurons through Soxc-mediated pathways and non-Soxc pathways.

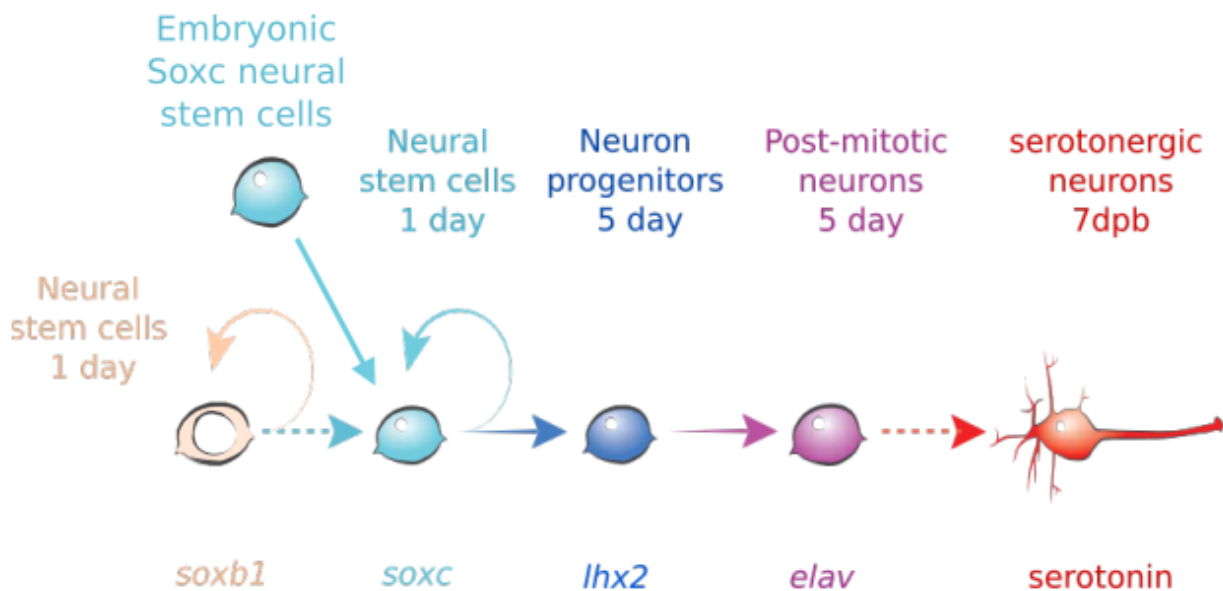


Fig 18. A model for the regeneration of the larval nervous system in sea stars.

Taken together, larvae of *P.miniata* maintain an embryonic neural stem cell lineage and a prime neural stem cell lineage. When the larvae sense the wound, possibly through early immune response, the stem cell lineages in the remaining posterior are reactivated to enter neurogenic pathways in order to generate lost neurons. On the other hand, the populations of neural stem cells and the prime neural stem cells expand from active cell proliferation and regeneration-activated specification. The specification events may involve the trans-differentiation of other tissues or neoblast progression.

6.3 Sox^{c+} stem cells are multipotent in regeneration.

Interestingly, we notice that the regenerative Sox^{c+} cell lineage (including the *de novo* green Sox^c cells and the yellow embryonic Sox^c lineage) becomes multiple types of neurons in regeneration. This demonstrates that Sox^{c+} stem cells are multipotent in regeneration, similar to their roles in embryo development. The regenerative Sox^{c+} cells not only form the serotonergic neurons distributed in the regenerated dorsal ganglia and the oral organs (mouth and esophagus), they also form non-serotonergic neurons in the regenerated pre-oral ciliary band and the re-proportioned post-oral ciliary band.

Although the subtypes of neurons need further characterization by molecular studies, the different locations suggest that there are multiple types of neurons. For example, only a particular population of differentiated neurons located at specific organs express serotonin whereas others do not. This is also supported by studies in sea urchins. In the apical organ, serotonergic neurons express tryptophan 5-hydroxylase for serotonin synthesis (Yaguchi and Katow 2003). Differentiated cholinergic neurons are distributed

throughout the ciliary band. And the post-oral neurons express both tyrosine hydroxylase and choline acetyltransferase for the synthesis of catecholamines and acetylcholine (Slota and McClay 2018). Neurons in the mouth and foregut are derived from the endoderm (Wei et al. 2011; Wei et al. 2016).

6.4 The regeneration leading edge is set back to an embryonic state

Early steps of neurogenesis are relatively conserved in animals (Hartenstein and Stollewerk 2015; Rentzsch et al. 2017; Florio and Huttner 2014). In most animals, neurogenesis begins when the ectoderm acquires the potential to form neural cells. Then neural progenitors arise from the ectoderm. These neural cells migrate, proliferate and differentiate to form neurons. The conserved neurogenesis regime is inherited in sea star embryos to form the larval nervous system and more interestingly is maintained in the regeneration of the larval nervous system. This suggests that to restore a complicated nervous system in the injured larvae, it is required to rewire the complex molecular environments in the remaining segments to a simple, primitive embryonic state.

The posterior segments contain multiple differentiated tissues including neurons, muscles, immune cells and the coeloms. Upon bisection, wound detection is activated possibly through the MAPK pathway. Immediately the regeneration leading edge is rewired to express Yamanaka factor genes including *soxb1* and *klf2/4*. *Soxb1*

expression is highly concentrated at the wound area and the regeneration leading edge on the ectoderm, specifying the anterior ectodermal cells with the potential to form neurons. This modifies the wound ectoderm to highly potent and proliferative epithelia resembling the embryonic state, ready for differentiation of particular tissues. Following the homologous neurogenesis regime, *Soxc*⁺ neural stem cells are specified and partitioned from the *Soxb1*⁺ neurogenic wound ectoderm. The resumed specification of *Soxc*⁺ cells at the anterior ectoderm initiates the differentiation of neurons. The *Soxc*⁺ neural cells proliferate and progress to become *lhx2*⁺ neural progenitors which then differentiate into neurons at the anterior ectoderm. Although whether the AP patterning genes regulate this process is unknown, we are confident to conclude that neurogenesis is recapitulated in the regeneration leading edge. Homologous wound detection in the remaining larvae connects tissue-loss injuries with the rewirement of the wound ectoderm. This resets the molecular environment at the regeneration leading edge back to the highly potent embryonic state and thereby re-initiates neurogenesis to restore the lost nervous system.

6.5 Regeneration capability and developmental plasticity in

Metazoa

Flexibility is the defining feature of regeneration. Whole-body regeneration is the most extreme example of developmental plasticity. This study preliminarily resolves the mechanisms in sea star larvae WBR. It demonstrates that WBR occurs through extensively reprogramming cell populations to different extents in sea star larvae. Upon

injuries, cells in proximity to the wound are reprogrammed naturally into highly potent, embryonic states through expressing genes like *Soxb1* that are important to promote proliferation and prime the chromatin for differentiation. Neural stem cell lineage at the posterior do not enter the serotonergic pathway in intact larvae. However, wounding activates the fate reprogramming of neural stem cells to enter the serotonergic pathway, possibly through providing primitive neurogenic potential and AP positioning cues. We believe that these early steps are key to the dramatic differences of regenerative potential across the animal kingdom in nature. The conclusions of this thesis inspire speculation that may explain the limited regeneration capability of other organisms.

In many organisms, the sealing of wounds is followed by the formation of scars instead of potent epithelia. The wound epithelia fail to reprogram into a primitive state. In other words, it fails to express a suite of master regulators like *Soxb1* (Clore 2016) and *Egr* (Gehrke et al. 2019). The master regulators have multiple functions in cell fate programming such as priming the epigenetic landscape (Amador-Arjona et al. 2015), opening the local chromatin (Muhr 2016), interacting with diverse stem cell regulators to direct proliferation and tissue formation (Kondoh and Kamachi 2016; Wong et al. 2016). Therefore, the poor regenerative capacity in later-branching animals may be caused by failure to activate or maintain these gene expressions, due to existing inhibition mechanisms, lack of activation signals, or lack of signal receiving and processing system (like cis-regulatory modules).

Many organisms may lack a reservoir of embryonic stem cell lineages that can serve as direct sources for regeneration. The embryonic lineage we identified here suggests that the stem cells are early derived, highly potent and self-maintaining. These stem cells can be totipotent or pluripotent to generate multiple tissues like the neoblast in planarians (Sánchez Alvarado 2006). They can also be lineage-specific and multipotent, similar to the Sox^c+ embryonic stem cell lineage giving rise to multiple types of neurons in sea star larvae. Absence of self-maintaining stem cell populations deprive organisms of a straightforward, transcriptionally-ready regeneration source. Consequently, the organisms may have limited regenerative ability. Some animals have restricted progenitors to replace dying cells in homeostasis (Brown and Pearson 2017). However, the less potent restricted progenitors need to be reprogrammed *in vivo* to obtain higher potency for regeneration upon severe injuries. Lack of this ability may be another reason for poor regeneration capacity.

References

- Almuedo-Castillo, M., Crespo-Yanez, X., Seebeck, F., Bartscherer, K., Salò, E. and Adell, T. 2014. JNK controls the onset of mitosis in planarian stem cells and triggers apoptotic cell death required for regeneration and remodeling. *PLoS Genetics* 10(6), p. e1004400.
- Amador-Arjona, A., Cimadamore, F., Huang, C.-T., et al. 2015. SOX2 primes the epigenetic landscape in neural precursors enabling proper gene activation during hippocampal neurogenesis. *Proceedings of the National Academy of Sciences of the United States of America* 112(15), pp. E1936-45.
- Ando, R., Hama, H., Yamamoto-Hino, M., Mizuno, H. and Miyawaki, A. 2002. An optical marker based on the UV-induced green-to-red photoconversion of a fluorescent protein. *Proceedings of the National Academy of Sciences of the United States of America* 99(20), pp. 12651–12656.
- Barsi, J.C. and Davidson, E.H. 2016. cis-Regulatory control of the initial neurogenic pattern of onecut gene expression in the sea urchin embryo. *Developmental Biology* 409(1), pp. 310–318.
- Beckervordersandforth, R., Deshpande, A., Schäffner, I., et al. 2014. In vivo targeting of adult neural stem cells in the dentate gyrus by a split-cre approach. *Stem cell reports* 2(2), pp. 153–162.
- Bergsland, M., Werme, M., Malewicz, M., Perlmann, T. and Muhr, J. 2006. The establishment of neuronal properties is controlled by Sox4 and Sox11. *Genes & Development* 20(24), pp. 3475–3486.
- Bisgrove, B.W. and Burke, R.D. 1986. Development of Serotonergic Neurons in Embryos of the Sea Urchin, *Strongylocentrotus purpuratus*. (serotonergic/neural development/embryo/echinoid). *Development, Growth & Differentiation* 28(6), pp. 569–574.
- Bishop, C.D., MacNeil, K.E.A., Patel, D., Taylor, V.J. and Burke, R.D. 2013. Neural development in *Eucidaris tribuloides* and the evolutionary history of the echinoid larval nervous system. *Developmental Biology* 377(1), pp. 236–244.
- Brown, D.D.R. and Pearson, B.J. 2017. A brain unfixed: unlimited neurogenesis and regeneration of the adult planarian nervous system. *Frontiers in Neuroscience* 11, p. 289.
- Bucher, D. and Anderson, P.A.V. 2015. Evolution of the first nervous systems - what can we surmise? *Journal of Experimental Biology* 218(4), pp. 501–503.
- Buckley, K.M., Dong, P., Cameron, R.A. and Rast, J.P. 2018. Bacterial artificial chromosomes as recombinant reporter constructs to investigate gene expression and regulation in echinoderms. *Briefings in functional genomics* 17(5), pp. 362–371.
- Buckley, K.M. and Etensohn, C.A. 2019. Techniques for analyzing gene expression using BAC-based reporter constructs. *Methods in Cell Biology* 151, pp. 197–218.
- Buckley, K.M., Ho, E.C.H., Hibino, T., et al. 2017. IL17 factors are early regulators in the gut epithelium during inflammatory response to *Vibrio* in the sea urchin larva. *eLife* 6.

- Bylund, M., Andersson, E., Novitsch, B.G. and Muhr, J. 2003. Vertebrate neurogenesis is counteracted by Sox1-3 activity. *Nature Neuroscience* 6(11), pp. 1162–1168.
- Byrne, M., Nakajima, Y., Chee, F.C. and Burke, R.D. 2007. Apical organs in echinoderm larvae: insights into larval evolution in the Ambulacraria. *Evolution & Development* 9(5), pp. 432–445.
- Cameron, R.A., Kudtarkar, P., Gordon, S.M., Worley, K.C. and Gibbs, R.A. 2015. Do echinoderm genomes measure up? *Marine genomics* 22, pp. 1–9.
- Cameron, R.A., Mahairas, G., Rast, J.P., et al. 2000. A sea urchin genome project: sequence scan, virtual map, and additional resources. *Proceedings of the National Academy of Sciences of the United States of America* 97(17), pp. 9514–9518.
- Cameron, R.A., Rast, J.P. and Brown, C.T. 2004. Genomic resources for the study of sea urchin development. *Methods in Cell Biology* 74, pp. 733–757.
- Carnevali, M.D.C. and Burighel, P. 2001. Regeneration in echinoderms and ascidians. In: John Wiley & Sons, Ltd ed. *Encyclopedia of life sciences*. Chichester, UK: John Wiley & Sons, Ltd.
- Cary, G.A., Cameron, R.A. and Hinman, V.F. 2018. Echinobase: tools for echinoderm genome analyses. *Methods in Molecular Biology* 1757, pp. 349–369.
- Cary, G.A., Cameron, R.A. and Hinman, V.F. 2019. *Genomic resources for the study of echinoderm development and evolution*.
- Cary, G.A., Cheatle Jarvela, A.M., Francolini, R.D. and Hinman, V.F. 2017. Genome-wide use of high- and low-affinity Tbrain transcription factor binding sites during echinoderm development. *Proceedings of the National Academy of Sciences of the United States of America* 114(23), pp. 5854–5861.
- Cary, G.A., Wolff, A., Zueva, O., Pattinato, J. and Hinman, V.F. 2019. Analysis of sea star larval regeneration reveals conserved processes of whole-body regeneration across the metazoa. *BMC Biology* 17(1), p. 16.
- Cheatle Jarvela, A.M. and Hinman, V.F. 2015. Evolution of transcription factor function as a mechanism for changing metazoan developmental gene regulatory networks. *EvoDevo* 6(1), p. 3.
- Cheatle Jarvela, A.M. and Hinman, V. 2014. A method for microinjection of *Patiria miniata* zygotes. *Journal of Visualized Experiments* (91), p. e51913.
- Cheatle Jarvela, A.M., Yankura, K.A. and Hinman, V.F. 2016. A gene regulatory network for apical organ neurogenesis and its spatial control in sea star embryos. *Development* 143(22), pp. 4214–4223.
- Chen, C.-C., Wu, J.-K., Lin, H.-W., et al. 2012. Visualizing long-term memory formation in two neurons of the *Drosophila* brain. *Science* 335(6069), pp. 678–685.
- Cimadamore, F., Amador-Arjona, A., Chen, C., Huang, C.-T. and Terskikh, A.V. 2013. SOX2-LIN28/let-7 pathway regulates proliferation and neurogenesis in neural precursors. *Proceedings of the National Academy of Sciences of the United States of America* 110(32), pp. E3017-26.

- Clore, G.M. 2016. Dynamics of SOX2 Interactions with DNA. In: *Sox2*. Elsevier, pp. 25–41.
- Corsinotti, A., Wong, F.C., Tatar, T., et al. 2017. Distinct SoxB1 networks are required for naïve and primed pluripotency. *eLife* 6.
- Currie, J.D., Kawaguchi, A., Traspas, R.M., Schuez, M., Chara, O. and Tanaka, E.M. 2016. Live imaging of axolotl digit regeneration reveals spatiotemporal choreography of diverse connective tissue progenitor pools. *Developmental Cell* 39(4), pp. 411–423.
- Currie, K.W. and Pearson, B.J. 2013. Transcription factors *lhx1/5-1* and *pitx* are required for the maintenance and regeneration of serotonergic neurons in planarians. *Development* 140(17), pp. 3577–3588.
- Czarkwiani, A., Ferrario, C., Dylus, D.V., Sugni, M. and Oliveri, P. 2016. Skeletal regeneration in the brittle star *Amphiura filiformis*. *Frontiers in zoology* 13, p. 18.
- David, C.N. 2012. Interstitial stem cells in Hydra: multipotency and decision-making. *The International Journal of Developmental Biology* 56(6–8), pp. 489–497.
- Elkouris, M., Balaskas, N., Poulou, M., et al. 2011. Sox1 maintains the undifferentiated state of cortical neural progenitor cells via the suppression of Prox1-mediated cell cycle exit and neurogenesis. *Stem Cells* 29(1), pp. 89–98.
- Florio, M. and Huttner, W.B. 2014. Neural progenitors, neurogenesis and the evolution of the neocortex. *Development* 141(11), pp. 2182–2194.
- Frank, U., Plickert, G. and Müller, W.A. 2009. Cnidarian Interstitial Cells: The Dawn of Stem Cell Research. In: *Stem Cells in Marine Organisms*. Dordrecht: Springer Netherlands, pp. 33–59.
- Frengen, E., Weichenhan, D., Zhao, B., Osoegawa, K., van Geel, M. and de Jong, P.J. 1999. A modular, positive selection bacterial artificial chromosome vector with multiple cloning sites. *Genomics* 58(3), pp. 250–253.
- Galliot, B. 2012. Hydra, a fruitful model system for 270 years. *The International Journal of Developmental Biology* 56(6–8), pp. 411–423.
- García-Arrarás, J.E., Lázaro-Peña, M.I. and Díaz-Balzac, C.A. 2018. Holothurians as a model system to study regeneration. *Results and Problems in Cell Differentiation* 65, pp. 255–283.
- Garner, S., Zysk, I., Byrne, G., et al. 2016. Neurogenesis in sea urchin embryos and the diversity of deuterostome neurogenic mechanisms. *Development* 143(2), pp. 286–297.
- Gehrke, A.R., Neverett, E., Luo, Y.J., et al. 2019. Acoel genome reveals the regulatory landscape of whole-body regeneration. *Science* 363(6432).
- Gerber, T., Murawala, P., Knapp, D., et al. 2018. Single-cell analysis uncovers convergence of cell identities during axolotl limb regeneration. *Science* 362(6413).
- Gold, D.A. and Jacobs, D.K. 2013. Stem cell dynamics in Cnidaria: are there unifying principles? *Development Genes and Evolution* 223(1–2), pp. 53–66.
- Guay, C.L., McQuade, S.T. and Nam, J. 2017. Single embryo-resolution quantitative analysis of reporters permits multiplex spatial cis-regulatory analysis. *Developmental*

Biology 422(2), pp. 92–104.

Hartenstein, V. and Stollewerk, A. 2015. The evolution of early neurogenesis. *Developmental Cell* 32(4), pp. 390–407.

Hatta, K., Tsujii, H. and Omura, T. 2006. Cell tracking using a photoconvertible fluorescent protein. *Nature Protocols* 1(2), pp. 960–967.

Hinman, V.F. and Burke, R.D. 2018. Embryonic neurogenesis in echinoderms. *Wiley interdisciplinary reviews. Developmental biology* 7(4), p. e316.

Hinman, V.F. and Cheattle Jarvela, A.M. 2014. Developmental gene regulatory network evolution: insights from comparative studies in echinoderms. *Genesis* 52(3), pp. 193–207.

Hinman, V.F., Nguyen, A.T. and Davidson, E.H. 2003. Expression and function of a starfish Otx ortholog, AmOtx: a conserved role for Otx proteins in endoderm development that predates divergence of the eleutherozoa. *Mechanisms of Development* 120(10), pp. 1165–1176.

Holmberg, J., Hansson, E., Malewicz, M., et al. 2008. SoxB1 transcription factors and Notch signaling use distinct mechanisms to regulate proneural gene function and neural progenitor differentiation. *Development* 135(10), pp. 1843–1851.

Hsu, Y.-C. 2015. Theory and practice of lineage tracing. *Stem Cells* 33(11), pp. 3197–3204.

Hsu, Y.-C., Pasolli, H.A. and Fuchs, E. 2011. Dynamics between stem cells, niche, and progeny in the hair follicle. *Cell* 144(1), pp. 92–105.

Jensen, P., Farago, A.F., Awatramani, R.B., Scott, M.M., Deneris, E.S. and Dymecki, S.M. 2008. Redefining the serotonergic system by genetic lineage. *Nature Neuroscience* 11(4), pp. 417–419.

Kao, D., Felix, D. and Aboobaker, A. 2013. The planarian regeneration transcriptome reveals a shared but temporally shifted regulatory program between opposing head and tail scenarios. *BMC Genomics* 14, p. 797.

Kondoh, H. and Kamachi, Y. 2016. Sox2–partner factor interactions and enhancer regulation. In: *Sox2*. Elsevier, pp. 131–144.

Kretschmar, K. and Watt, F.M. 2012. Lineage tracing. *Cell* 148(1–2), pp. 33–45.

Kugelberg, E., Norström, T., Petersen, T.K., Duvold, T., Andersson, D.I. and Hughes, D. 2005. Establishment of a superficial skin infection model in mice by using *Staphylococcus aureus* and *Streptococcus pyogenes*. *Antimicrobial Agents and Chemotherapy* 49(8), pp. 3435–3441.

Lai, C. 2016. BAC Transgenesis: Cell-Type Specific Expression in the Nervous System☆. In: *Reference module in biomedical sciences*. Elsevier.

Lenhoff, S.G., Lenhoff, H.M. and Trembley, A. 1986. Hydra and the birth of experimental biology, 1744: Abraham Trembley's Mémoires concerning the polyps.

de-Leon, S.B.-T. and Davidson, E.H. 2010. Information processing at the foxa node of the sea urchin endomesoderm specification network. *Proceedings of the National*

- Academy of Sciences of the United States of America* 107(22), pp. 10103–10108.
- Mashanov, V.S., Dolmatov, I.Y. and Heinzeller, T. 2005. Transdifferentiation in holothurian gut regeneration. *The Biological Bulletin* 209(3), pp. 184–193.
- Mashanov, V.S., Zueva, O.R. and Garcia-Arraras, J.E. 2012. Expression of Wnt9, TCTP, and Bmp1/Tll in sea cucumber visceral regeneration. *Gene Expression Patterns* 12(1–2), pp. 24–35.
- Mashanov, V.S., Zueva, O.R., Rojas-Catagena, C. and Garcia-Arraras, J.E. 2010. Visceral regeneration in a sea cucumber involves extensive expression of survivin and mortalin homologs in the mesothelium. *BMC Developmental Biology* 10, p. 117.
- McCauley, B.S., Akyar, E., Filliger, L. and Hinman, V.F. 2013. Expression of wnt and frizzled genes during early sea star development. *Gene Expression Patterns* 13(8), pp. 437–444.
- McCauley, B.S., Akyar, E., Saad, H.R. and Hinman, V.F. 2015. Dose-dependent nuclear β -catenin response segregates endomesoderm along the sea star primary axis. *Development* 142(1), pp. 207–217.
- McCauley, B.S., Weideman, E.P. and Hinman, V.F. 2010. A conserved gene regulatory network subcircuit drives different developmental fates in the vegetal pole of highly divergent echinoderm embryos. *Developmental Biology* 340(2), pp. 200–208.
- McClay, D.R., Miranda, E. and Feinberg, S.L. 2018. Neurogenesis in the sea urchin embryo is initiated uniquely in three domains. *Development* 145(21).
- McMahon, A.P., Novak, T.J., Britten, R.J. and Davidson, E.H. 1984. Inducible expression of a cloned heat shock fusion gene in sea urchin embryos. *Proceedings of the National Academy of Sciences of the United States of America* 81(23), pp. 7490–7494.
- Miyagi, S., Kato, H. and Okuda, A. 2009. Role of SoxB1 transcription factors in development. *Cellular and Molecular Life Sciences* 66(23), pp. 3675–3684.
- Muhr, J. 2016. Genomic occupancy in various cellular contexts and potential pioneer factor function of SOX2. In: *Sox2*. Elsevier, pp. 145–159.
- Nakajima, Y., Kaneko, H., Murray, G. and Burke, R.D. 2004. Divergent patterns of neural development in larval echinoids and asteroids. *Evolution & Development* 6(2), pp. 95–104.
- Oosterveen, T., Kurdija, S., Ensterö, M., et al. 2013. SoxB1-driven transcriptional network underlies neural-specific interpretation of morphogen signals. *Proceedings of the National Academy of Sciences of the United States of America* 110(18), pp. 7330–7335.
- Oulhen, N., Heyland, A., Carrier, T.J., et al. 2016. Regeneration in bipinnaria larvae of the bat star *Patiria miniata* induces rapid and broad new gene expression. *Mechanisms of Development* 142, pp. 10–21.
- Paul, C.R. 2001. Echinodermata. In: John Wiley & Sons, Ltd ed. *Encyclopedia of life sciences*. Chichester, UK: John Wiley & Sons, Ltd.

- Petersen, C.P. and Reddien, P.W. 2009. A wound-induced Wnt expression program controls planarian regeneration polarity. *Proceedings of the National Academy of Sciences of the United States of America* 106(40), pp. 17061–17066.
- Petersen, H.O., Höger, S.K., Looso, M., et al. 2015. A comprehensive transcriptomic and proteomic analysis of hydra head regeneration. *Molecular Biology and Evolution* 32(8), pp. 1928–1947.
- Porter, F.D., Drago, J., Xu, Y., et al. 1997. Lhx2, a LIM homeobox gene, is required for eye, forebrain, and definitive erythrocyte development. *Development* 124(15), pp. 2935–2944.
- Rakic, P. 2009. Evolution of the neocortex: a perspective from developmental biology. *Nature Reviews. Neuroscience* 10(10), pp. 724–735.
- Reddien, P.W. 2018. The cellular and molecular basis for planarian regeneration. *Cell* 175(2), pp. 327–345.
- Reddien, P.W., Bermange, A.L., Kicza, A.M. and Sánchez Alvarado, A. 2007. BMP signaling regulates the dorsal planarian midline and is needed for asymmetric regeneration. *Development* 134(22), pp. 4043–4051.
- Reinardy, H.C., Emerson, C.E., Manley, J.M. and Bodnar, A.G. 2015. Tissue regeneration and biomineralization in sea urchins: role of Notch signaling and presence of stem cell markers. *Plos One* 10(8), p. e0133860.
- Rentzsch, F., Layden, M. and Manuel, M. 2017. The cellular and molecular basis of cnidarian neurogenesis. *Wiley interdisciplinary reviews. Developmental biology* 6(1).
- Reyer, R.W., Woolfitt, R.A. and Withersty, L.T. 1973. Stimulation of lens regeneration from the newt dorsal iris when implanted into the blastema of the regenerating limb. *Developmental Biology* 32(2), pp. 258–281.
- Ross, K.G., Molinaro, A.M., Romero, C., et al. 2018. Sox1 activity regulates sensory neuron regeneration, maintenance, and function in planarians. *Developmental Cell* 47(3), pp. 331–347.e5.
- Sánchez Alvarado, A. 2006. Planarian regeneration: its end is its beginning. *Cell* 124(2), pp. 241–245.
- Schmidt, A., Wiesner, B., Weissbart, K., et al. 2009. Use of Kaede fusions to visualize recycling of G protein-coupled receptors. *Traffic* 10(1), pp. 2–15.
- Slota, L.A. and McClay, D.R. 2018. Identification of neural transcription factors required for the differentiation of three neuronal subtypes in the sea urchin embryo. *Developmental Biology* 435(2), pp. 138–149.
- Spanjaard, B., Hu, B., Mitic, N., et al. 2018. Simultaneous lineage tracing and cell-type identification using CRISPR-Cas9-induced genetic scars. *Nature Biotechnology* 36(5), pp. 469–473.
- Suster, M.L., Abe, G., Schouw, A. and Kawakami, K. 2011. Transposon-mediated BAC transgenesis in zebrafish. *Nature Protocols* 6(12), pp. 1998–2021.
- Tanaka, E.M. and Reddien, P.W. 2011. The cellular basis for animal regeneration.

Developmental Cell 21(1), pp. 172–185.

Tasaki, J., Shibata, N., Nishimura, O., et al. 2011. ERK signaling controls blastema cell differentiation during planarian regeneration. *Development* 138(12), pp. 2417–2427.

Tomura, M., Yoshida, N., Tanaka, J., et al. 2008. Monitoring cellular movement in vivo with photoconvertible fluorescence protein “Kaede” transgenic mice. *Proceedings of the National Academy of Sciences of the United States of America* 105(31), pp. 10871–10876.

Tumbar, T., Guasch, G., Greco, V., et al. 2004. Defining the epithelial stem cell niche in skin. *Science* 303(5656), pp. 359–363.

Vickery, M.C., Vickery, M.S., McClintock, J.B. and Amsler, C.D. 2001. Utilization of a novel deuterostome model for the study of regeneration genetics: molecular cloning of genes that are differentially expressed during early stages of larval sea star regeneration. *Gene* 262(1–2), pp. 73–80.

Vickery, M.S. and McClintock, J.B. 1998. Regeneration in metazoan larvae. *Nature* 394(6689), pp. 140–140.

Vickery, M.S., Vickery, M.C.L. and McClintock, J.B. 2002. Morphogenesis and organogenesis in the regenerating planktotrophic larvae of asteroids and echinoids. *The Biological Bulletin* 203(2), pp. 121–133.

Wang, H., Lööf, S., Borg, P., Nader, G.A., Blau, H.M. and Simon, A. 2015. Turning terminally differentiated skeletal muscle cells into regenerative progenitors. *Nature Communications* 6, p. 7916.

Wang, H. and Simon, A. 2016. Skeletal muscle dedifferentiation during salamander limb regeneration. *Current Opinion in Genetics & Development* 40, pp. 108–112.

Wang, P., Chen, T., Sakurai, K., et al. 2012. Intersectional Cre driver lines generated using split-intein mediated split-Cre reconstitution. *Scientific reports* 2, p. 497.

Wei, Z., Angerer, L.M. and Angerer, R.C. 2016. Neurogenic gene regulatory pathways in the sea urchin embryo. *Development* 143(2), pp. 298–305.

Wei, Z., Angerer, R.C. and Angerer, L.M. 2011. Direct development of neurons within foregut endoderm of sea urchin embryos. *Proceedings of the National Academy of Sciences of the United States of America* 108(22), pp. 9143–9147.

Wei, Z., Yaguchi, J., Yaguchi, S., Angerer, R.C. and Angerer, L.M. 2009. The sea urchin animal pole domain is a Six3-dependent neurogenic patterning center. *Development* 136(7), pp. 1179–1189.

Wong, F.C.K., Chambers, I. and Mullin, N.P. 2016. SOX2-Dependent Regulation of Pluripotent Stem Cells. In: *Sox2*. Elsevier, pp. 163–185.

Yaguchi, S. and Katow, H. 2003. Expression of tryptophan 5-hydroxylase gene during sea urchin neurogenesis and role of serotonergic nervous system in larval behavior. *The Journal of Comparative Neurology* 466(2), pp. 219–229.

Yankura, K.A., Koechlein, C.S., Cryan, A.F., Cheatle, A. and Hinman, V.F. 2013. Gene regulatory network for neurogenesis in a sea star embryo connects broad neural

specification and localized patterning. *Proceedings of the National Academy of Sciences of the United States of America* 110(21), pp. 8591–8596.

Yankura, K.A., Martik, M.L., Jennings, C.K. and Hinman, V.F. 2010. Uncoupling of complex regulatory patterning during evolution of larval development in echinoderms. *BMC Biology* 8, p. 143.

Zafar, H., Lin, C. and Bar-Joseph, Z. 2019. Single-cell Lineage Tracing by Integrating CRISPR-Cas9 Mutations with Transcriptomic Data. *BioRxiv*.